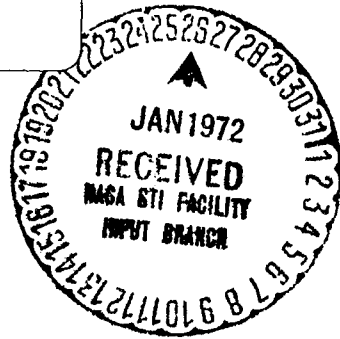


TECHNICAL REPORT NO. 9

Project A-852

COMMUNICATION SYSTEM MODELING



L. D. Holland, J. R. Walsh and R. D. Wetherington

CONTRACT NAS8-20054

CR 123554

19 November 1971

Prepared for

National Aeronautics and Space Administration
George C. Marshall Space Flight Center
Marshall Space Flight Center, Alabama

(NASA-CR-123554) COMMUNICATION SYSTEM
MODELING L.D. Holland, et al (Georgia
Inst. of Tech.) 19 Nov. 1971 163 p
CSCL 17B

N72-19201

Unclas

G3/07 15116



Engineering Experiment Station

GEORGIA INSTITUTE OF TECHNOLOGY

Atlanta, Georgia

FF No. 60	(ACCESSION NUMBER)	(THRU)
	163	23
	(PAGES)	(CODE)
	CR 123554	07
	(NASA CR OR TMX OR AD NUMBER)	(CATEGORY)

Reproduced by
NATIONAL TECHNICAL
INFORMATION SERVICE
U S Department of Commerce
Springfield VA 22151

GEORGIA INSTITUTE OF TECHNOLOGY
Engineering Experiment Station
Atlanta, Georgia

TECHNICAL REPORT NO. 9

PROJECT A-852

COMMUNICATION SYSTEM MODELING

By

L. D. Holland, J. R. Walsh and R. D. Wetherington

19 November 1971

Prepared for

NATIONAL AERONAUTICS AND SPACE ADMINISTRATION
GEORGE C. MARSHALL SPACE FLIGHT CENTER
MARSHALL SPACE FLIGHT CENTER, ALABAMA

ABSTRACT

This report presents the results of work on communications systems modeling and covers three different areas of modeling. The first of these deals with the modeling of signals in communication systems in the frequency domain and the calculation of spectra for various modulations. These techniques are applied in determining the frequency spectra produced by a unified carrier system, the down-link portion of the Command and Communications System (CCS).

The second modeling area covers the modeling of portions of a communication system on a block basis. A detailed analysis and modeling effort based on control theory is presented along with its application to modeling of the automatic frequency control system of an FM transmitter. Both linear and nonlinear models for the system are developed.

A third topic discussed is a method for approximate modeling of stiff systems using state variable techniques. Such systems are characterized by having one or more very fast time constants along with much slower time constants. A technique for removing "fast" roots associated with fast time constants from the state equations characterizing a linear system is described, and an example presented.

A number of the computer routines developed and used in the above efforts are listed in the report Appendices.

PRECEDING PAGE BLANK NOT FILMED

TABLE OF CONTENTS

	<u>PAGE</u>
ABSTRACT	iii
I. INTRODUCTION	1
II. SOME SPECIAL CONSIDERATIONS IN MODELING UNIFIED CARRIER SYSTEMS	3
A. Introduction	3
B. The CCS Down-Link Configuration of Interest	4
C. Theoretical Considerations and Computer Programs	5
1. Baseband Spectral Calculations	5
2. Radio Frequency Spectral Calculations	7
3. Filter Transfer Functions	8
D. Discussion of Binary PCM Baseband Systems	15
E. Examples of Some Calculations and Experimental Measurements for a Proposed use of a Unified Carried System	20
F. Conclusions	30
III. AUTOMATIC FREQUENCY CONTROL SYSTEM ANALYSIS AND SIMULATION	37
A. Introduction	37
B. System Description	38
1. Direct FM Transmitters	38
2. AFC Loop	41
C. Math Models	42
1. Subsystem Models	42
2. AFC Loop Model	48
D. Linear System Analysis	48
1. Closed-Loop Difference Equation	50
2. Stability Regions	53
3. Transient Response Parameters	58
4. Sensitivity Analysis	60
5. Summary of Analysis	64
E. Simulation-Linear	64
1. Development of Simulation Program	64
2. Verification of Linear Simulation	65

TABLE OF CONTENTS (CONTINUED)

	<u>PAGE</u>
F. Simulation - Nonlinear	77
1. Limiter	77
2. Nonlinear VCO	80
3. Limiter and Nonlinear VCO	83
G. An Alternate Sampling System	85
1. Analysis	85
2. Simulation	87
H. Conclusions	89
IV. DETAILED CIRCUIT SIMULATION: STIFF SYSTEMS	93
A. Introduction	93
B. Derivation of Root Removal Technique	94
C. Reconstructing the Original State Vector	99
D. Practical Application: RLC Bandpass Filter	101
E. Complex Pairs of Fast Roots	103
F. Conclusions	108
V. REFERENCES	109
APPENDIX A	111
APPENDIX B	113
APPENDIX C	115
APPENDIX D	117
APPENDIX E	121
APPENDIX F	129
APPENDIX G	135
APPENDIX H	143
APPENDIX I	151

LIST OF FIGURES

	<u>PAGE</u>
1. CCS telemetry bandpass filter	9
2. Equivalent representations of the CCS telemetry filter . .	11
3. Amplitude and phase response of CCS telemetry bandpass filter	14
4. Experimentally determined amplitude response of the CCS bandpass telemetry filter	16
5. Time waveform into the low-pass RC sections and the CCS telemetry filter	17
6. Baseband frequency spectrum of the signal of Figure 5	18
7. Output time waveform of two RC low-pass filters and the CCS telemetry filter for the input time waveform shown in Figure 5	19
8. Block diagram of the test set-up	23
9. Time waveform for biphase modulated subcarrier signal and biphase PCM signal with a pattern of all ones or all zeros. Amplitude relationships for $\beta_{sc} = 1.0$, $\beta_{pcm} = 0.7$	24
10. Frequency spectrum of time waveform shown in Figure 9	25
11. Low-passed time waveform of Figure 9. Filter is a two-section RC low-pass with $f_c = 1$ MHz	26
12. Frequency spectrum of the time waveform shown in Figure 11	27
13. Baseband spectra of modulating signals. Amplitude relationships for modulation indices of $\beta_{sc} = 1.0$ and $\beta_{pcm} = 0.7$	28
14. Time waveform for biphase modulated subcarrier signal and PCM signal with a random pattern of bits. Ampli- tude relationship for $\beta_{sc} = 1.0$ and $\beta_{pcm} = 0.7$	29
15. Frequency spectrum for time waveform shown in Figure 14 .	31
16. S-band spectrum of a biphase modulated telemetry sub- carrier only, $\beta = 1.0$. No low-pass simulation of modulator characteristic	32

LIST OF FIGURES (CONTINUED)

	<u>PAGE</u>
17. S-band spectrum of a biphase modulated telemetry subcarrier, $\beta = 1.0$, and Manchester PCM signal consisting of all ones or zeros, $\beta = 0.7$, no low-pass simulation of phase modulator characteristics	33
18. S-band spectra, $\beta_{sc} = 1.0$, $\beta_{pcm} = 0.7$	34
19. Baseband signal spectra at output of 1024 kHz Generalized Concept Receiver telemetry bandpass filter, $\beta_{sc} = 1.0$, and $\beta_{pcm} = 0.7$	35
20. Block diagram of FM transmitter	39
21. Block diagram showing AFC details	40
22. Typical VCO characteristics	43
23. Linearized VCO model	44
24. Discriminator model	45
25. Error feedback sampling model	47
26. AFC loop model	49
27. Stability regions for linear AFC system	56
28. Transient responses of linear AFC system for various loop gains	57
29. AFC system approximate time constant	66
30. Steady-state frequency error	67
31. Step response of the VCO frequency in a sampling AFC loop for various values of loop gain in the linear simulation	69
32. AFC loop simulation response with limiter set at 12 volts	79
33. VCO characteristic (exaggerated)	81
34. AFC simulation transient response with nonlinear VCO	82
35. AFC simulation transient response with nonlinear VCO and with ± 12 volt limiter	84
36. Alternate Sampler Model	86
37. Alternate sampler AFC simulation transient response with nonlinear VCO and with ± 12 volt limiter	90
38. Transient response of the CCS telemetry bandpass filter obtained by using state variable techniques	107

LIST OF TABLES

	<u>PAGE</u>
I. TRANSIENT RESPONSES OF LINEAR AFC SYSTEM	54
II. COMPARISON OF THEORETICAL AND SIMULATED FREQUENCY ERRORS	68
III. COMPARISON OF THEORETICAL AND SIMULATED TIME CONSTANTS . .	76
IV. STAEADY STATE FREQUENCY ERRORS WITH NONLINEAR VCO AND LIMITER IN THE AFC SYSTEM	83
V. COMPARISON OF AFC EFFECTIVE TIME CONSTANTS OF TWO SAMPLING SCHEMES FOR $R = 20,000$ OHMS, $C = 1 \times 10^{-7}$ FARADS, AND $t_o = 1.5 \times 10^{-6}$ SECONDS	88
VI. PHYSICAL INTERPRETATION OF THE BANDPASS FILTER STATE VARIABLES	102
VII. NON-ZERO ELEMENTS OF STATE AND CONTROL DISTRIBUTION MATRICES FOR BANDPASS FILTER SHOWN IN FIGURES 1 AND 2 . .	104
VIII. EIGENVALUES OF THE BANDPASS FILTER A-MATRIX	106

I. INTRODUCTION

This report presents the results of a portion of the technical program conducted under Contract NAS8-20054, and covers three different areas of communication system modeling. These are: (1) the modeling of signals in communication systems in the frequency domain and the calculation of spectra for various modulations, (2) the modeling of portions of a communication system on a block basis using control theory techniques, and (3) a technique for approximate modeling of a "stiff" linear system that can reduce the solution time significantly and still produce acceptable estimates of the system response.

Section II presents results of work in signal modeling and calculation of spectra, in particular, determination of frequency spectra produced by a unified carrier system, the down-link portion of the Command and Communications System (CCS). Both calculated spectra and experimentally measured spectra are presented for comparison. Also discussed is a technique for modeling the transfer function of filters.

Section III describes a detailed analysis and modeling effort based on control theory and its application to modeling of the automatic frequency control system of an FM transmitter. The modeling was done on a block basis and both linear and nonlinear models for the system are developed. The linear model was verified with an analytic solution; nonlinear effects were introduced one at a time by remodeling a single block. The models were used to investigate various AFC characteristics, such as stability, transient time, and frequency sensitivity. Results of these investigations are presented.

Section IV discusses the method for approximate modeling of stiff systems using state variable techniques. Such systems are characterized by having one or more very fast time constants along with much slower time constants. Straightforward digital simulation of such systems is generally unsatisfactory in that excessive

round-off errors occur. A technique for removing "fast" roots associated with fast time constants from the state equations is described, and an example presented.

Since the three sections deal with three different topics which are not closely related, the conclusions applicable to each effort are included in each individual section.

A number of the computer routines developed and used in the above efforts are listed in the Appendices. All of the programs are written in FORTRAN-V for use on a UNIVAC-1108 computer.

II. SOME SPECIAL CONSIDERATIONS IN MODELING UNIFIED CARRIER SYSTEMS

A. Introduction

An investigation was made of the spectra of both baseband and RF signals in the CCS transponder when the modulating signals are a PCM data stream, a biphasic modulated telemetry subcarrier, or both. The specific objective of the investigation was to develop techniques applicable to unified carrier systems which would permit ready determination of the effects on radiated spectra of such factors as number and types of modulating signals, modulation indices, and baseband filtering of signals. The work included modeling of various signals, modeling of filter transfer functions, and automating procedures for calculating and plotting spectra. During the course of the work one particular application was made; evaluation of the effect on the operation of the CCS transponder of replacing the PN range code on the down-link with a wide band data signal. This task was performed on a quick-response basis and has been previously reported [1]. This report covers the particular areas investigated and the techniques developed on a more general basis. Recommendations are included on additional tasks that need to be carried out.

Particular aspects of the CCS have been investigated in two previous studies. The work reported here makes use of techniques developed on these programs. These include mathematical derivation of expressions for certain baseband and RF spectra, development of computer programs for computing the spectra, automated plot routines for constructing graphs of spectra and of time waveforms from computed results, and an efficient mechanization of the fast Fourier transform (FFT). For detailed discussions of these developments, reference should be made to the reports of these studies [2,3]. Some of the more pertinent points applicable to this study are reviewed briefly in the following sections.

B. The CCS Down-Link Configuration of Interest

The CCS is a unified carrier system which combines the functions of command, communication, and ranging on a single S-band carrier for each direction of transmission [4]. The up-link portion of the system usually carries both command and ranging signals and was the subject of an earlier study [2]. The modulation applied to the down-link is more complex. The transponder aboard the spacecraft demodulates the up-link signal and re-modulates it onto the down-link. In addition, a biphase modulated 1024 kHz telemetry subcarrier is also modulated onto the down-link. The down-link portion of the system was also investigated in a previous study [3]. More detailed discussions of the system and its characteristics are given in the reports on these earlier efforts [2,3].

In the CCS transponder, the telemetry subcarrier is normally biphase modulated by data at a rate of 72 kilobits per second. In the study reported here a data rate of 27.5 kilobits per second was assumed to correspond to a proposed use of the transponder. Also this study does not consider an actual turned-around up-link signal, but substitutes a PCM signal having approximately the same clock rate as the range code in lieu thereof. Thus for purposes of this study, the signals applied to the S-band modulator of the down link consisted of (1) a PCM signal replacing the turned-around up-link signal, and (2) a 1024 kHz subcarrier which was biphase modulated with a data rate of 27.5 kilobits per second. Of special interest in this study were the time waveforms and spectra of the original baseband signals, the transfer function of various filters, time waveforms and spectra of the filtered baseband signals, and the S-band spectra produced by these signals.

The techniques developed here should be useful in the general area of communication system modeling and evaluation.

C. Theoretical Considerations and Computer Programs

This section presents a brief discussion of the theoretical basis for calculating frequency spectra and time waveforms. In addition, the calculation of selected filter transfer functions is discussed. Computer programs developed for the calculations are also discussed, and listings of these programs are included in the Appendix. For more detailed discussion of the spectral calculation techniques, see Technical Reports Nos. 3 and 7 [2,3].

1. Baseband Spectral Calculations

The input signal considered was a time waveform representing the PCM signal, the modulated telemetry subcarrier, or their sum. The input signal is evaluated at equally spaced time intervals which gives the sampled version of the signal as a real-time function. The baseband frequency spectrum of the time waveform for the continuous signal case is given by

$$x(f) = \int_{-\infty}^{\infty} x(t)e^{-2\pi jft} dt \quad (1)$$

where $x(f)$ is the frequency domain representation, and $x(t)$ is the time domain representation. For a sampled signal the discrete Fourier transform (DFT) must be used. An efficient means of computing the discrete Fourier transform (DFT) is provided by the FFT. The mechanization of the FFT used in these investigations is described in Appendix C of Technical Report No. 7 [3]. The frequency domain representation, A_r , of the samples, X_k , of the time waveform is given by

$$A_r = \frac{1}{N} \sum_{k=0}^{n-1} X_k e^{-\frac{2\pi jrk}{N}} \quad (2)$$

$$= \frac{1}{N} \sum_{k=0}^{n-1} X_k W^{-rk}, \quad r = 0, 1, \dots, n-1, \text{ and} \quad (3)$$

$W^{-rk} = \left[e^{\frac{2\pi i}{N}} \right]^{-rk}$ is the phase function of the DFT. Index "r" is referred to as the frequency of the transform component. The transform provides the spectral components, A_r , corresponding to the series of time samples, X_k . The inverse transform is obtained in a similar manner with the elimination of the $1/N$ term in front of the summation and by use of a positive sign in the exponential.

The continuous signal representation of a filter transfer function is given by

$$H(j\omega) = A(\omega)e^{j\theta(\omega)} = a + jb \quad (4)$$

where $A(\omega)$ is the amplitude response of the filter and $\theta(\omega)$ is the phase function. The latter is given by

$$\theta(\omega) = \tan^{-1} \left[\frac{b}{a} \right] \quad (5)$$

where a and b are the real and imaginary parts of $H(j\omega)$.

For the continuous case the filtered time function, $g(t)$, may be obtained from the inverse transform of the product of $H(j\omega)$ and $F(j\omega)$ as

$$g(t) = \int_{-\infty}^{\infty} H(j\omega) \cdot F(j\omega) e^{j\omega t} d\omega \quad (6)$$

For the discrete case, the filtered time function is given by

$$C(k) = \sum_{i=0}^{n-1} [G(i) \cdot H(i)] W^{ik} \quad (7)$$

where $C(k)$ is the sampled output time function, $G(i)$ is the transform of the sampled input time function, and $H(i)$ is the transform of the filter impulse response. W^{ik} is the Fourier transform phase function.

This procedure is easily mechanized for computation. The filtered time function can be generated by transforming the sampled time function to the frequency domain, evaluating the filter transfer function at these transform frequencies, producing the product of the transform frequency component with the value of the transfer function (in general both complex numbers), and retransforming the result to the time domain.

2. Radio Frequency Spectral Calculations

The time waveform representing a phase modulated carrier such as that present in the CCS can be expressed as

$$e_{pm}(t) = \frac{A}{2} \left[e^{j\omega_c t + j\beta\psi(t)} + e^{-j\omega_c t - j\beta\psi(t)} \right] \quad (8)$$

where

- A = the carrier peak amplitude,
- ω_c = the carrier radian frequency,
- β = the phase modulation index, and
- $\psi(t)$ = the modulation time function.

The two terms in brackets in Equation (8) represent the positive and negative frequency components of the modulated carrier, respectively. The carrier frequency in the CCS is high enough so that only the positive frequency terms need to be considered. Also, since only relative magnitudes are of interest in the spectral calculations, the time function representing the modulated carrier can be considered to be

$$e'_{pm}(t) = e^{j\omega_c t + j\beta\psi(t)} \quad (9)$$

The Fourier transform of the modulated carrier signal is

$$E'(\omega) = \delta(\omega - \omega_c) * F(\omega) \quad (10)$$

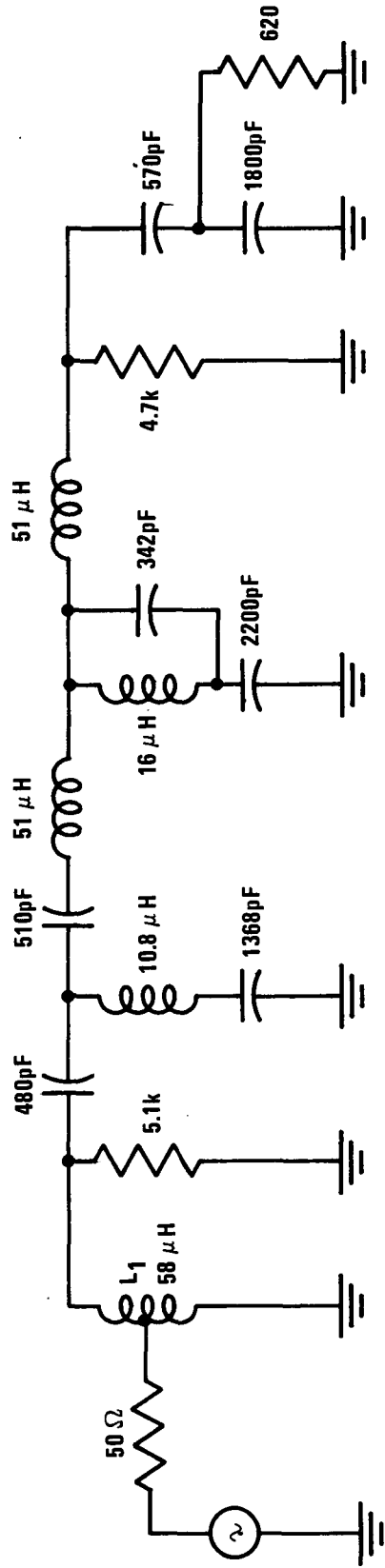
where $\delta(\omega - \omega_c)$ represents a delta function at the carrier frequency, the symbol "*" denotes convolution, and $F(\omega) = \mathcal{F}(e^{j\beta\psi(t)})$. The Fourier transform, $F(\omega)$, of the modulating signal can be obtained by evaluating the exponential function by knowing the modulation indices and the values of the time function. Evaluating this exponential function and taking the FFT of the result yields the radio frequency spectrum. (Subroutine FOFT which evaluates $e^{j\beta\psi(t)}$ is given in Appendix A.)

3. Filter Transfer Functions

Several filter transfer functions were modeled for the wideband PCM data down-link studies. Two representations of filter transfer functions were used. One of these expresses the filter transfer characteristics as a function of the ratio of the frequency at which the transfer function is to be evaluated to the filter cutoff frequency (3 dB point). For this representation, component values of the filter are not required to evaluate the transfer function -- only the cutoff frequency of the filter need be considered. This method of generating the transfer function was used in modeling a RC low-pass filter and is discussed in Technical Report No. 7 [3].

The other representation of a transfer function considers the actual component values of the filter. The loop equation of the filters are written and solved in determinate form. Examples of the application of this technique to several filters are also discussed in Technical Report No. 7 [3]. The application of this technique to the 1024 kHz bandpass telemetry filter in the Generalized Concept Receiver will be discussed here. This filter has a transformer coupled stage and presents a good example for demonstrating computer modeling of a representative filter.

The schematic diagram of the telemetry bandpass filter is shown in Figure 1. The equivalent circuit of the filter in which the input transformer is replaced by a "T" network is shown in



BANDPASS FILTER

Figure 1. CCS telemetry bandpass filter.

Figure 2a. The equivalent network of Figure 2b is used for writing the loop equations. Each impedance shown in Figure 2b was represented by its appropriate combination of circuit elements as shown in Figure 2a. The various impedances are

$$Z_{11} = R_{11} + j\omega L_{11} ,$$

$$Z_{12} = j\omega L_{12} ,$$

$$Z_{13} = R_{13} + j\omega L_{13} ,$$

$$Z_2 = \frac{R_2}{1 + j\omega R_2 C_{22}} ,$$

$$Z_3 = -\frac{1}{\omega C_1} ,$$

$$Z_4 = R_4 + j\left(\omega L_2 - \frac{1}{\omega C_2}\right) ,$$

$$Z_5 = \frac{R_5 + j\omega L_3}{1 - \omega^2 L_3 C_{33} + j\omega R_5 C_{33}} - \frac{j}{\omega C_3} ,$$

$$Z_6 = \frac{R_6 + j\omega L_4}{1 - \omega^2 L_4 C_{44} + j\omega R_6 C_{44}} - j\frac{1}{\omega C_4} ,$$

$$Z_7 = \frac{R_7 + j\omega L_5}{1 - \omega^2 L_5 C_{55} + j\omega R_7 C_{55}} ,$$

$$Z_8 = R_3 ,$$

$$Z_9 = -\frac{j}{\omega C_6} , \text{ and}$$

$$Z_{10} = \frac{R_L}{1 + j\omega R_L C_7} . \tag{11}$$

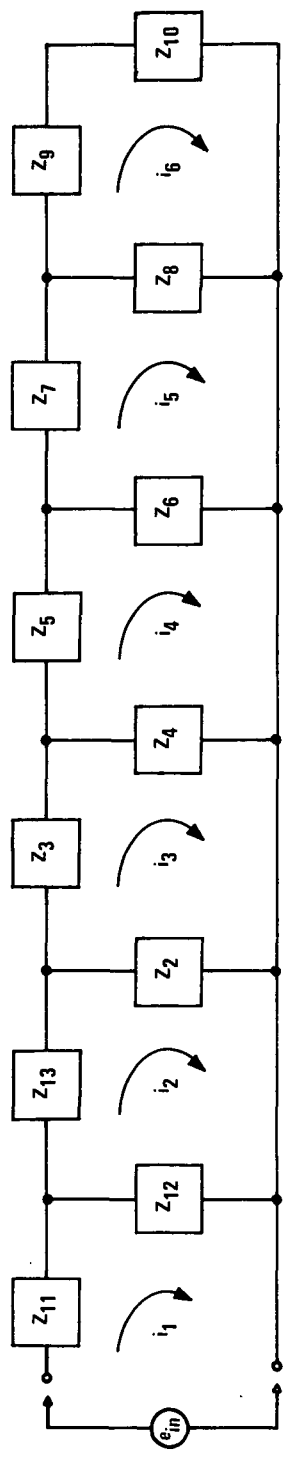
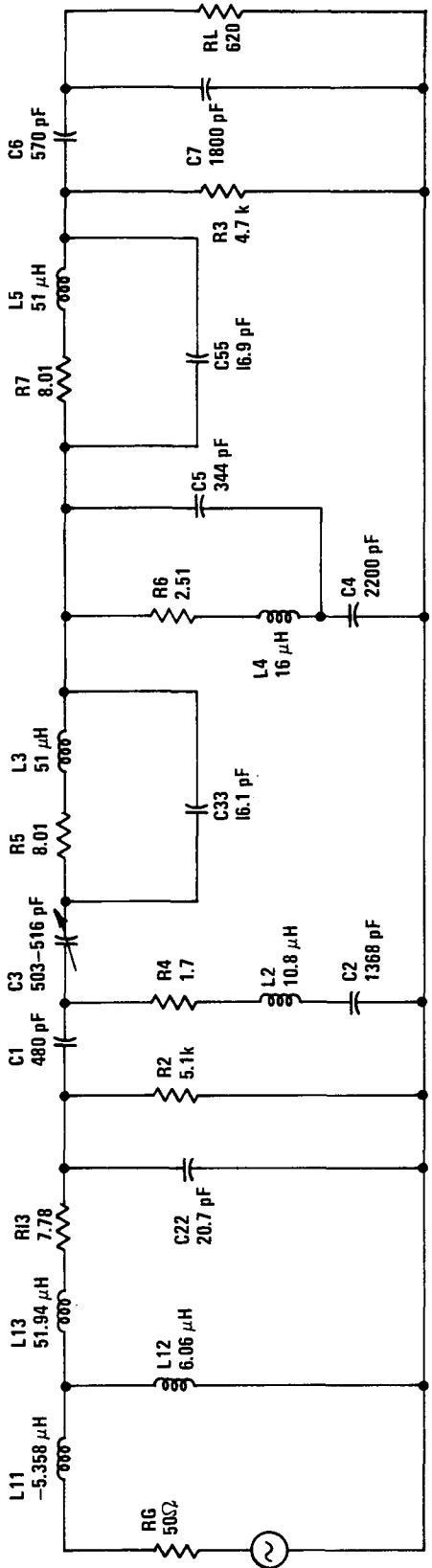


Figure 2. Equivalent representations of the CCS telemetry filter.

Writing the loop equations and solving for the transfer function gives

$$H = \frac{Z_N}{Z_{DD}} , \quad (12)$$

where $Z_N = Z_{12} Z_2 Z_4 Z_6 Z_8 Z_{10} ,$

$$Z_{DD} = Z_F (-Z_{D1} - Z_{D2} + Z_{D3} + Z_{D4} - Z_{D5}) \\ + Z_{D6} (-Z_{D7} + Z_{D8} + Z_{D9}) ,$$

and $Z_{A1} = Z_{11} + Z_{12} ,$

$$Z_{A2} = Z_{12} + Z_{13} + Z_2 ,$$

$$Z_B = Z_2 + Z_3 + Z_4 ,$$

$$Z_C = Z_4 + Z_5 + Z_6 ,$$

$$Z_D = Z_6 + Z_7 + Z_8 ,$$

$$Z_E = Z_8 + Z_9 + Z_{10} ,$$

$$Z_F = Z_{A1} Z_{A2} - Z_{12}^2 ,$$

$$Z_{D1} = Z_D Z_E Z_4^2 ,$$

$$Z_{D2} = Z_B Z_E Z_6^2 ,$$

$$Z_{D3} = Z_4^2 Z_8^2 ,$$

$$Z_{D4} = Z_B Z_C Z_D Z_E ,$$

$$Z_{D5} = Z_B Z_C Z_8^2 ,$$

$$Z_{D6} = Z_{A1} Z_2^2 ,$$

$$Z_{D7} = Z_C Z_D Z_E ,$$

$$Z_{D8} = Z_C Z_8^2 , \quad \text{and}$$

$$Z_{D9} = Z_E Z_6^2 .$$

(13)

The expressions (11) relating the impedances with numbered subscripts to circuit parameters include resistances (e.g., R11, R13, etc.) which determine the Q of the inductances. The Q used for all inductances had a value of 100. Also included is the self capacitance of the larger inductances. These appear in (11) as the C values with the double subscripts. The self capacitance of the coils was experimentally obtained using the relationship

$$C_S = \frac{C_1 - 4C_2}{3} ,$$

where C_S = self capacitance of the coil,

C_1 = capacitance required to resonate the coil at a frequency f_1 , and

C_2 = capacitance required to resonate the coil at a frequency $f_2 = 2f_1$.

The self capacitance of the coils was determined experimentally from the filter inductances to be

$$C_{11} = 20.7 \text{ pf,}$$

$$C_{22} = 4.27 \text{ pf,}$$

$$C_{33} = 16.07 \text{ pf,}$$

$$C_{44} = 4.1 \text{ pf, and}$$

$$C_{55} = 16.93 \text{ pf.}$$

The self capacitance was included in the circuit only for coils with large inductances for which the self capacitance produced self resonance in the 5 MHz region. The self resonance of the smaller coils was in the region of 20 MHz, well removed from the filter passband.

The telemetry filter transfer function was evaluated using subroutine TLMFLT included in Appendix B. The results of the computations are shown in Figure 3 which displays the normalized amplitude response as well as the phase response. The amplitude

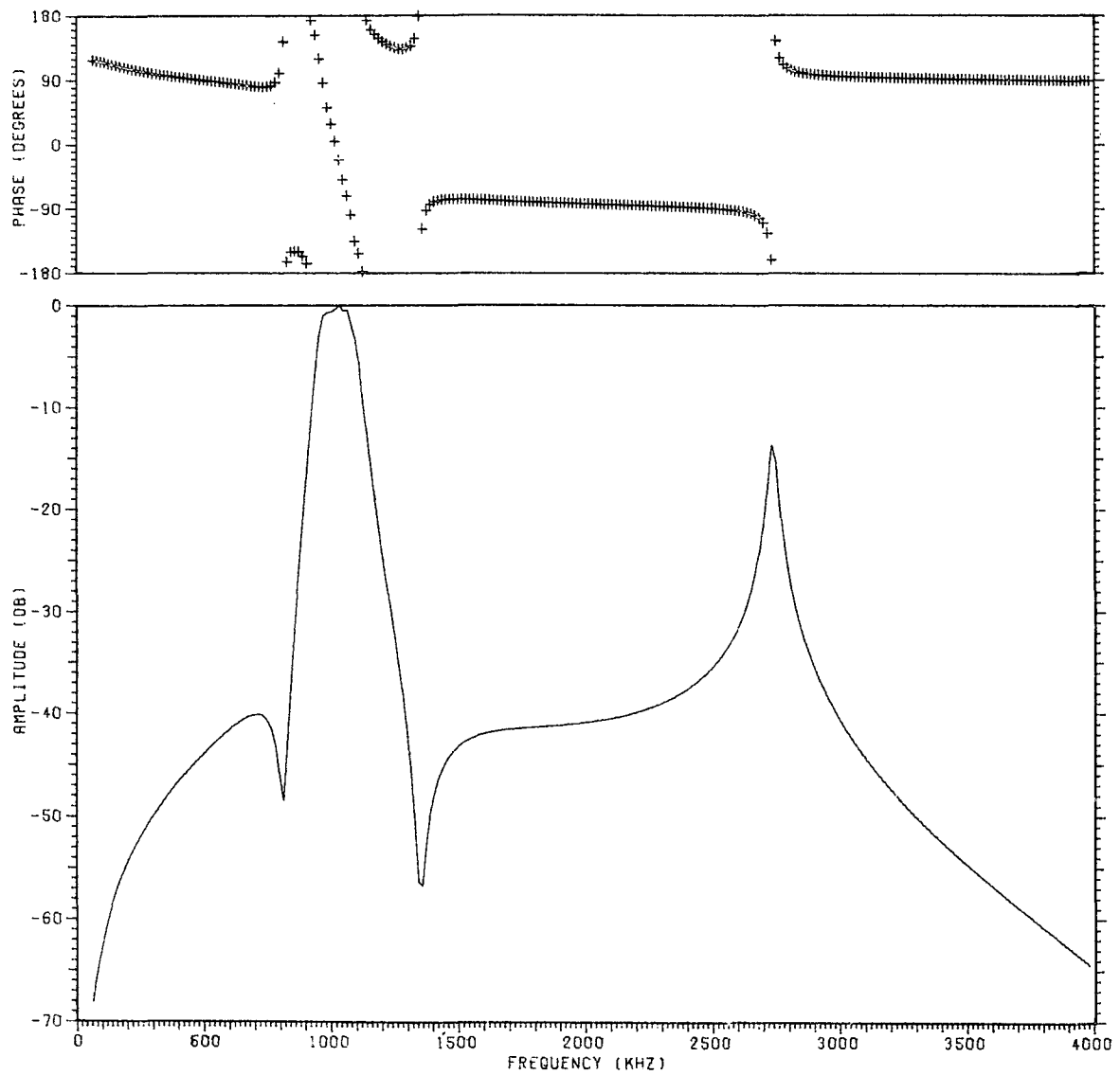


Figure 3. Amplitude and phase response of CCS telemetry bandpass filter.

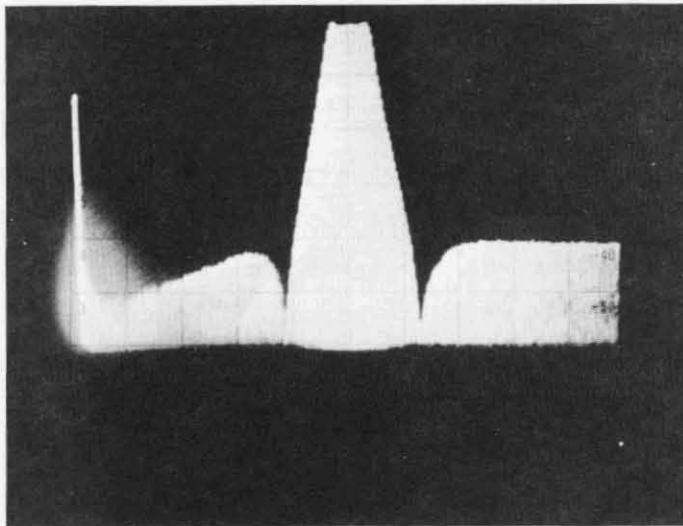
response of the filter obtained in the laboratory is shown in Figure 4. This display of the amplitude response of the filter was obtained using a spectrum analyzer and a constant amplitude signal generator whose frequency was swept very slowly. The response at zero frequency in Figure 4 is the "zero beat" of the spectrum analyzer and does not represent the value of the transfer function of the filter which is zero at this frequency. The calculated response shows good agreement with the experimentally obtained value.

The effect of the telemetry bandpass filter transfer function on the square wave modulated telemetry subcarrier is shown in Figures 5 through 7. Figure 5 shows the computed biphase modulated telemetry subcarrier modulated at the nominal CCS data rate of 72 kilobits per second. Figure 6 shows the frequency spectrum of the signal. The telemetry filter transfer function was then applied to this spectrum and the results retransferred to the time domain. Figure 7 shows the time waveform at the output of the filter.

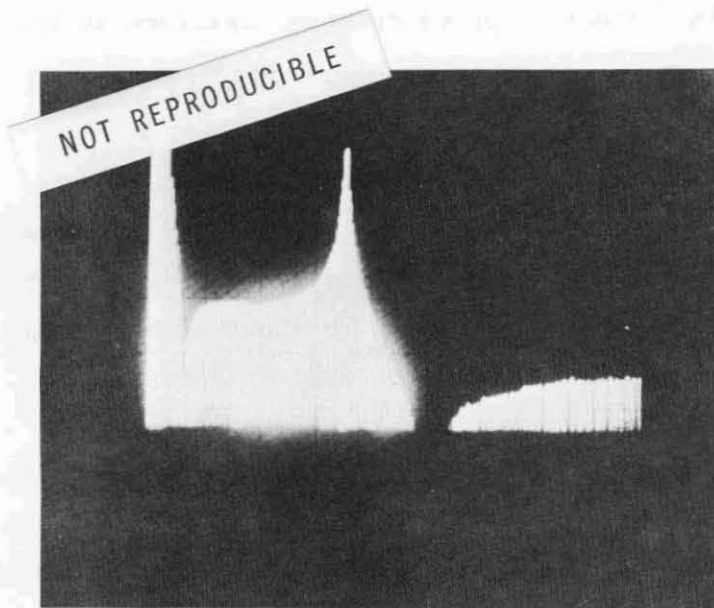
D. Discussion of Binary PCM Baseband Systems

Binary PCM data waveforms can take several forms depending on the method used to indicate a one or a zero. The IRIG telemetry standards specify seven different methods of bit coding. Two common methods of bit coding were considered in this analysis. These are specified in the standards as NRZ-Level, in which a one is represented by one level and a zero by the other, and Biphase-Level, in which a one is represented by a one-zero transition during a bit time and a zero is represented by a zero-one transition during a bit time. NRZ-Level will be referred to here simply as non-return-to-zero (NRZ) and Biphase-Level as return-to-zero (RZ).

For NRZ data having a bit time of one microsecond the bit rate is one megabit per second and the fundamental clock rate is 500 kHz. For RZ data with the same time for each state of the



(a) HORIZONTAL CALIBRATION 200 kHz PER DIVISION.
VERTICAL CALIBRATION 10 dB PER DIVISION.



(b) HORIZONTAL CALIBRATION 0.5 MHz PER DIVISION
STARTING AT 1 MHz.
VERTICAL CALIBRATION 10 dB PER DIVISION.

Figure 4. Experimentally determined amplitude response of the CCS bandpass telemetry filter.

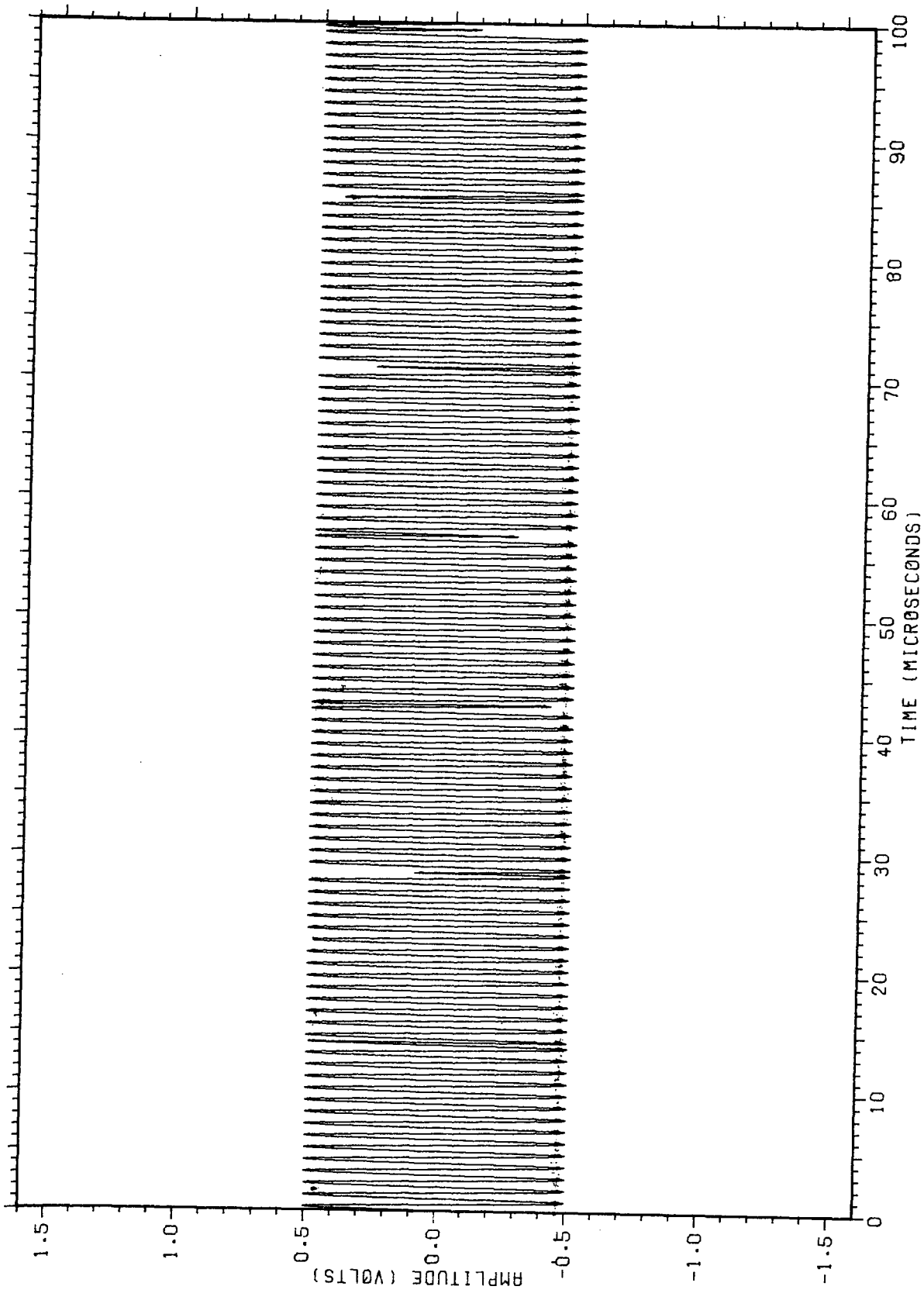


Figure 5. Time waveform into the low-pass RC sections and the CCS telemetry filter.

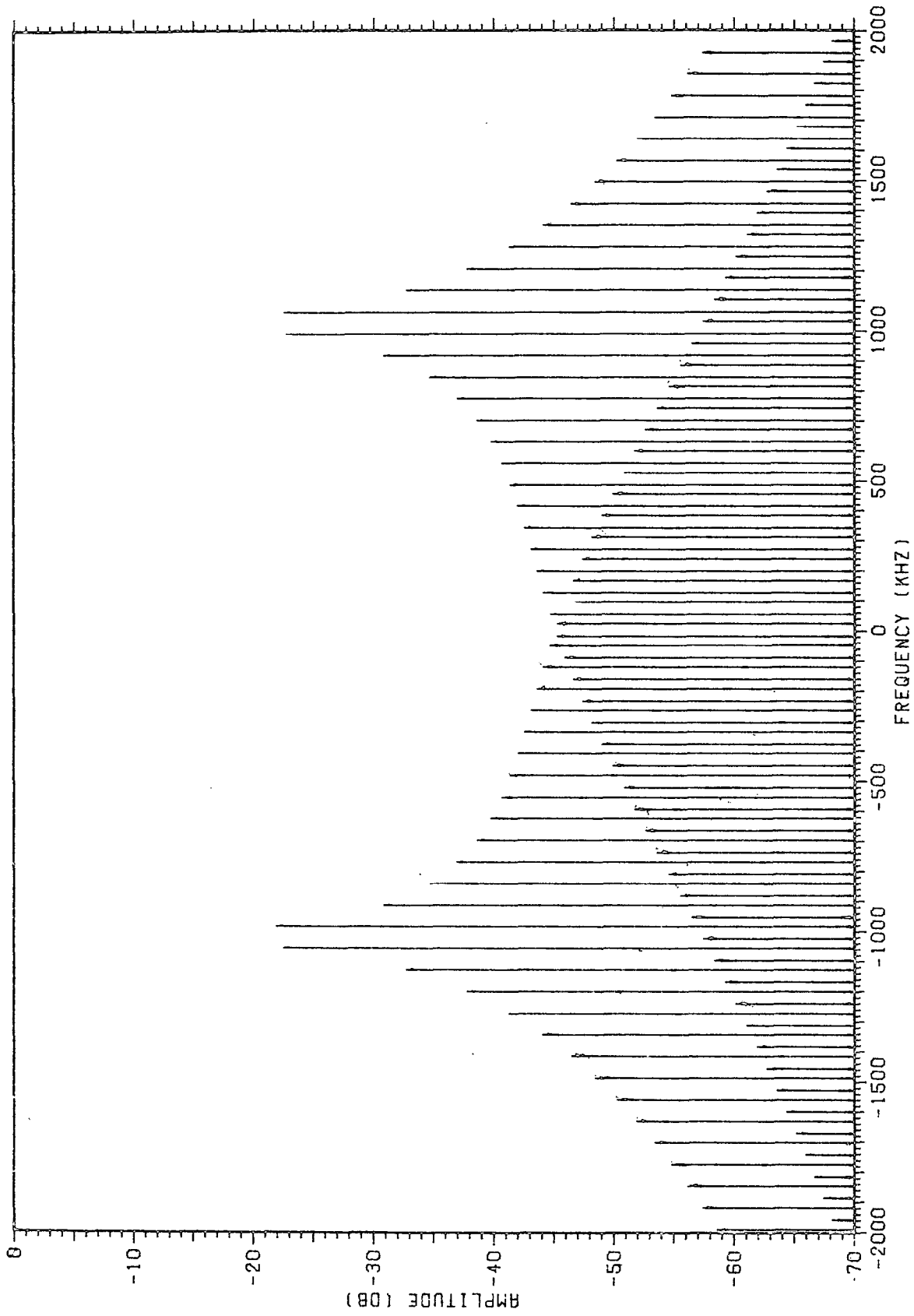


Figure 6. Baseband frequency spectrum of the signal of Figure 5.

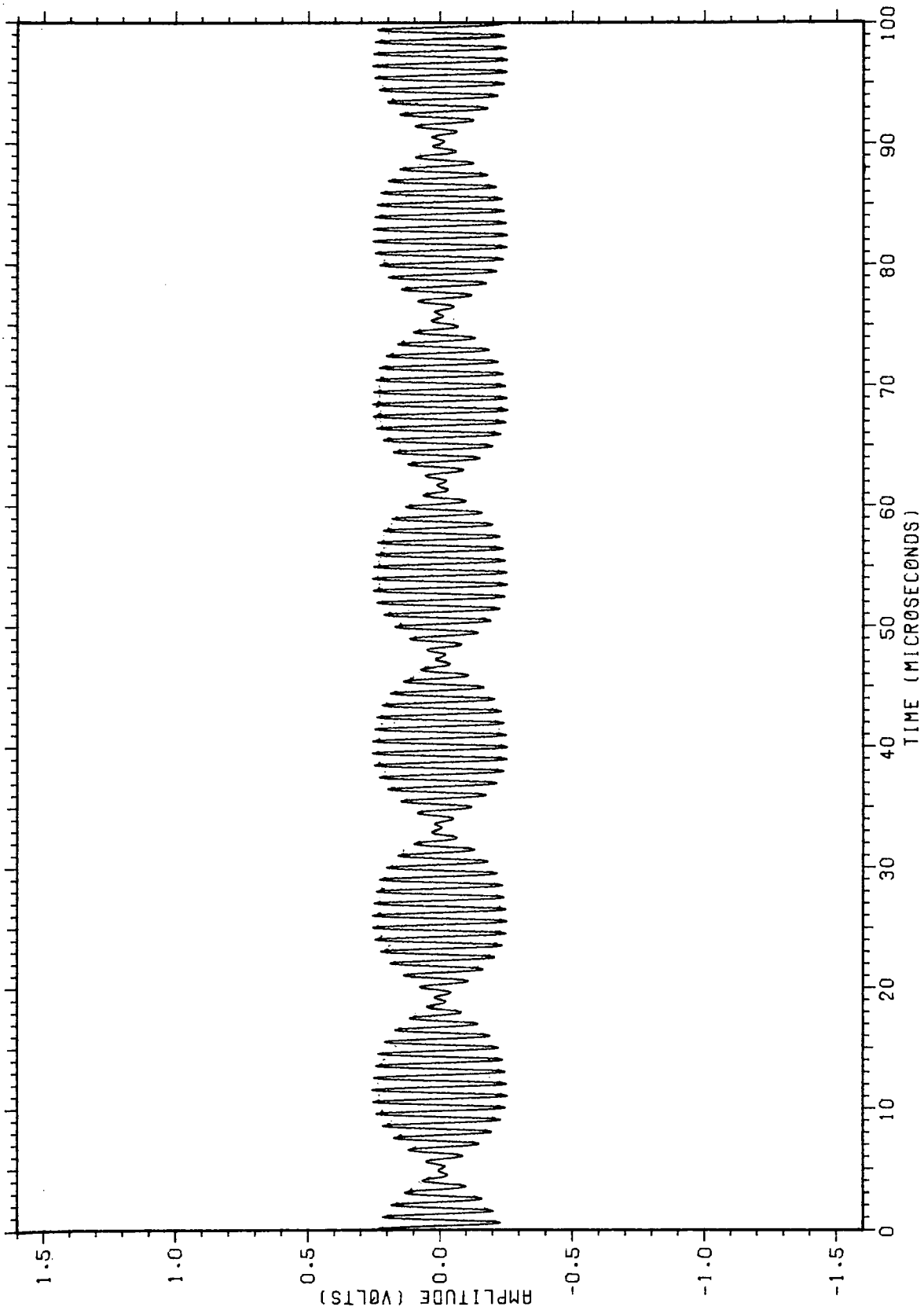


Figure 7. Output time waveform of two RC low-pass filters and the CCS telemetry filter for the input time waveform shown in Figure 5.

signal one bit time would occupy two microseconds and the bit rate would be one half that of the NRZ mode. NRZ data with an alternating string of ones and zeros would have a fundamental frequency of 500 kHz. Similarly, a string of ones or zeros with RZ data would also produce a square wave at 500 kHz. If the data were a perfect square wave passed through a linear filter, harmonic components of the data would exist only at odd harmonics of the data fundamental frequency. For an alternating bit pattern for RZ data the fundamental frequency would be one-half of that for NRZ data and again harmonics would exist at odd harmonics of the fundamental. For strings of ones or zeros in RZ data it would appear as NRZ data with an alternating bit pattern since a transition is forced to occur in each time slot assigned to a bit. Data such as those just discussed would have no detrimental effect on the telemetry system operating in a bandwidth of approximately 150 kHz centered at 1024 kHz. Although NRZ data would provide a higher data rate, RZ data is often preferred because of the additional signal transitions forced into the data leading to better performance of tape recorders and bit synchronizers.

E. Examples of Some Calculations and Experimental Measurements for a Proposed use of a Unified Carrier System

The techniques developed for the time waveform and frequency spectrum modeling of communication systems, such as the CCS down-link, were used for the analysis of the signals involved in a projected use of a unified carrier system such as the CCS. Parts of the results of this investigation were reported earlier in a special technical memorandum which provided, on a quick-look basis, data relative to the problem [1]. Some additions to the data available at that time have been made. This intended use of a unified carrier system provides a good example of the modeling of systems using frequency domain techniques.

The investigation of the spectral content of baseband and radio frequency signals in the CCS transponder down-link for specific baseband signals was of interest.

These signals were a biphasic modulated 1024 kHz telemetry subcarrier signal and a 500 kilobit per second split phase modulated PCM data signal. For the case of interest the modulation on the telemetry subcarrier was nominally a 13.75 kHz square wave simulating NRZ data at a rate of 27.5 kilobits per second. The split phase modulated PCM signal was simulated by a 500 kHz square wave. This simulation represents a continuous string of ones or zeros in the split phase modulated data stream. A bit time in this signal occupies two microseconds. For a split phase signal, a one in the input data stream is represented by a one-to-minus-one transition at the midpoint of the bit interval, while a zero is represented by a minus-one-to-one transition at the midpoint of the bit interval. Thus, a continuous stream of ones or zeros results in a square wave having a period of two microseconds or a frequency of 500 kHz.

Calculation of the spectra of the various signals involved was accomplished using programs developed earlier for CCS spectral studies. To adapt the input signals to the FFT, slight adjustments were made in the frequencies of some of the signals. The biphasic modulating signal frequency was adjusted to be 13.65333 kHz and the wideband PCM signal frequency adjusted to 498.3467 kHz. This made all signals periodic on a period of two cycles of the biphasic subcarrier modulating signal (146.484375 μ sec) with 73 cycles of the PCM signal and 150 cycles of the 1024 kHz subcarrier frequency present during this period. These adjustments were made to avoid some unknowns about the discrete transform when the transform coefficients do not match the frequencies present in the input signal.

Measured spectra were obtained from laboratory measurements for comparison with computed spectra. The modulation indices were set experimentally by determining the peak-to-peak input voltage to the phase modulator of a sine wave signal at either 500 kHz or 1024 kHz required to give the desired index. The

phase modulation index for the two modulating signals was then set by matching the peak-to-peak amplitude of each of the signals to the amplitude of the appropriate sine wave.

The experimental test setup is shown in Figure 8. The telemetry subcarrier portion of the baseband signal was generated by applying the biphasic modulating signal and the telemetry subcarrier signal to the proper inputs of a balanced modulator. The output signal of the balanced modulator is the desired biphasic modulated telemetry subcarrier signal. The 500 kilobit per second data signal was obtained from a pulse generator adjusted to give a 500 kHz square wave signal. These two signals were added in an oscilloscope and the vertical output of the oscilloscope was used as the input to the CCS transponder phase modulator. The amplitudes of the two signals could be adjusted independently by use of the controls on the two channel vertical amplifier of the oscilloscope.

Modulation indices used in the calculated and experimental data were 0.7 radian for the wideband PCM signal (β_{PCM}) and 1.0 radian for the telemetry subcarrier signal (β_{sc}). Figure 9 shows the time waveform of such a modulating signal, and Figure 10 shows its frequency spectrum. Figure 11 shows the same time waveform after filtering through two ideal RC low pass filters having a cutoff frequency of 1 MHz each. The spectrum of the output of the two low-pass sections is shown in Figure 12. This signal serves as the input to the down-link phase modulator.

Experimentally obtained baseband spectra are shown in Figure 13. Figure 13a shows the biphasic modulated subcarrier spectrum for the above example; Figure 13b is that of the wideband PCM signal; and Figure 13c shows the sum of the two spectra.

An example of the time waveform for a random selection of the 73 bits possible in the PCM signal is shown in Figure 14. The selection of the bit pattern was made using a pseudo-random number generator in a Univac 1108 computer. That is, each of the 73 bits of the PCM signal present in the time waveform was

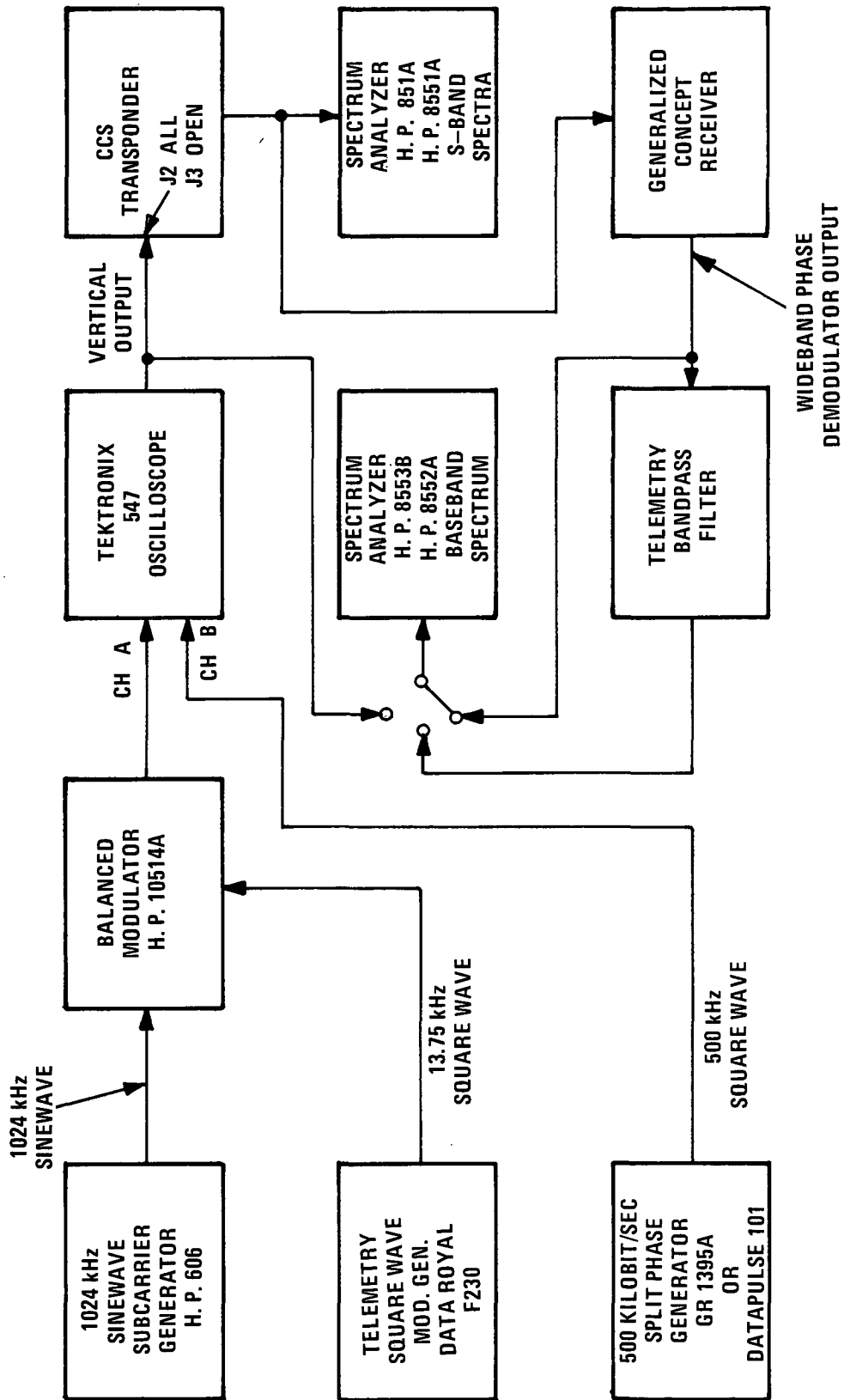


Figure 8. Block diagram of the test set-up.

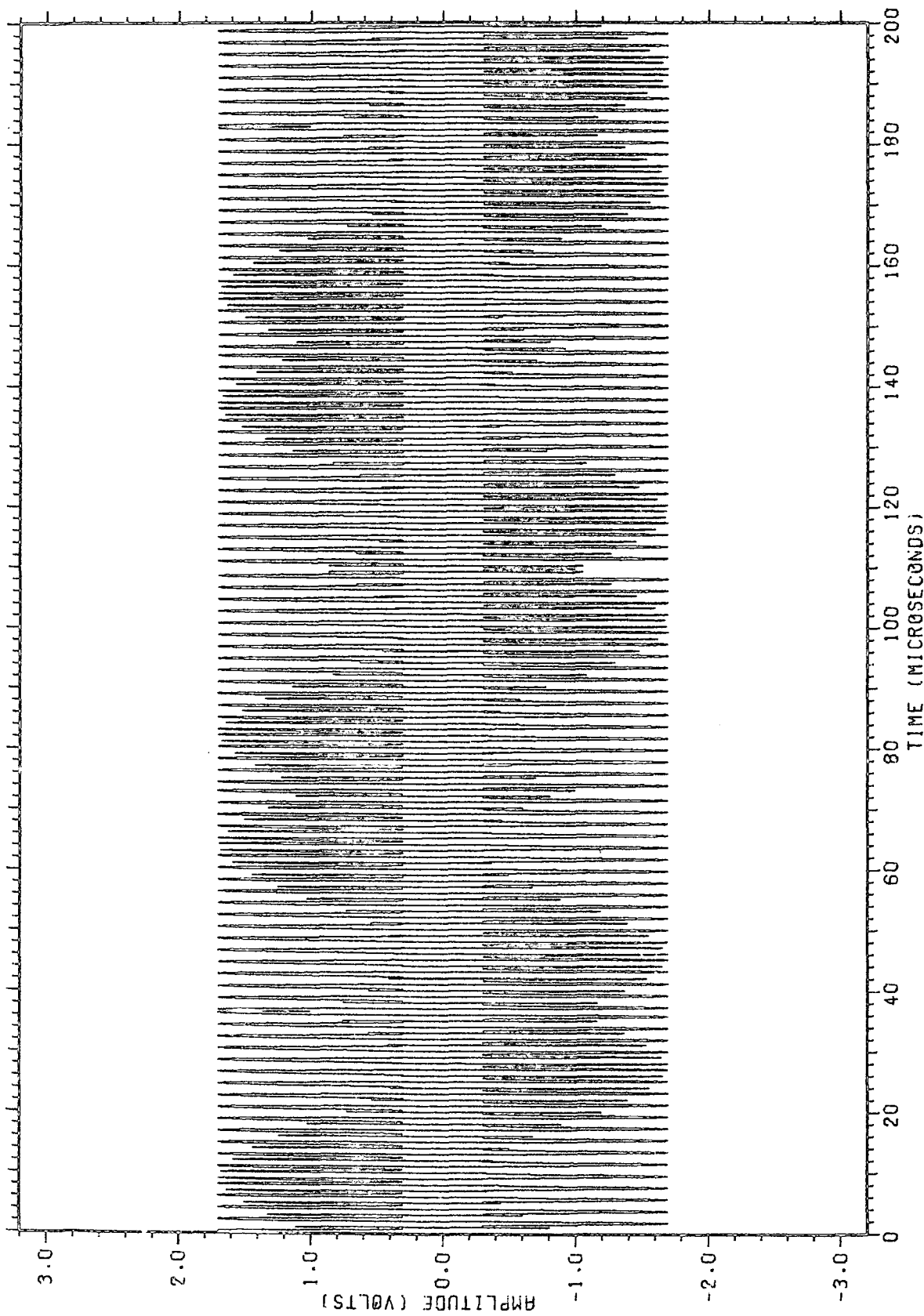


Figure 9. Time waveform for biphase modulated subcarrier signal and biphase PCM signal with a pattern of all ones or all zeros. Amplitude relationships for $\beta_{sc} = 1.0$, $\beta_{pcm} = 0.7$.

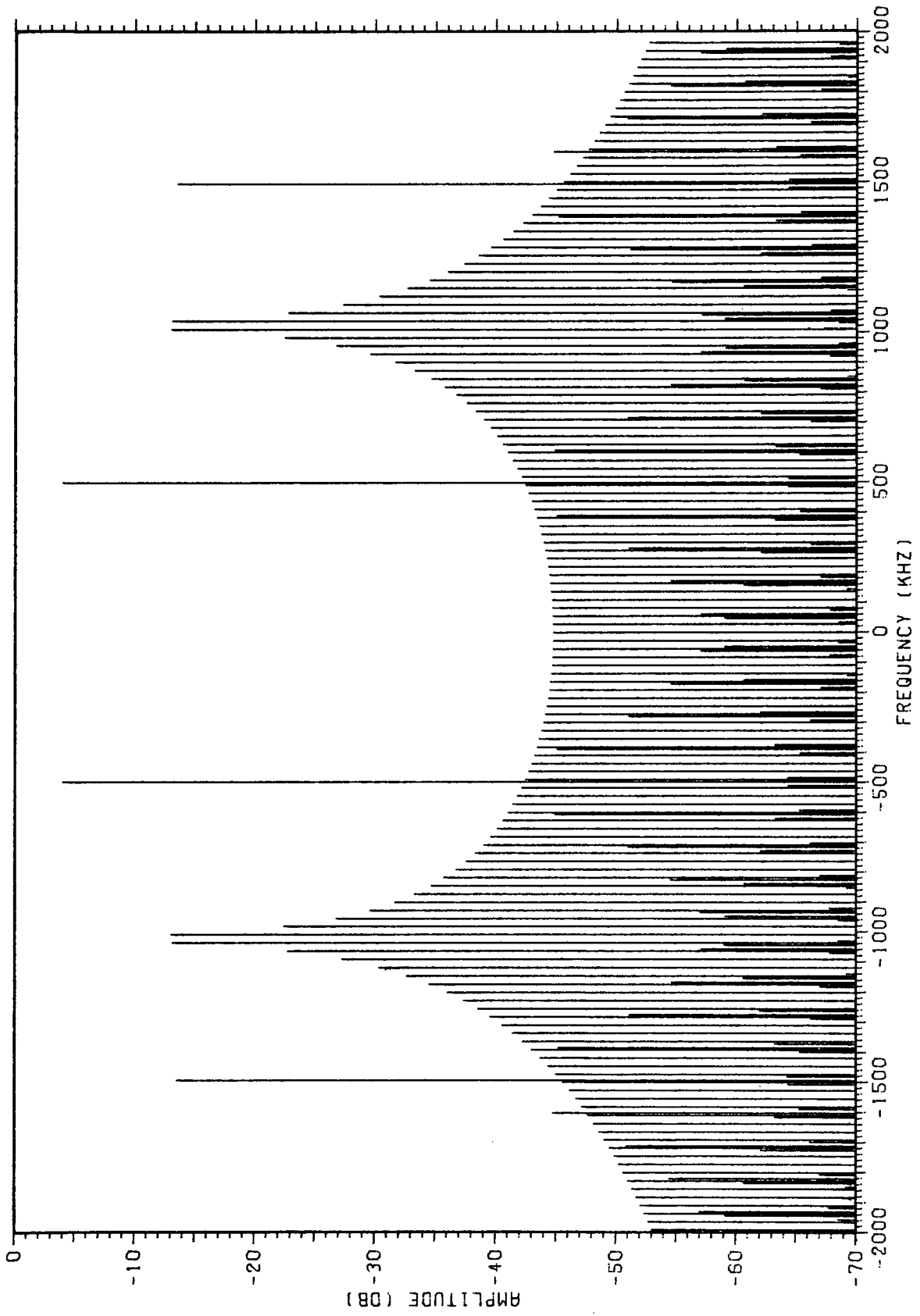


Figure 10. Frequency spectrum of time waveform shown in Figure 9.

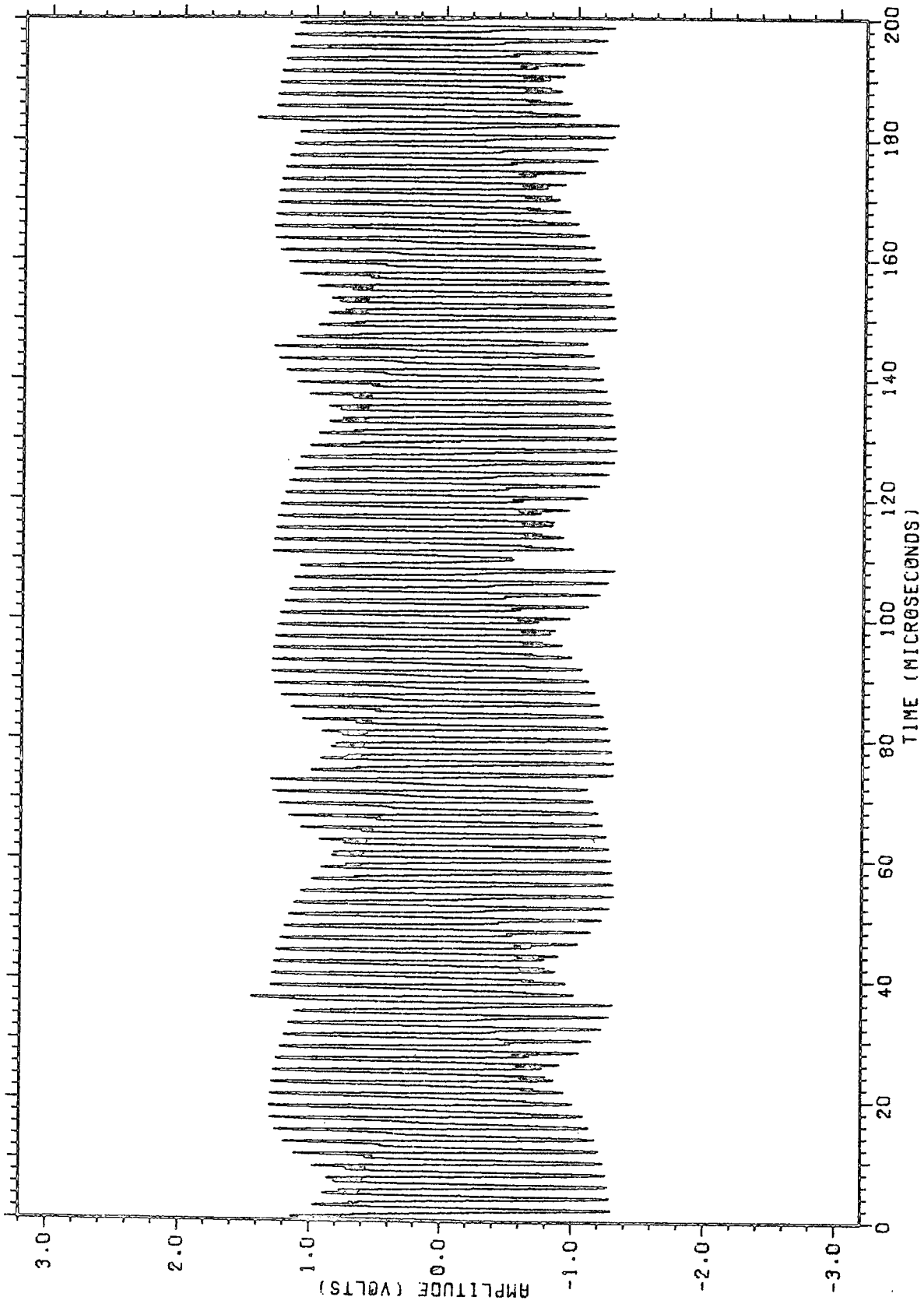


Figure 11. Low-passed time waveform of Figure 9. Filter is a two-section RC low-pass with $f_c = 1$ MHz.

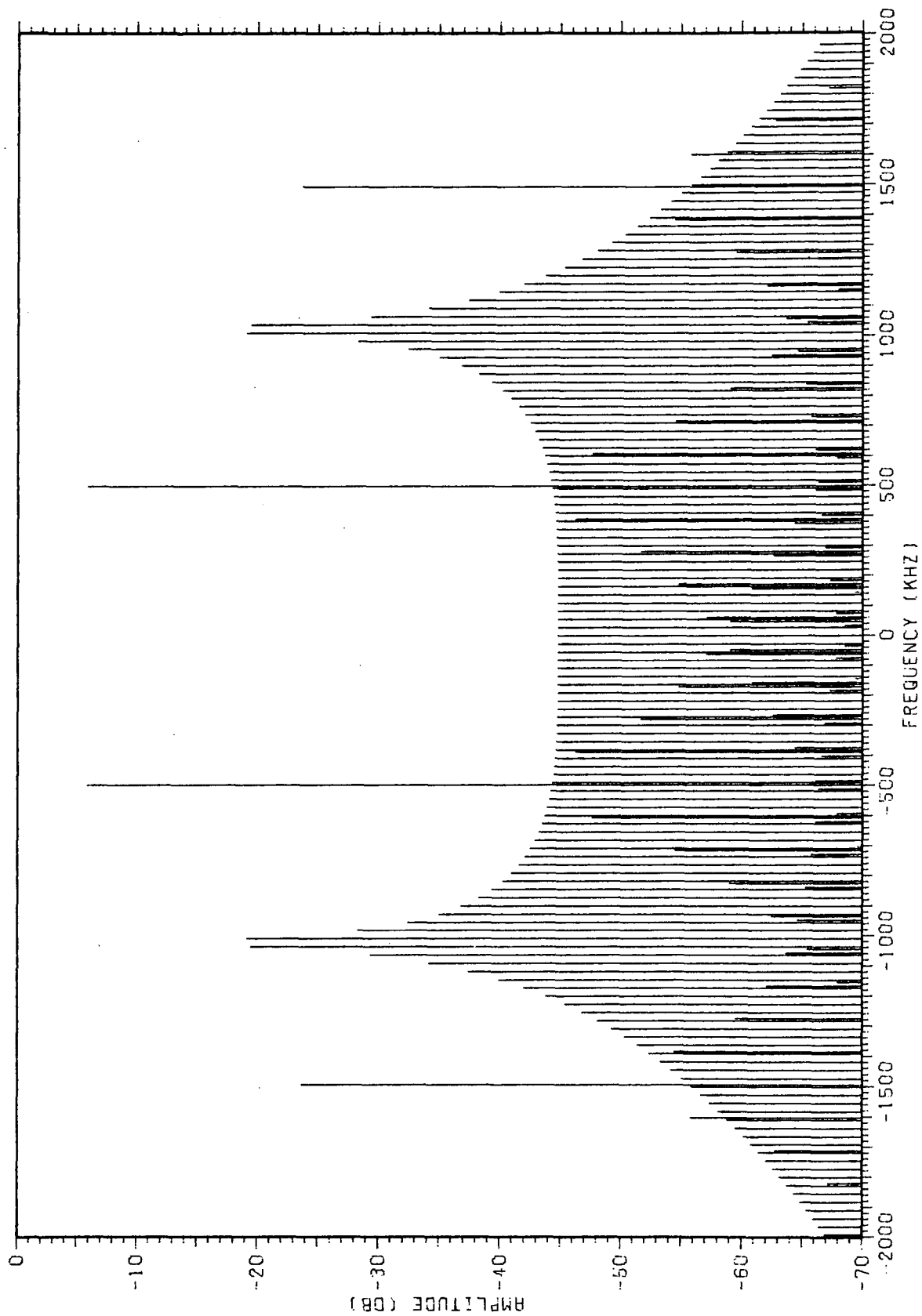
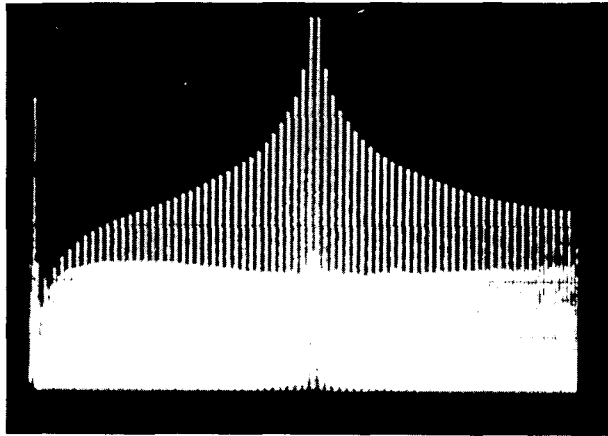


Figure 12. Frequency spectrum of the time waveform shown in Figure 11.

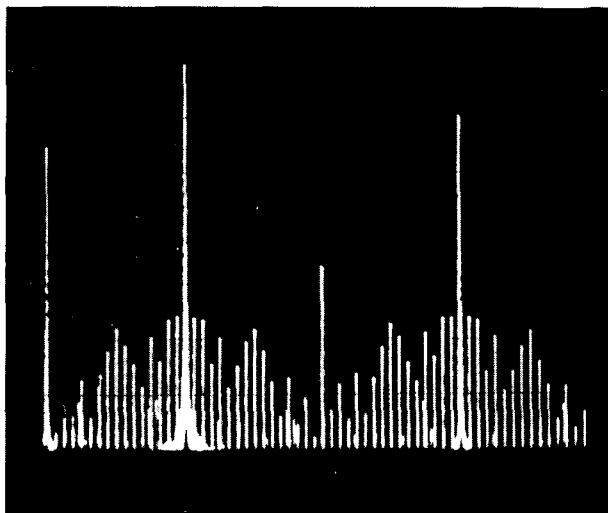
(a) BIPHASE MODULATED (SQUARE WAVE MODULATION) 1024 kHz TELEMETRY SUBCARRIER.

VERTICAL 10 dB/DIV.
HORIZONTAL 200 kHz/DIV.



(b) 500 KILOBIT/SEC SPLIT PHASE SIGNAL CONSISTING OF ALL ONES OR ZEROS. (SIMULATED BY A 500 kHz SQUARE WAVE.)

NOTE: Sidebands around square wave fundamental and 3rd harmonic frequencies were found to be produced by the square wave signal generator.



(c) BOTH SIGNALS PRESENT.

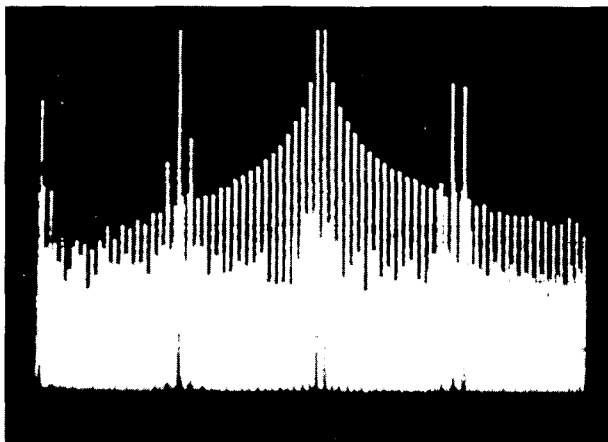


Figure 13. Baseband spectra of modulating signals. Amplitude relationships for modulation indices of $\beta_{sc} = 1.0$ and $\beta_{pcm} = 0.7$.

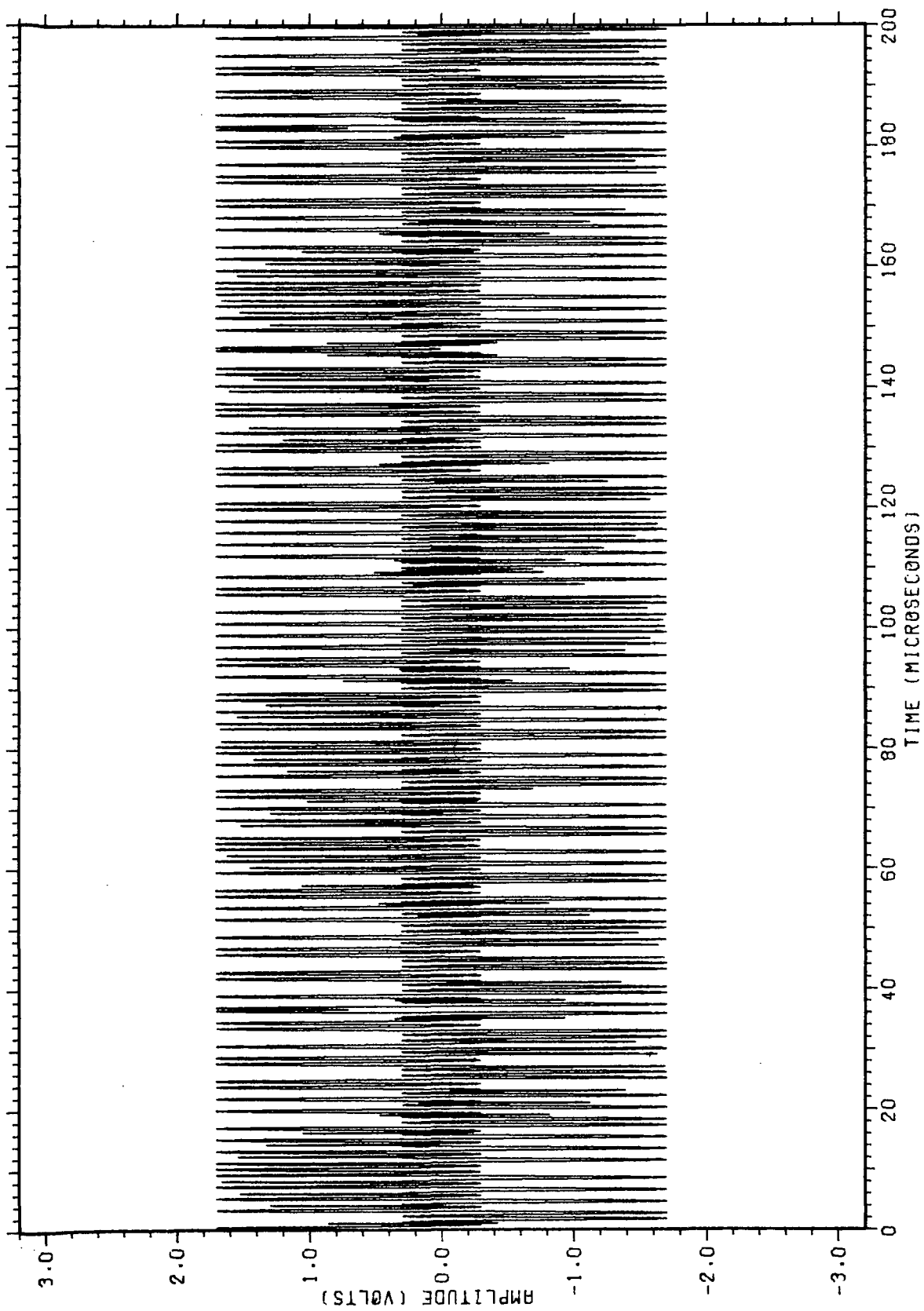


Figure 14. Time waveform for biphase modulated subcarrier signal and PCM signal with a random pattern of bits. Amplitude relationship for $\beta_{sc} = 1.0$ and $\beta_{pcm} = 0.7$.

selected in a random fashion with a probability of 0.5. Figure 15 shows the baseband spectra of the signal shown in Figure 14. Note the disappearance of the single line in the spectrum at 500 kHz, and the spreading of the spectrum around this frequency. Note also the null in the spectrum of the PCM data signal near the telemetry subcarrier frequency.

Next the S-band spectra of some of these signals were investigated. Figure 16 shows the calculated S-band spectrum for the biphase modulated telemetry subcarrier signal only. The calculated S-band spectrum for both modulating signals present is shown in Figure 17. Experimentally obtained S-band spectra for each modulation present separately and both at the same time are shown in Figure 18.

Ideally, the effect of phase demodulation should be evaluated to complete the study, but time did not permit developing modeling techniques for the phase demodulator. For the particular application investigated, experimental assessment of the demodulator action was made, and the results are shown in Figure 19. This figure shows the output of the telemetry bandpass filter in the subcarrier phase demodulator in the Generalized Concept Receiver [5] for the case of each signal presented individually and both at the same time. Note that when both signals are present the second harmonic component of the 500 kilobit per second signal (imperfect square wave) is some 10 dB below the amplitude of the first sideband pair of the biphase modulated telemetry subcarrier signal.

F. Conclusions

Modeling studies have been carried out which were aimed at developing techniques and procedures applicable to unified carrier systems which would permit analytical determination of the effect of changing modulation types, modulating indices, etc. Techniques have been developed for modeling biphase modulated subcarrier signals and PCM data streams. Automated procedures were developed

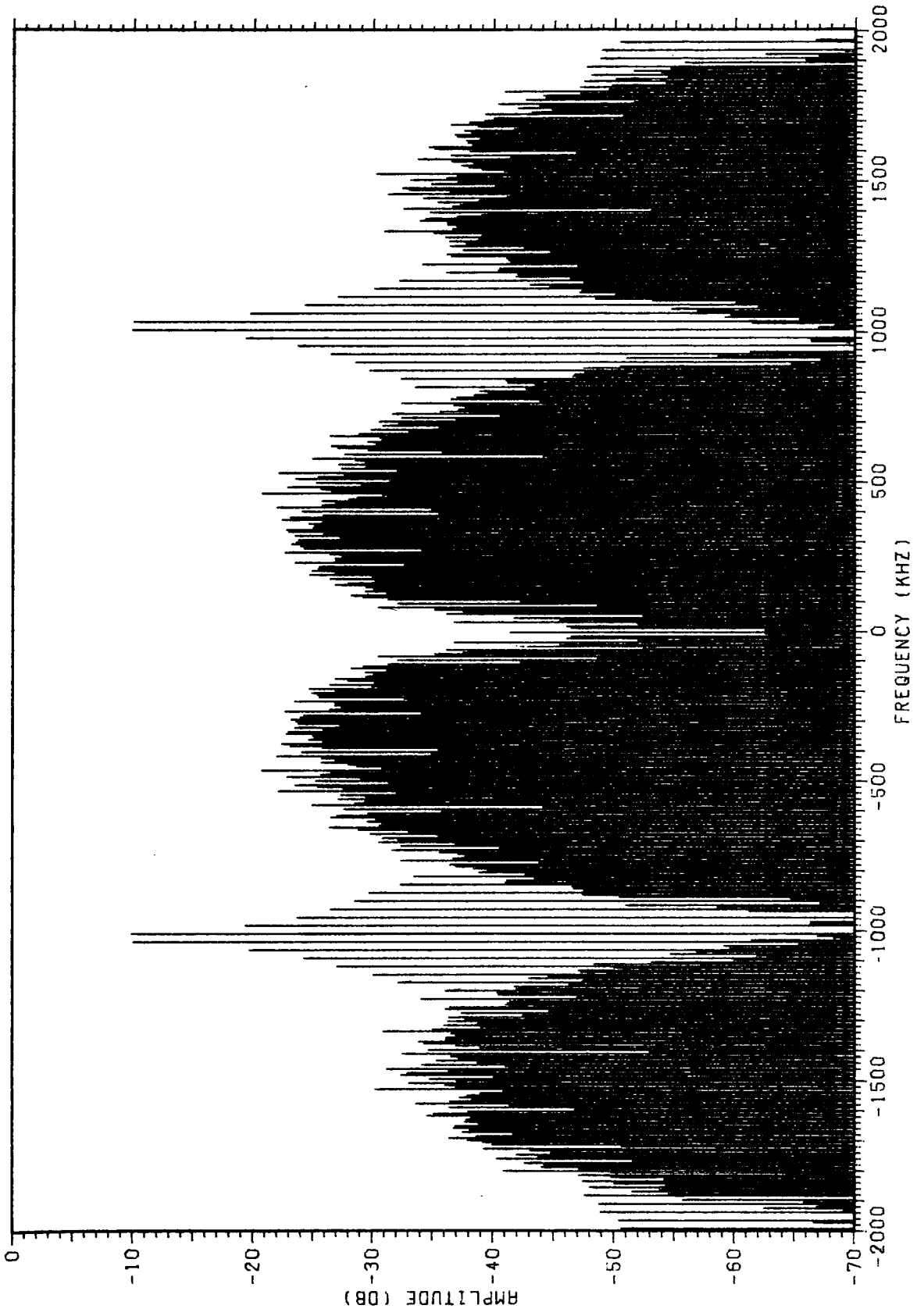


Figure 15. Frequency spectrum for time waveform shown in Figure 14.

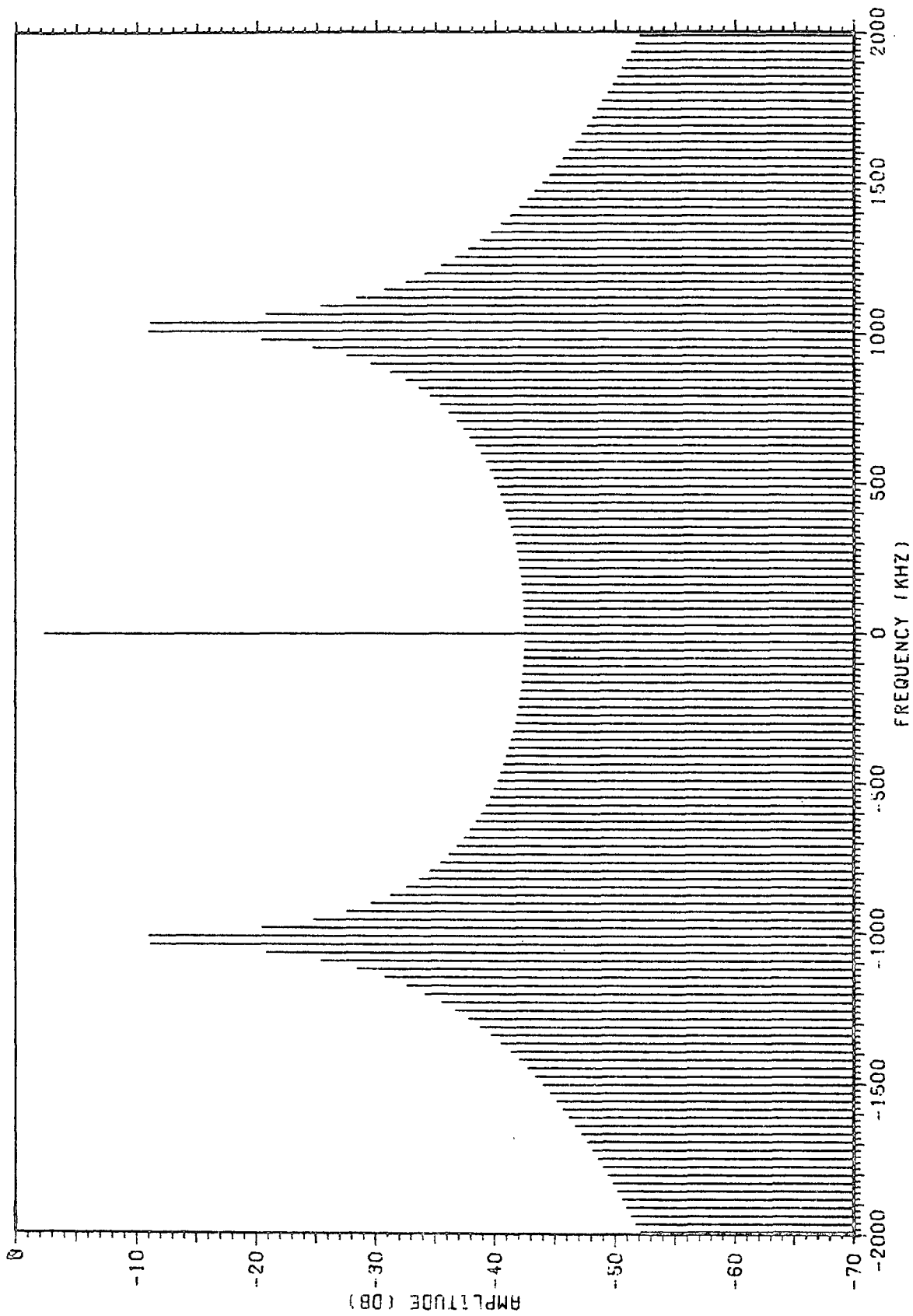


Figure 16. S-band spectrum of a biphas modulated telemetry subcarrier only, $\beta = 1.0$. No low-pass simulation of modulator characteristic.

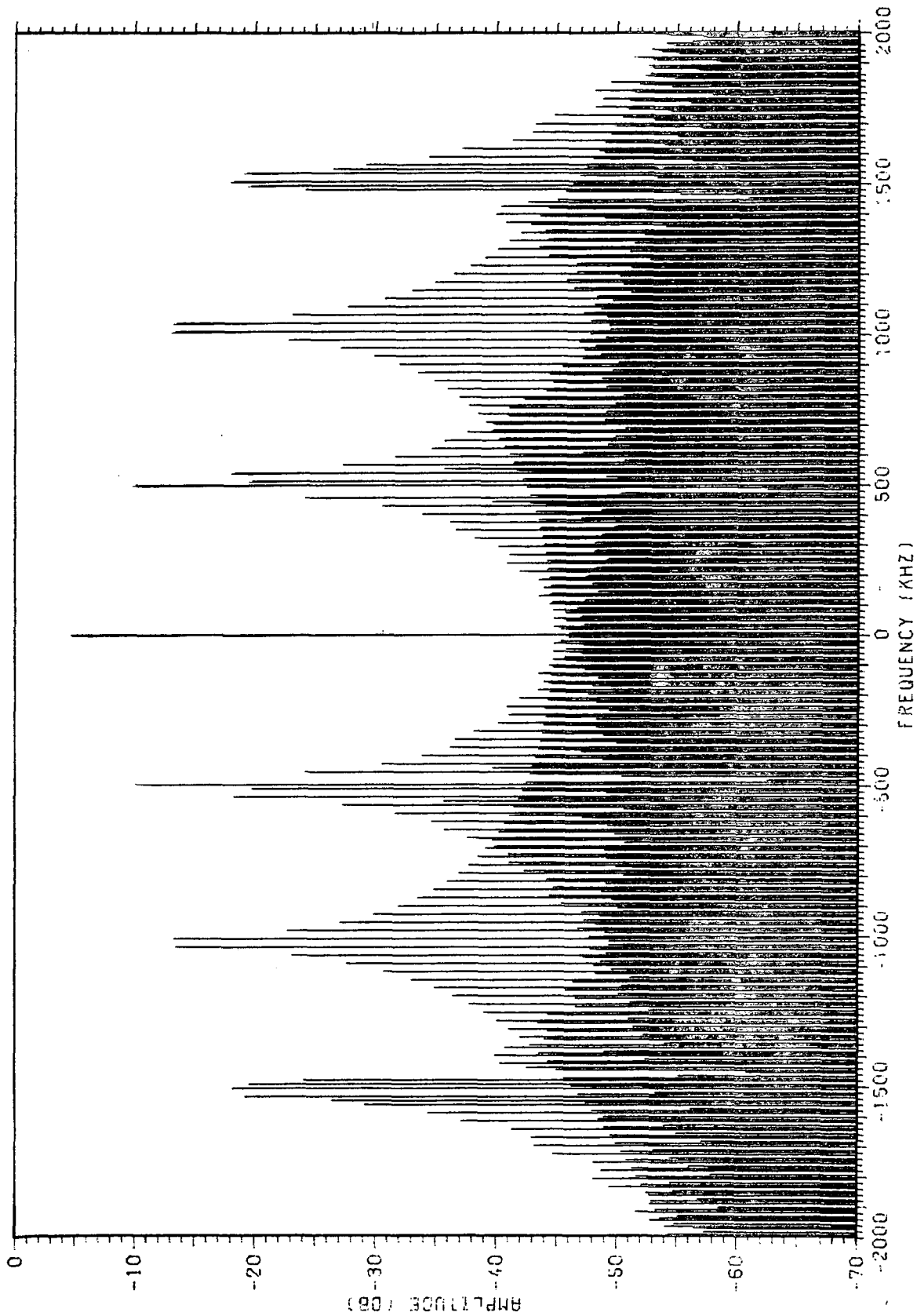
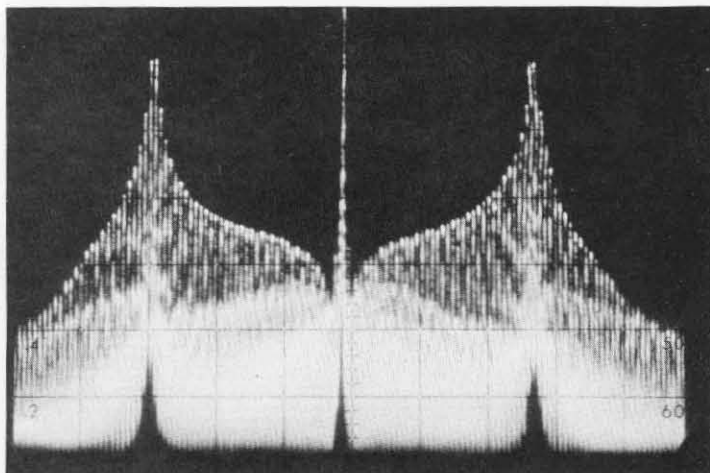


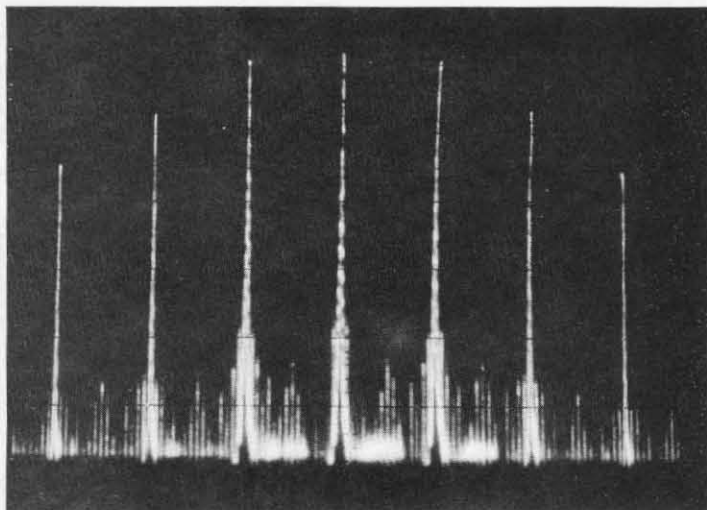
Figure 17. S-band spectrum of a biphasely modulated telemetry subcarrier, $\beta = 1.0$, and Manchester PCM signal consisting of all ones or zeros, $\beta = 0.7$, no low-pass simulation of phase modulator characteristics.

(a) MODULATED (SQUARE WAVE)
1024 kHz TELEMETRY SUB-
CARRIER'

VERTICAL 10 dB/DIV.
HORIZONTAL 360 kHz/DIV.



(b) 500 KILOBIT SPLIT PHASE
PCM SIGNAL.



(c) BOTH SIGNALS PRESENT.

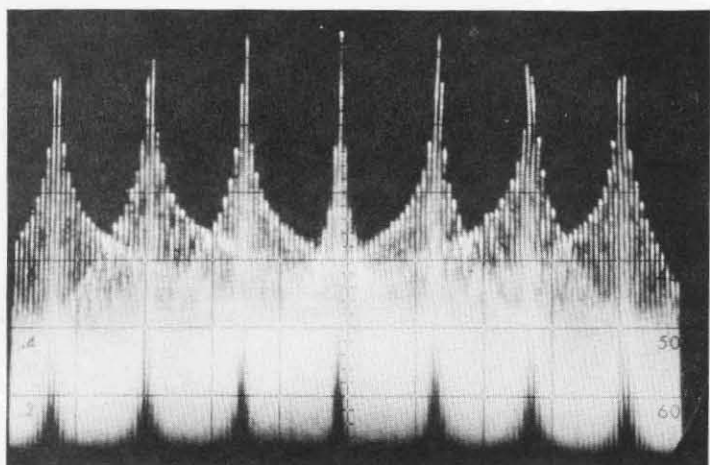
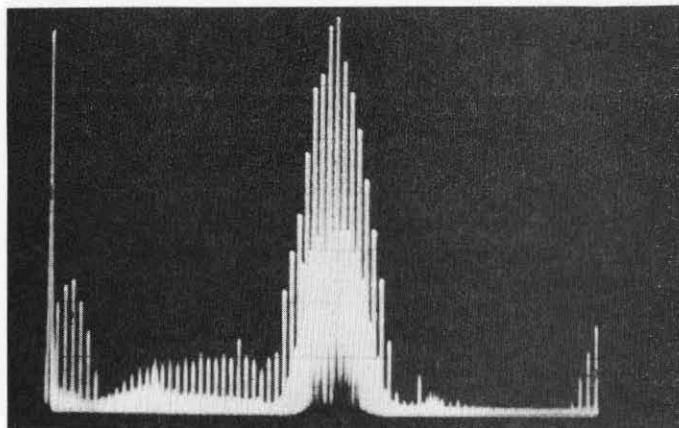
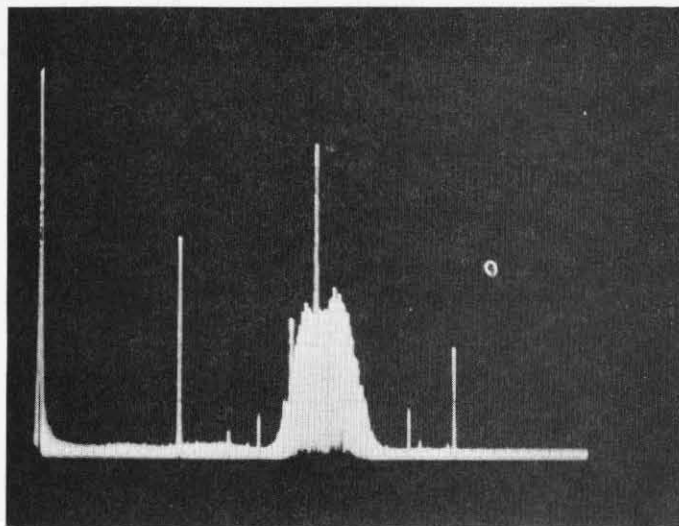


Figure 18. S-band spectra, $\beta_{sc} = 1.0$, $\beta_{pcm} = 0.7$.

(a) MODULATED 1024 kHz
TELEMETRY SUBCARRIER
ONLY.
VERTICAL 10 dB/DIV.
HORIZONTAL 200 kHz/DIV.



(b) 500 KILOBIT/SEC SPLIT PHASE
MODULATED SIGNAL ONLY.



(c) BOTH SIGNALS PRESENT.

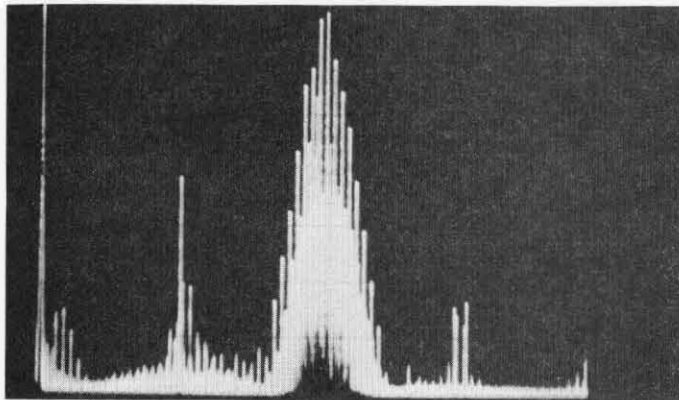


Figure 19. Baseband signal spectra at output of 1024 kHz Generalized Concept Receiver telemetry bandpass filter, $\beta_{sc} = 1.0$, and $\beta_{pcm} = 0.7$.

for plotting the time waveform of baseband signals; for computing both baseband and RF spectra; and for plotting the spectra. These procedures permit easy determination of the spectral content of a phase modulated carrier when both biphasic modulated subcarriers and PCM data streams are used as modulating signals.

A need exists for extending this work to modeling of a phase demodulator, so that the time waveform and spectral content of the recovered baseband signal can be predicted. Time available for this program did not permit modeling of the demodulator.

During the course of the work a specific application of the techniques was made in examining the effects of replacing the PN range code on the CCS down-link with a wideband PCM signal. It was found that the effects of the PCM signal on the recovered telemetry waveform were small.

III. AUTOMATIC FREQUENCY CONTROL SYSTEM ANALYSIS AND SIMULATION

A. Introduction

An Automatic Frequency Control (AFC) loop for a typical direct Frequency Modulation (FM) transmitter is considered in this section. A digital simulation (nonlinear) of the AFC system is developed and, together with a linear analysis, is used to determine the relationships between system behavior and the parameters and other characteristics of the subsystems. Using such a simulation, the design engineer can evaluate and improve his preliminary system design without setting up the associated hardware and test equipment. Two methods of frequency sampling are considered.

After a brief description of a direct FM transmitter and its AFC system, math models are described for the subsystems of the AFC loop. Using linearized models, important AFC system features such as stability, transient time, and frequency sensitivity are estimated analytically. These linear system results provide insight into the significance of subsystem parameters and serve as a test case for verifying the programming of the simulation.

After the linear version of the simulation has been verified, certain linear blocks or subsystems in the simulation are replaced by nonlinear models. The Voltage Controlled Oscillator (VCO) input-output characteristic is modeled by a nonlinear curve-fit, and a limiter is included in the feedback path to simulate saturation in the error-processing electronics.

The results of the analysis and simulation show how such parameters as the system gains, sampling period and duration, and the RC time constant of the sampling network influence the AFC system behavior. A numerical example is included.

B. System Description

1. Direct FM Transmitters

A typical direct FM transmitter with its associated Automatic Frequency Control (AFC) loop is shown in block diagram form in Figure 20 and again in more detail in Figure 21. In direct frequency modulation, the modulating voltage (input signal) varies the natural frequency of an LC oscillator whose nominal unmodulated frequency is the carrier frequency or some submultiple of it. The variation in natural frequency of the oscillator (ideally, proportional to the input signal) results when a change in the input voltage varies the capacitance of a voltage-dependent capacitor in the oscillator resonant circuit.

This technique can produce large-index frequency modulation directly (i.e., without requiring large frequency multiplication ratios to produce the desired modulation index at the carrier frequency as in the Armstrong indirect frequency modulation technique), but since it uses an LC Voltage Controlled Oscillator (VCO) which tends to have drift in its nominal frequency, some method of stabilizing the carrier frequency to meet its stability requirements is required. (A typical stability requirement may be 0.005% at S-band.) To obtain such stabilities, the frequency of the LC oscillator is "slaved" to the frequency of a crystal reference oscillator through comparison and control circuitry (AFC loop). To accomplish this, a sample of the output signal can be heterodyned against a reference signal generated by multiplication of the frequency of a crystal oscillator. The difference-frequency between the transmitter carrier signal and the multiplied reference signal is applied to a discriminator (usually operating in the 1 MHz region) to produce an error signal for correction of the VCO nominal frequency. A low-pass filter (or sample and hold circuit) prevents the tracking-out of useful modulation components while providing for the correction of the long term frequency of the VCO. Frequency stabilization techniques

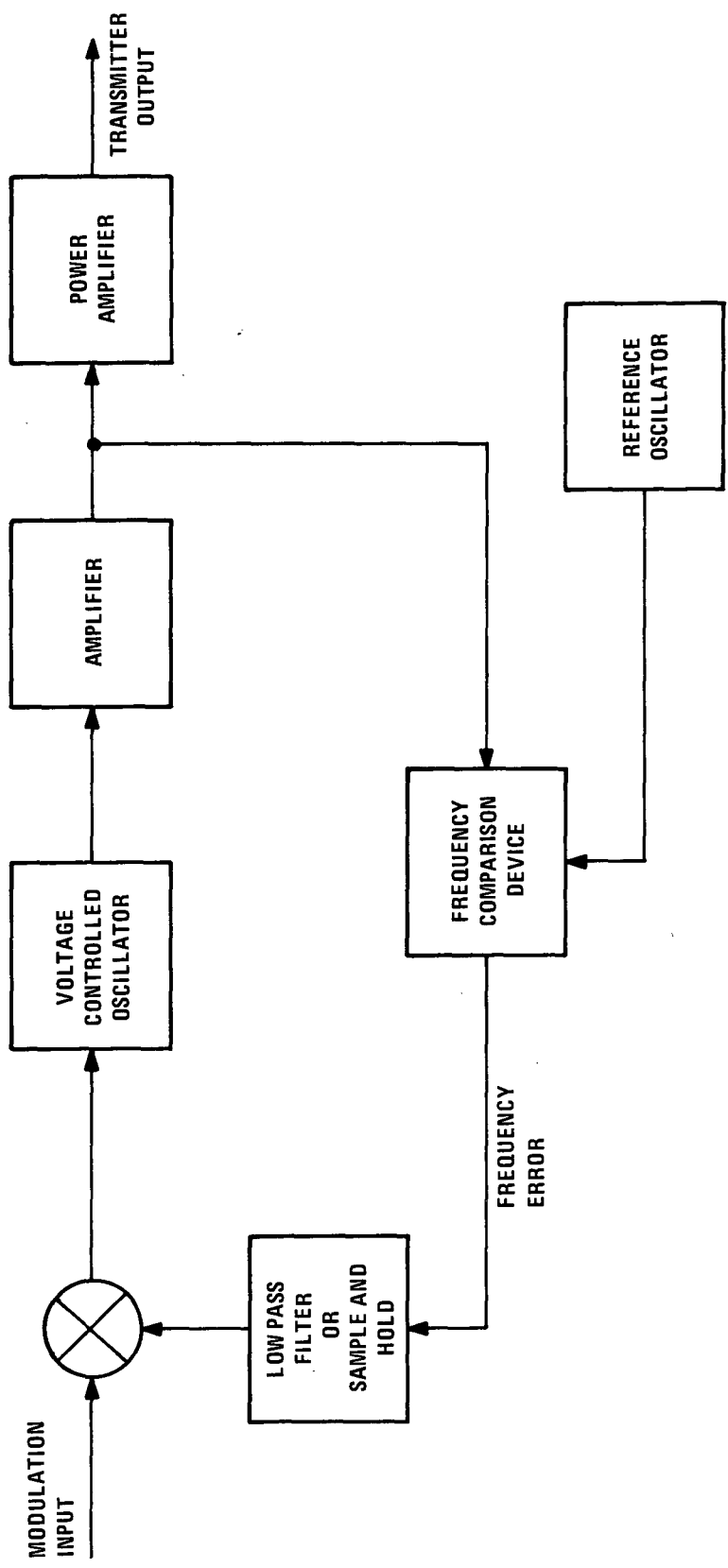


Figure 20. Block diagram of FM transmitter.

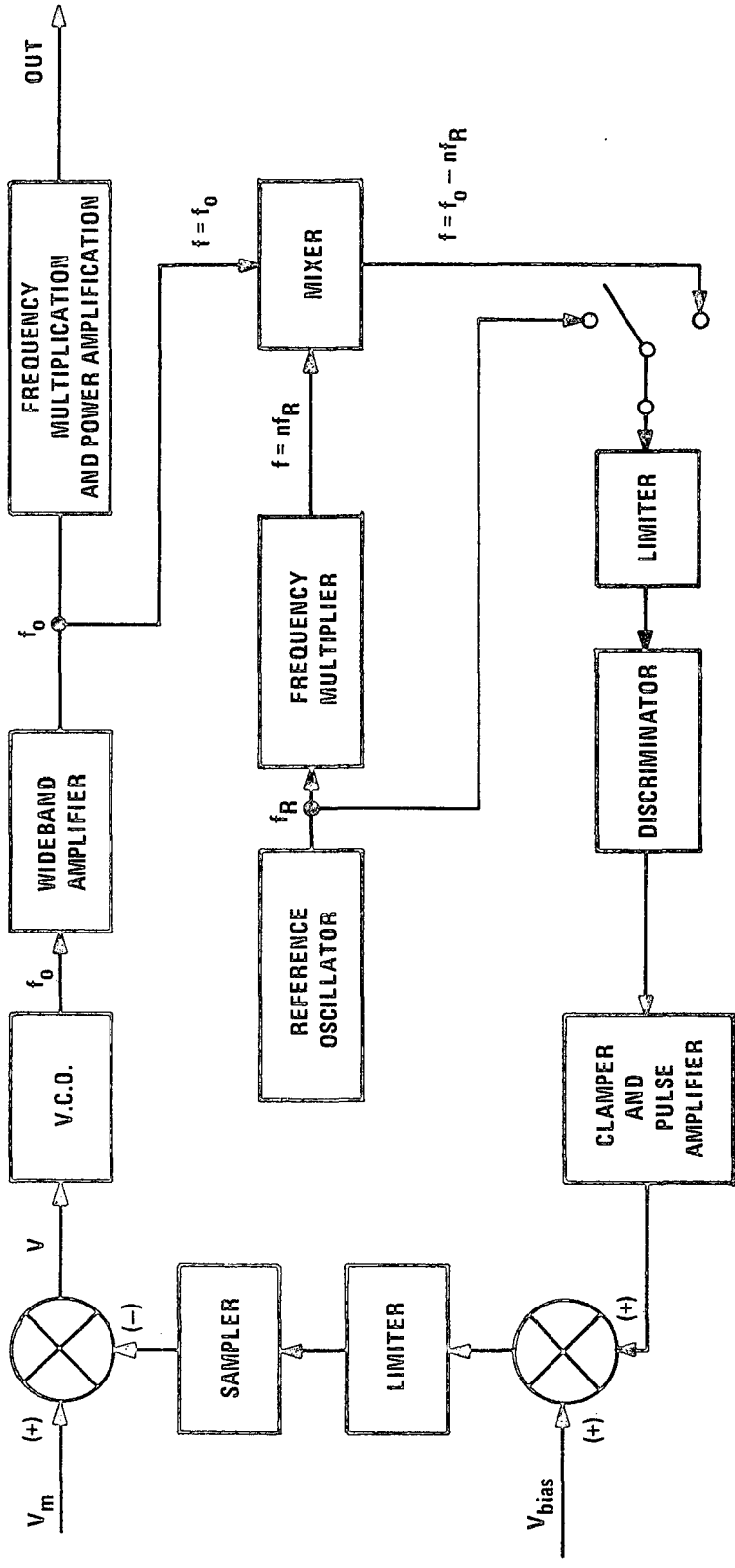


Figure 21. Block diagram showing AFC details.

for direct frequency modulation may operate to hold the mean frequency of the transmitted signal within a specified tolerance or they may sample the modulating signal at some repetitive position of the time waveform which is then held to some specific frequency (Figure 21). An example of the latter system would be a sampled automatic frequency control system used with a television modulating signal.

2. AFC Loop

In the analysis and simulation of the AFC system, the variable of interest is the frequency of the output signal rather than the output voltage waveform. Thus any RF block in Figures 20 or 21 which does not influence the fundamental frequency of the waveform can be ignored in this study, regardless of any voltage gain or waveform distortion the block (subsystem) might introduce. In the following, only that portion of the direct FM transmitter in the AFC loop will be discussed, and the discussion will treat frequency, rather than voltage, as the variable of interest.

The heart of a direct FM transmitter is the voltage controlled oscillator (VCO). Ideally, the VCO output frequency would be proportional to the modulating voltage; in reality it is a nonlinear function of the applied voltage. The VCO output (modulated signal) is amplified and perhaps frequency multiplied by succeeding stages in the transmitter. Although some of these stages included in the AFC loop may introduce phase shift and distortion in the modulated signal, it is assumed that no change in the fundamental frequency is introduced (other than intentional frequency multiplication). Thus for simulation and analysis of the AFC system these stages may be modeled as constant gains.

It is assumed that periodically in the input modulating signal there is a reference level in the time waveform such as one level of a frequency shift keyed signal or the signal level during the sync pulse interval of a standard television video signal.

During the time of occurrence of this reference level, the output frequency of the transmitter is measured and compared with the desired nominal frequency. The difference frequency is then used as an error signal to adjust the bias voltage on the VCO so as to reduce the error in its output frequency. By sampling the error signal pulse during the center of its duration, the effects of the dynamics of the error detection system upon the AFC loop are minimized. Since the error signal is available only as a sampled signal and since a continuous bias for the VCO is required, there must be a sample-and-hold device between the error frequency signal and the VCO bias input. Note that if the feedback (including sample and hold) contains no integration, the steady state error of the AFC system will be non-zero for a constant disturbance and will be inversely proportional to the AFC loop gain. The inclusion of an integrator would convert the AFC system to a control system which would reduce the steady-state error in the output frequency to zero for a constant disturbance caused by a frequency shift internal to the VCO.

In the next section of this report, math models will be established for each block of the AFC loop. These models are used for both analysis and digital simulation of an automatic frequency control system of a typical direct FM transmitter.

C. Math Models

In the following, math models for the individual blocks of the AFC loop shown in Figure 21 are described. Linearized models will be used in both the analysis and digital simulation of the AFC system, while the more complete nonlinear models will be used in the simulation only.

1. Subsystem Models

The Voltage Controlled Oscillator (VCO) produces a sinusoidal voltage signal whose frequency is dependent upon the input voltage, V , in a nonlinear manner as shown in Figure 22.

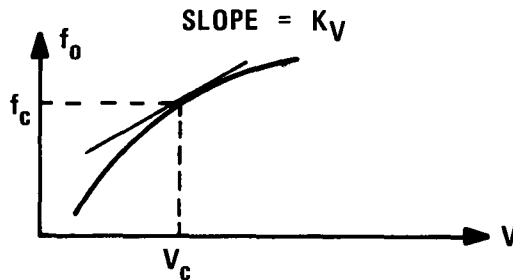


Figure 22. Typical VCO characteristics.

Since the VCO frequency is the variable of interest, it is not necessary to model the VCO with circuit details. The change in VCO frequency for a change in input voltage is assumed to occur "rapidly" with respect to other time-constants in the AFC loop so that the dynamics of the VCO may be ignored.

The nonlinear model sketched in Figure 22 can be used in the simulation either by (1) finding an analytic expression which approximates $f_c(V)$ sufficiently close, or (2) by interpolating between data points from a measured $f_c - V$ curve.

Alternately, as indicated in Figure 22, the VCO characteristics can be approximated for "small" deviations in V from its nominal value by the following linear expression:

$$f_o = f_c + k_V (V - V_c) .$$

The associated block diagram for a linearized VCO model is as given in Figure 23.

Although the Amplifier (see Figure 21) following the VCO definitely influences the waveshape of the signal (amplitude and phase), it is assumed not to influence the frequency of the signal.

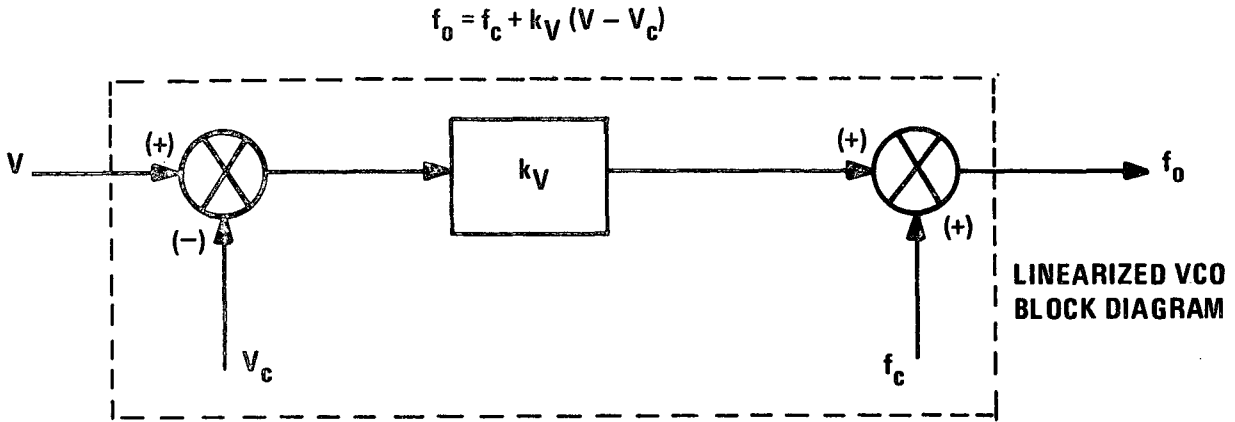


Figure 23. Linearized VCO model.

Since the AFC loop analysis and simulation is concerned with only the frequency of the transmitted signal, the amplifier will be modeled here by a unity transfer function. Also, the output signal Frequency Multiplication and Power Amplification blocks can be ignored for the purpose here since they are outside the AFC loop.

The low-power, fixed-frequency Reference Oscillator, whose frequency is a sub-harmonic of the desired nominal transmitter frequency, is modeled as a constant-frequency source. The reference signal is fed into a Frequency Multiplier circuit with a multiplication factor n where the desired nominal transmitter frequency is $(n + 1) f_R$. The frequency multiplier is modeled as a gain factor, n . The VCO signal, after amplification, and the frequency multiplied reference signal are fed into a Mixer whose output signal has frequency equal to the difference frequency, $(f_o - n f_R)$. The deviation of this frequency from f_R represents the "error" in the nominal VCO output signal frequency.

The Limiter-Discriminator in Figure 21 is time-shared in the AFC loop to develop a voltage which represents alternately the frequencies $(f_o - nf_R)$ and f_R . Since the two signals may not have the same amplitude, any "amplitude dependence" of the limiter-discriminator produces outputs as if the two input signals were processed by separate discriminators with different gains. This amplitude dependence will be modeled by using two discriminators whose gains are not necessarily the same. Nonlinear models for the discriminators could be used, but linear models with non-identical gains should be sufficient here. The (linearized) discriminator output voltage, V_1 , can be expressed in terms of the frequency of the input signal (f), the nominal discriminator frequency (f_o), and the nominal slope of the limiter-discriminator characteristic curve as follows:

$$V_1 = k_{01} (f - f_o) . \quad (14)$$

The linearized block diagram for the discriminator (modeled as a pair) is shown in Figure 24.

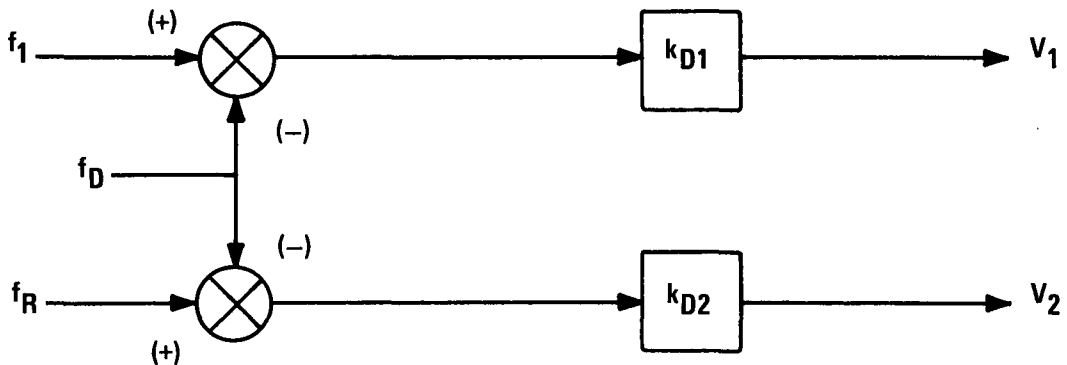


Figure 24. Discriminator Model

The difference between the two discriminator output voltages (or between the single discriminator's output voltages at the two different times) is proportional to the "frequency error" of the VCO. After amplification, the difference voltage is combined with the "set" voltage, V_{bias} , to form the feedback error signal. The voltage V_{bias} is set initially such that the output frequency, f_o , is at or near the desired nominal frequency for the reference value of the input voltage, V_m (see Figure 21). Provision is made in the model to limit the signal at this point for modeling saturation throughout the feedback loop.

Since the error signal is assumed available only on a sampled basis, and since the input voltage to the VCO must be continuously present, some Sample and Hold device must be used to buffer the feedback error signal. Depending upon how the time-sharing discriminator is implemented, the frequency error sample may be either a flat-topped pulse whose amplitude represents the error at the time the pulse began, or it may be a time-varying pulse whose amplitude follows the frequency error during the duration of the pulse. The former case, which allows a "deadbeat response," will be assumed here, and the other case discussed later.

For the constant amplitude pulse, the error feedback can be modeled as two electronic switches, a zero-order sample-and-hold, and a simple RC charging circuit (Figure 25).

The initial value of the sampled waveform is held as a constant input to the RC circuit. The switch S_2 is assumed to close for t_0 seconds once each T seconds.

This sample-and-hold circuit is piecewise linear and has a continuous output voltage, e_o . However, the output is used in such a way in the AFC system that it is its new value, after S_2 has reopened, that is of interest. Accordingly, the sample-and-hold circuit can be modeled by the linear, first order, difference equation derived in the following.

Consider one cycle or period for the sample-and-hold circuit.

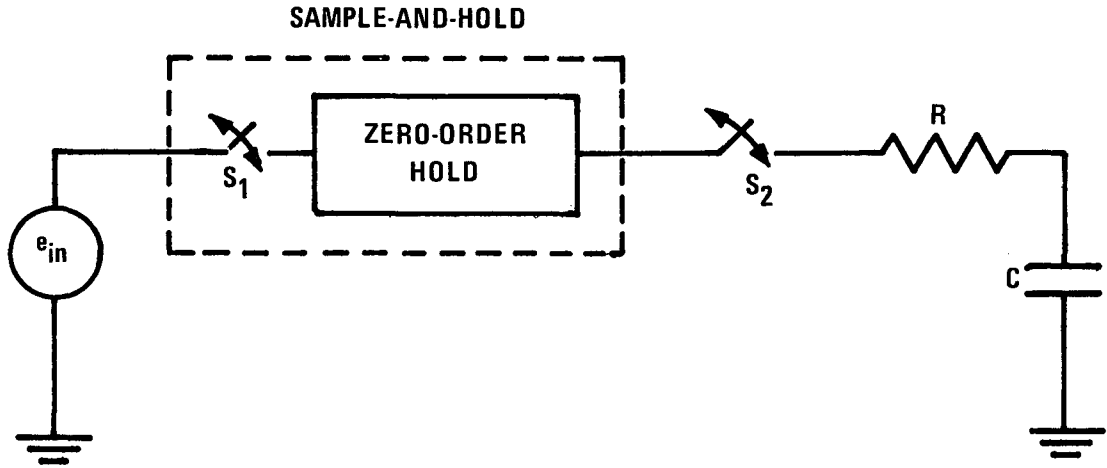


Figure 25. Error feedback sampling model.

Let the switch close at $t = 0$ and reopen at $t = t_o$ and then stay open until $t = T$. Transient analysis shows that, while the switch is closed, the output voltage is given by

$$e_o(t) = e_o(0) + [e_{in}(0) - e_o(0)][1 - e^{-t/RC}], \quad 0 \leq t \leq t_o, \quad (15)$$

and after the switch opens, the output voltage remains fixed at

$$e_o(t) = e_o(0) + [e_{in}(0) - e_o(0)][1 - e^{-t_o/RC}], \quad t_o \leq t < T. \quad (16)$$

Thus,

$$e_o(T) = e_o(0) + C_1 [e_{in}(0) - e_o(0)], \quad (17)$$

where $C_1 = 1 - e^{-t_o/RC}$.

This is generalized to the n^{th} sampling period as

$$e_o[(N + 1) T] = e_o(NT) + C_1 [e_{in}(NT) - e_o(NT)],$$

which can be expressed as a difference equation without the factor T as follows:

$$e_o(N + 1) = e_o(N) + C_1[e_{in}(N) - e_o(N)] . \quad (18)$$

Thus the updated sampler output will be equal to the current value plus a term proportional to the difference between the present input and output voltages. Note that this acts like a zero-order, or box-car, sample-and-hold device only if $RC \ll t_o \ll T$; that is, if $C_1 \approx 1$. However, even for $t_o < RC$, the AFC system closed loop response can be made similar to that of a box-car hold circuit by using a large AFC feedback loop gain. This is shown in the analysis section of the report.

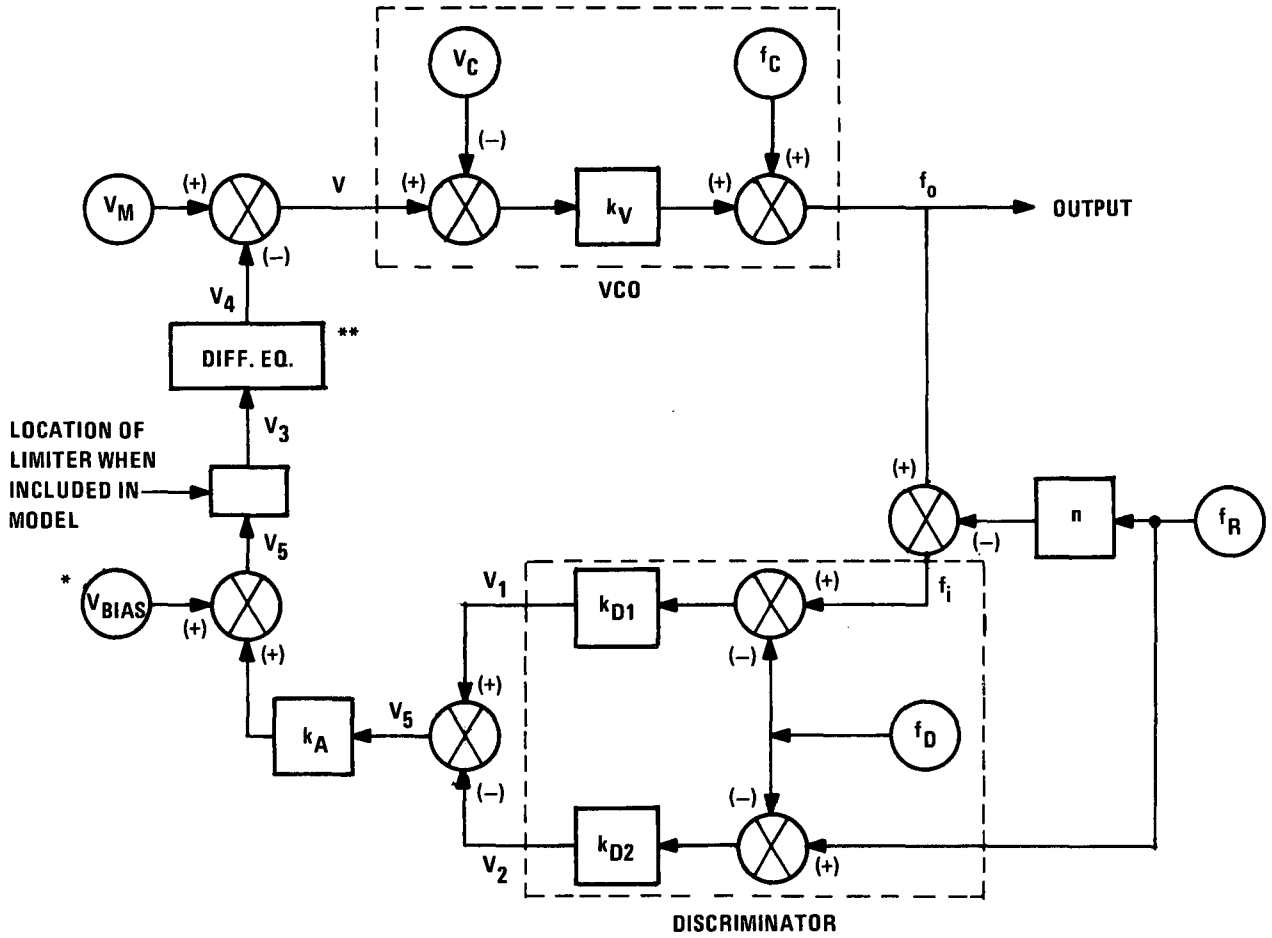
2. AFC Loop Model

Using the math models just described for the blocks of Figure 21, the block diagram is redrawn as shown in Figure 26.

A digital simulation program can be written directly from the block diagram, allowing a programming block for each diagram block. The program can of course use either the linearized models as shown in Figure 26 or the more complete nonlinear models described earlier. However, in order to verify a simulation, a reasonable test case is required; since the linear model response can be predicted analytically, it will be used as the test case. Individual blocks of the simulation will be replaced with nonlinear models after the simulation program has been verified. The analysis of the linearized system (Figure 26) is given in the following section.

D. Linear System Analysis

The linearized model (Figure 26) of the AFC loop is analyzed in this section to (1) provide insight into the relationships between system parameters and the effectiveness of the frequency



** THE DIFFERENCE EQUATION IS $v_4(N+1) = v_4(N) + c_1 [v_3(N) - v_4(N)]$.

* NOTE: $v_{BIAS} \doteq V_C - (V_M)_{REF}$

Figure 26. AFC loop model.

control system and to (2) provide data for verifying or de-bugging the digital simulation program to be developed. The simulation will be developed initially using the linearized model, will be de-bugged, and will then have some of its (linear) blocks replaced by more complete models for further system evaluation.

Since this system is a sampled-data system, the Laplace transform technique is not applicable for systems analysis. A similar technique using the Z-transform is normally used for sampled-data system analysis, but its use requires that the order of the denominator of the closed loop transfer function exceed that of the numerator by at least two [6]. Thus the Z-transform is not applicable here.

Fortunately, the system is sufficiently simple that one can learn a lot about the system from its closed loop difference equation. From this equation, such items of interest as stability of the closed loop system, sensitivity of the output frequency to variations in system parameters, and the time constant of the transient response can be determined.

1. Closed-Loop Difference Equation

Referring to the linearized model of the AFC system (Figure 26) the only subsystem which contains dynamics is the sampler block; all other subsystems are modeled simply as combinations of gains and summations. Thus, with the exception of the difference equation^{*} modeling the sampler, the system math model is algebraic. Using the sampler difference equation and the algebraic relationships given by the linearized AFC block diagram, the closed-loop difference equation can be derived as follows.

* A difference equation is the discrete analogy of a differential equation.

Let $V_4(N)$ refer to the value of the "sample and hold" output after the sampler switch has closed and reopened for the N^{th} time. Similarly, let $V_m(N)$ be the reference value of the modulating voltage just before the switch is closed and reopened for the $(N + 1)^{\text{th}}$ time.

The algebraic equation for the VCO is as follows:

$$f_o(N + 1) = f_c + k_v [V(N + 1) - V_c] . \quad (19)$$

But,

$$V(N + 1) = V_m(N + 1) - V_4(N + 1) ,$$

so that

$$f_o(N + 1) = f_c - k_v V_c + k_v [V_m(N + 1) - V_4(N + 1)] . \quad (20)$$

The difference equation for the sample and hold device is

$$V_4(N + 1) = [1 - C_1] V_4(N) + C_1 V_3(N) . \quad (21)$$

Substituting,

$$f_o(N + 1) = f_c - k_v V_c + k_v V_m(N + 1) - k_v [(1 - C_1)V_4(N) + C_1 V_3(N)] . \quad (22)$$

Now, writing $V_4(N)$ in terms of $V_m(N)$ and $f_o(N)$, writing $V_3(N)$ in terms of $f_o(N)$, and substituting into Equation (22) will complete the development of the closed loop difference equation.

Rewrite Equation (19) for N rather than $(N + 1)$:

$$f_o(N) = f_c - k_v V_c + k_v V_m(N) - k_v V_4(N) , \quad (23)$$

from which

$$k_v V_4(N) = -f_o(N) + f_c - k_v V_c + k_v V_m(N) . \quad (24)$$

From the block diagram,

$$\begin{aligned}
 V_3(N) &= V_{\text{bias}} + k_A V_5 , \\
 &= V_{\text{bias}} + k_A [V_1 - V_2] , \\
 &= V_{\text{bias}} + k_A [k_{D1} (f_o(N) - n f_R - f_D) - k_{D2} (f_R - f_D)] ;
 \end{aligned}$$

or

$$V_3(N) = (k_A k_{D1}) f_o(N) + V_{\text{bias}} - f_R k_A (n k_{D1} + k_{D2}) - k_A f_D (k_{D1} - k_{D2}) . \quad (25)$$

The loop is closed by substituting Equations (24) and (25) into Equation (22) to obtain

$$\begin{aligned}
 f_o(N+1) + [C_1 k_v k_A k_{D1} - 1 + C_1] f_o(N) &= k_v V_m(N+1) \\
 + ([C_1 - 1] k_v) V_m(N) + E , & \quad (26)
 \end{aligned}$$

where

$$\begin{aligned}
 E \triangleq C_1 f_c - C_1 k_v V_c - C_1 k_v V_{\text{bias}} + C_1 k_v k_A (n k_{D1} + k_{D2}) f_R \\
 + C_1 k_v k_A (k_{D1} - k_{D2}) f_D . \quad (27)
 \end{aligned}$$

Equation (26) with the constant E as defined in Equation (27) is the first-order difference equation which describes the behavior of the Automatic Frequency Control System. Although an analytic expression (a finite sum series) exists for the solution to such a difference equation [7], the form of the expression is such that it is difficult to use in other than numerical examples. A better understanding of the significance of the parameters of the system

2

can be had by examining the difference equation directly for stability, sensitivity, and transient time.

2. Stability Regions

From the closed loop difference equation, Equation (26), much information about the response of the linearized model of the AFC system can be determined without actually solving the difference equation. For example, one can determine the set of gains for which the closed loop system is stable, the "speed" of response of the system, the steady state response, and the system sensitivities (i.e., how the steady state output frequency varies with perturbations in the system elements).

To determine the transient response characteristics of a linear system, the driving functions may be set to zero and the resulting homogeneous differential equations or difference equations analyzed. The homogeneous portion of Equation (26) is

$$f_o(N + 1) + [C_1(k + 1) - 1] f_o(N) = 0, \quad (28)$$

where

$$k \triangleq k_v k_{D1} k_A .$$

Regardless of the initial condition, $f(N = 0)$, the system described by Equation (28) can be seen to be stable for

$$|[C_1(k + 1) - 1]| < 1 \quad (29)$$

since

$$f_o(N + 1) = - [C_1(k + 1) - 1] f_o(N) ; \quad (30)$$

i.e., the magnitude of $f_o(N)$ will be decreasing with each increment in N . Furthermore, the response is stable and non-oscillatory if $-1 < [C_1(k + 1) - 1] < 0$, since $f_o(N + 1)$ would have the same sign as $f_o(N)$. Similarly,

$$0 < [C_1(k + 1) - 1] < 1 \quad (31)$$

corresponds to a stable but oscillatory response with f_o decreasing in magnitude but reversing signs at each increment. Note the special form of response (called dead beat) which results when

$$[C_1(k + 1) - 1] = 0. \quad (32)$$

Under this condition, the AFC loop reaches its "steady state" response within one sampling period of the occurrence of a step disturbance.

The gain conditions for each type response are given in Table I.

TABLE I
TRANSIENT RESPONSES OF LINEAR AFC SYSTEM

Loop Gain (k)	Factor [1 - C ₁ (k + 1)]	Transient Response
$k > \left[\frac{2}{C_1} - 1 \right]$	Less than -1	unstable, alternating sign
$k = \left[\frac{2}{C_1} - 1 \right]$	-1	square wave
$\left(\frac{1}{C_1} - 1 \right) < k < \left(\frac{2}{C_1} - 1 \right)$	-1 to 0	stable, alternating sign
$k = \left(\frac{1}{C_1} - 1 \right)$	0	deadbeat
$-1 < k < \left(\frac{1}{C_1} - 1 \right)$	0 to +1	stable, monotonic
$k = -1$	+1	constant
$k < -1$	Greater than +1	unstable, monotonic

Note: $C_1 = 1 - e^{-t_o/RC}$

Consider a numerical example for which

$$R = 20 \times 10^3 \text{ ohms,}$$

$$C = 0.1 \times 10^{-6} \text{ farads, and}$$

$$t_o = 1.5 \times 10^{-6} \text{ seconds.}$$

Then

$$\left(\frac{1}{C_1} - 1 \right) = 1333, \text{ and}$$

$$\left(\frac{2}{C_1} - 1 \right) = 2667.$$

Figure 27 shows the previously described stability regions.

Typical AFC systems operate in the monotonically stable region with loop gain, k , well below the deadbeat value. The use of a deadbeat system, which gives the "best" frequency regulation as far as response time is concerned, requires a high loop gain which can make the system very susceptible to noise. Deadbeat control also requires more stages of error signal amplification; large perturbations can produce saturation in the loop.

The stable-but-alternating portion of Figure 27 requires larger loop gain than deadbeat; it has no advantages over the stable and monotonic operation.

As to the applicability of this linear model, it should be noted that the linearization of the VCO required the assumption that frequency perturbations were small. Thus the model is not applicable when the frequency deviation, Δf , gets "large." The linear model does nonetheless provide a basis for choosing the loop gain. Figure 28 shows the transient response in frequency error for a step change in VCO nominal frequency for various values of AFC loop gain.

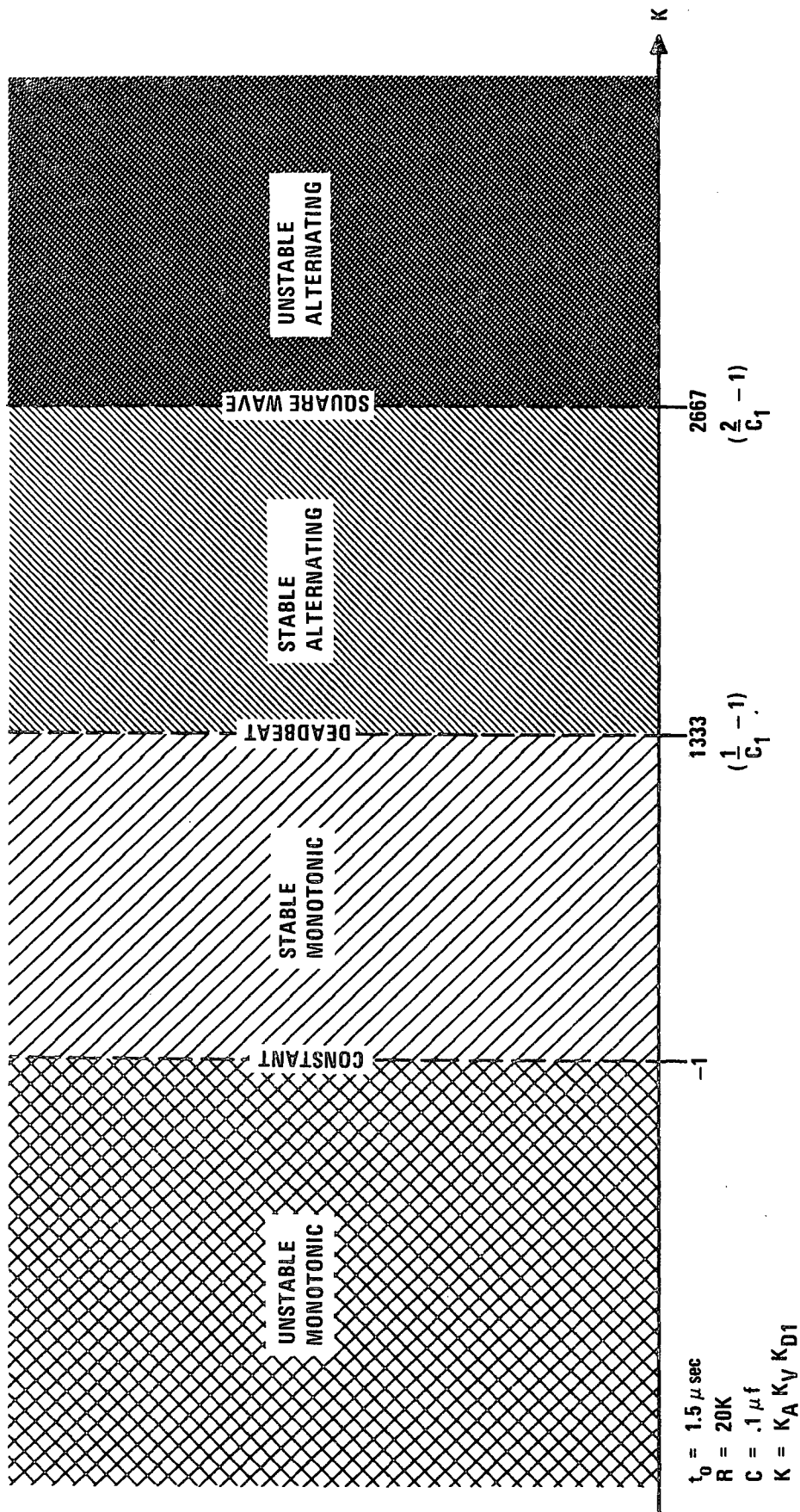


Figure 27. Stability regions for linear AFC system.

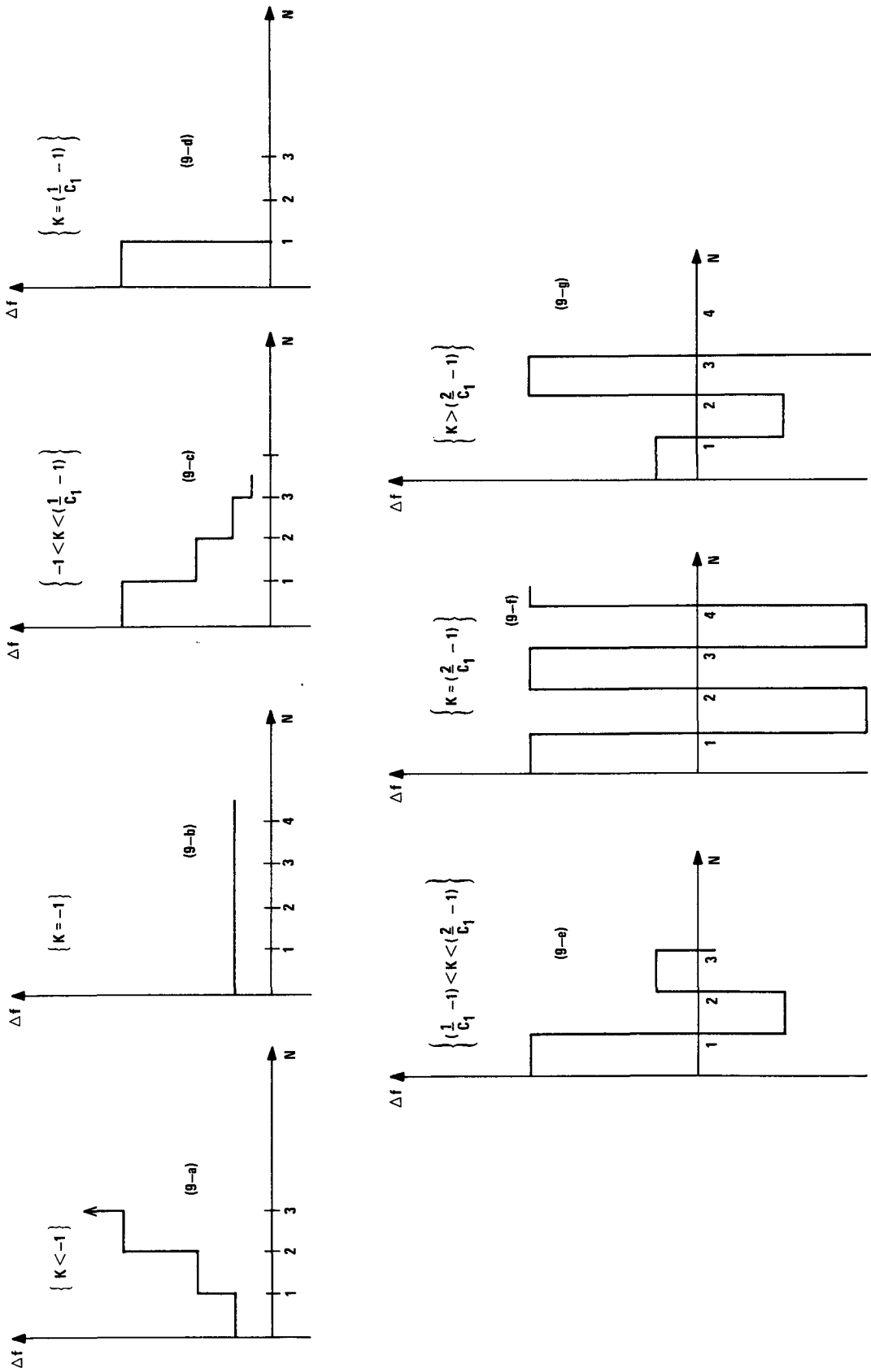


Figure 28. Transient responses of linear AFC system for various loop gains.

3. Transient Response Parameters

The linear model can also be used to predict an approximate time constant, τ , for the closed-loop AFC system response when k is in the stable, monotonic region. Since the approximate time constant is associated with the envelope of the steps in Δf , it is significant only if several (> 10) sampling intervals are required for 90% of the frequency error to be removed, i.e., only for relatively small loop gains.

Recall that the homogeneous closed-loop difference equation is

$$f_o(N+1) = \gamma_1 f_o(N) \quad (33)$$

where

$$\gamma_1 \triangleq 1 - C_1(k+1) = 1 - (k+1)(1 - e^{-t_o/RC}) .$$

For the stable monotonic response,

$$0 < \gamma_1 < 1 .$$

By looking at the progression

$$f_o(T) = \gamma_1 f_o(0) ,$$

$$f_o(2T) = \gamma_1 f_o(T) = \gamma_1^2 f_o(0) ,$$

$$f_o(3T) = \gamma_1 f_o(2T) = \gamma_1^3 f_o(0) ,$$

etc.,

one can see that the general homogeneous response is given by

$$f_o(NT) = \gamma_1^N f_o(0) ,$$

or

$$f_o(t) = (\gamma)^{(t/\tau)} f_o(0), \text{ where } t = NT.$$

But the approximate time constant, τ , is defined such that*

$$f_o(\tau) = (e^{-1}) f_o(0) .$$

Since

$$f_o(\tau) = (\gamma)^{(\tau/T)} f_o(0) = (e^{-1}) f_o(0) ,$$

$$\gamma^{(\tau/T)} = e^{-1}, \text{ and}$$

$$\tau = \frac{-T}{\ln(\gamma)} ,$$

$$\tau = \frac{-T}{\ln [1 - (k + 1) (1 - e^{-t_o/RC})]} \quad (34)$$

Also, if $t_o \ll RC$,

$$\tau \approx \frac{-T}{\ln [1 - (k + 1) t_o/RC]} ; \quad (35)$$

if further $[(k + 1) t_o/RC] \approx 1$, then

$$\tau \approx \frac{T}{(k + 1) (t_o/RC)} . \quad (36)$$

Thus by using either Equation (34) or Equations (35) or (36), one can choose the AFC system open-loop gain to obtain the desired transient response time constant.

For higher gain (if ever desirable) and stable but alternating response, the overshoot is found from the homogeneous closed loop difference equation to be $-\gamma_1$.

* Note that the approximate time constant may not be an integer multiple of the sample period, T.

4. Sensitivity Analysis

In the analysis up to this point, the homogeneous difference equation has been used to investigate the system transient response. Now that it has been shown that for a wide range of system parameters the closed-loop AFC system is stable, it is reasonable to ask how well the AFC system does its job. That is, how much will the VCO frequency deviate from nominal for a given parameter change in the AFC loop. Although the term "frequency stability" is commonly used to describe the sensitivity of the VCO frequency to system changes, one must be careful not to confuse this with stability in the transient sense; i.e., stable versus unstable.

The system frequency stability or sensitivity can be determined from the AFC closed-loop difference equation without actually solving the difference equation. Assume that step-changes in all system parameters occur at $t = 0$ (changes are assumed small enough that the linear model remains applicable). It is known that the system will converge eventually to a steady-state or constant frequency if the loop gain has been chosen to satisfy the inequality

$$-1 < k < \left(\frac{2}{C_1} - 1 \right).$$

The steady-state frequency is determined from the AFC closed-loop difference equation by equating $f_o(N)$ and $f_o(N + 1)$. (Note that this can only be done after one is assured that the closed-loop system is not unstable.) The closed-loop difference equation is repeated here.

$$\begin{aligned} f_o(N + 1) + [C_1(k + 1) - 1] f_o(N) &= k_v V_m(N + 1) \\ &+ (k_v [C_1 - 1] V_m(N) + E \end{aligned} \quad (37)$$

where E is a function of the AFC system parameters, assumed constant at their new values:

$$E = C_1 \left\{ f_c - k_v (V_c + V_{\text{bias}}) + k_v k_A [(nk_{D1} + k_{D2}) f_R + (k_{D1} - k_{D2}) f_D] \right\} . \quad (38)$$

For steady-state analysis, one has

$$f_o(N) = f_o(N + 1) = f_o$$

and

$$V_m(N) = V_m(N + 1) = V_m .$$

The difference equation then reduces to the following algebraic equation:

$$C_1(k + 1) f_o = C_1 k_v V_m + E ,$$

or

$$f_o = \left(\frac{k_v}{k + 1} \right) V_m + \frac{E}{C_1(k + 1)} . \quad (39)$$

This is the equation for the steady-state VCO frequency. Note that C_1 is a multiplying factor of E and thus does not influence the steady-state VCO frequency. That is, the system sampling parameter

$$C_1 = 1 - e^{-t_o/RC}$$

influences only the transient response of the AFC system. Substituting for E from Equation (38), the steady-state frequency is written as follows.

$$f_o = \left(\frac{k_v}{k+1} \right) (V_m - V_c - V_{\text{bias}}) + \left(\frac{1}{k+1} \right) f_c + f_R \left[\frac{k_v k_A (nk_{D1} + k_{D2})}{k+1} \right] + f_D \left[\frac{k_v k_A (k_{D1} - k_{D2})}{k+1} \right] \quad (40)$$

Nominally, V_{bias} is set (experimentally) such that when the reference input voltage is present, the output frequency has its desired value of

$$(f_o)_{\text{nom}} = (n+1) f_R .$$

Also, the nominal values of other parameters are as follows:

$$f_c = (n+1) f_R ,$$

$$f_D = f_R , \text{ and}$$

$$k_{D2} = k_{D1} = k_o .$$

From this expression for the steady state nominal output frequency, it can be seen that system parameter perturbations influence the frequency output as follows. Let

Δf_c = shift in VCO frequency for fixed input voltage,

Δf_R = shift in reference oscillator frequency,

Δf_D = shift in discriminator center frequency,

ΔV_m = shift in reference input voltage,

ΔV_b = shift in bias voltage, and

Δf_o = resultant shift in nominal VCO frequency.

Then the resultant output frequency error is given by

$$\Delta f_o = \left(\frac{k_v}{k+1} \right) \Delta V_m - \left(\frac{k_v}{k+1} \right) \Delta V_b + \left(\frac{1}{k+1} \right) \Delta f_c + \frac{k_v k_A (nk_{D1} + k_{D2})}{k+1} \Delta f_R + \frac{k_v k_A (k_{D1} - k_{D2})}{k+1} \Delta f_D \quad (41)$$

(Note: $k = k_v k_A k_{D1}$)

which is approximated as follows for $k \gg 1$ and $k_{D1} \approx k_{D2}$

$$\Delta f_o \approx \left(\frac{k_v}{k} \right) \Delta V_m - \left(\frac{k_v}{k} \right) \Delta V_b + \frac{\Delta f_c}{k} + (n+1) \Delta f_R + \left(\frac{k_{D1} - k_{D2}}{k_{D1}} \right) \Delta f_D \quad (42)$$

The terms of Equation (42) are considered one-by-one in the following. The first shows the prime function of and a reason for the existence of the AFC loop; any shift in the reference voltage level of the input signal will result (steady state) in an error in the output VCO frequency that is $(1/k)$ times that for an open-loop system. The second term shows that variations in the input bias voltage have a steady-state effect similar to shifts in the input reference level. The third term is the most important term. It shows that VCO frequency shifts due to any internal (to the VCO) changes will also be corrected by the AFC loop such that the resultant f_o error will be reduced by a factor of $(1/k)$. The fourth term points out that percentage perturbations in the reference frequency appear directly (un-attenuated) in the VCO output frequency (note that $f_o \approx (n+1) f_R$). The remaining term is small since it is of second order: both $(k_{D1} - k_{D2})$ and Δf_D are normally small.

5. Summary of Analysis

The preceding AFC system analysis serves two purposes. The insight gained in the functioning of the system enables one to better choose system parameters in design or re-design efforts and evaluate (without hardware) proposed changes in the system gains, etc. The linear analysis also can serve as a checkcase in the development of a computer simulation of the AFC system. Note that the simulation, after initial debugging, will use more complete, nonlinear models for the subsystems and will thus provide more realistic estimates of system behavior, especially for large frequency deviations which may produce saturation in the real system. The next section of this report describes the development of the computer simulation from the system block diagram.

E. Simulation-Linear

1. Development of Simulation Program

The actual development of an AFC system simulation program requires only a small step beyond the development of the math model indicated by the block diagram in Figure 26 and does not depend directly upon the analysis in the previous section (except for de-bugging of the resulting program).

The program is written so as to repeatedly "go around" the AFC loop evaluating the (algebraic) transfer functions and updating the variables representing the states and/or outputs of each block. A "memory" of the previous (i.e., previous time around the loop) value of variables is required only for the variables associated with the dynamic transfer function(s). The predominance of algebraic rather than dynamic blocks in the AFC system model makes the simulation program especially simple.

The heart of the program is the repeated evaluation of only eight equations. Referring again to Figure 26, and beginning at the feedback point, the following equations are written:

$$\begin{aligned}
V &= V_m - V_4 , \\
f_o &= f_c + k_v (V - V_c) , \\
f_i &= f_o - n f_R , \\
V_1 &= k_{D1} (f_i - f_D) , \\
V_2 &= k_{D2} (f_R - f_D) , \\
V_5 &= V_1 - V_2 , \\
V_3 &= V_{\text{bias}} + k_A V_5 , \\
V_4(N+1) &= V_4(N) + [V_3(N) - V_4(N)] C_1 . \tag{43}
\end{aligned}$$

The basic linear AFC system simulation program consists of (1) an initialization section, (2) a DO LOOP to evaluate repeatedly the above equations, and (3) instructions for printing the simulation results. A listing of this basic program, including explanatory comments, is given in Appendix E. Note that with the aid of the comments it is easy to see where to insert any desired non-linear model for a block or subsystem.

A sample output from the basic program is also given in Appendix E. The loop gain for this run is 100. Note that the input step in V_m occurred at the 10th sample interval and that the system had essentially recovered (error frequency down by 90%) by the 40th step.

2. Verification of Linear Simulation

For those loop gains for which the transient response is stable and monotonic, the system time constant is given by Equation (34) as derived earlier, or in graphical form by Figure 29. Similarly, the resultant system steady state frequency error for a shift in nominal VCO frequency is given by Equation (41) and sketched in Figure 30. To verify the simulation (linear), the response time constants and steady state errors of simulation runs for several loop gains will be compared with the theoretical

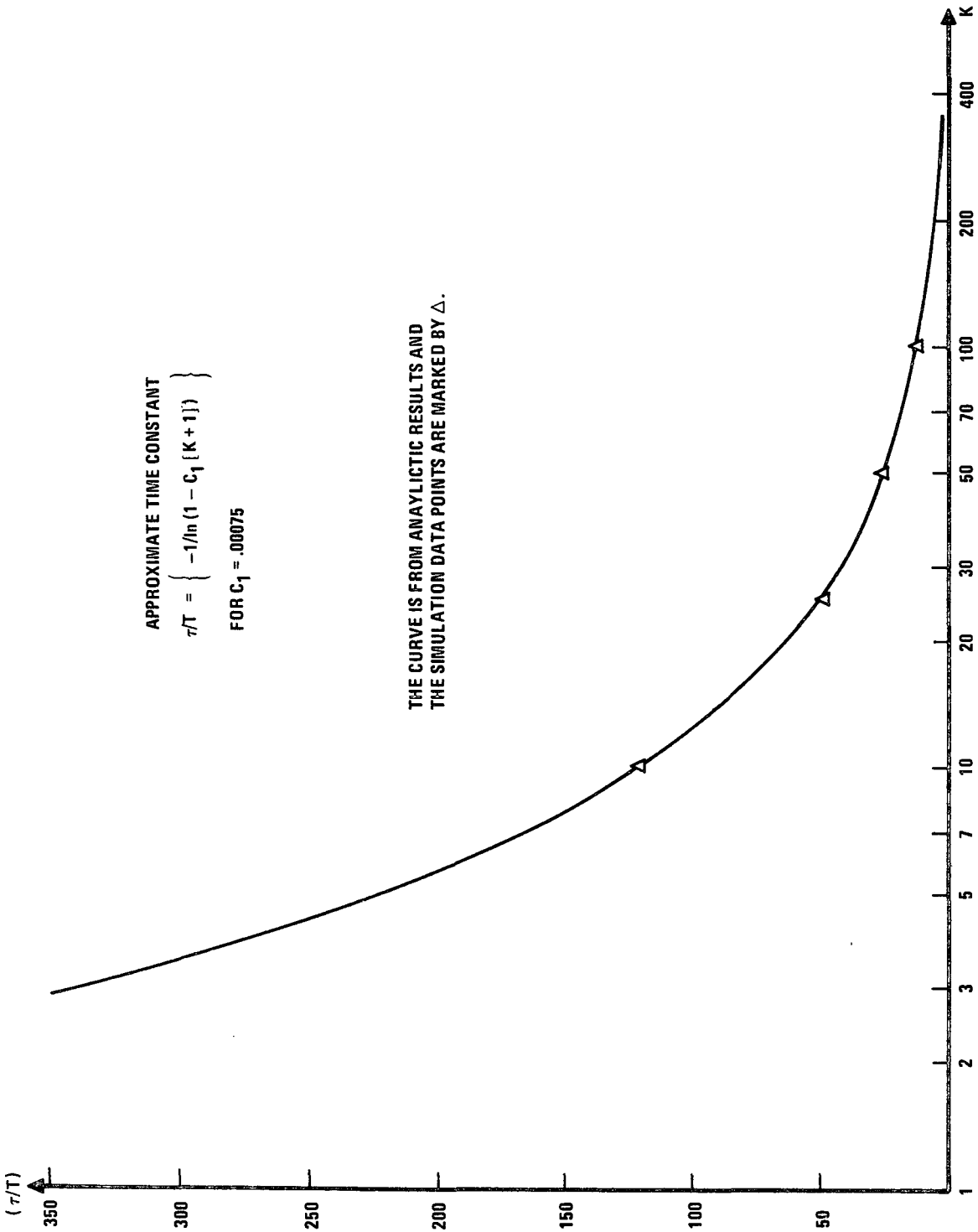


Figure 29. AFC system approximate time constant.

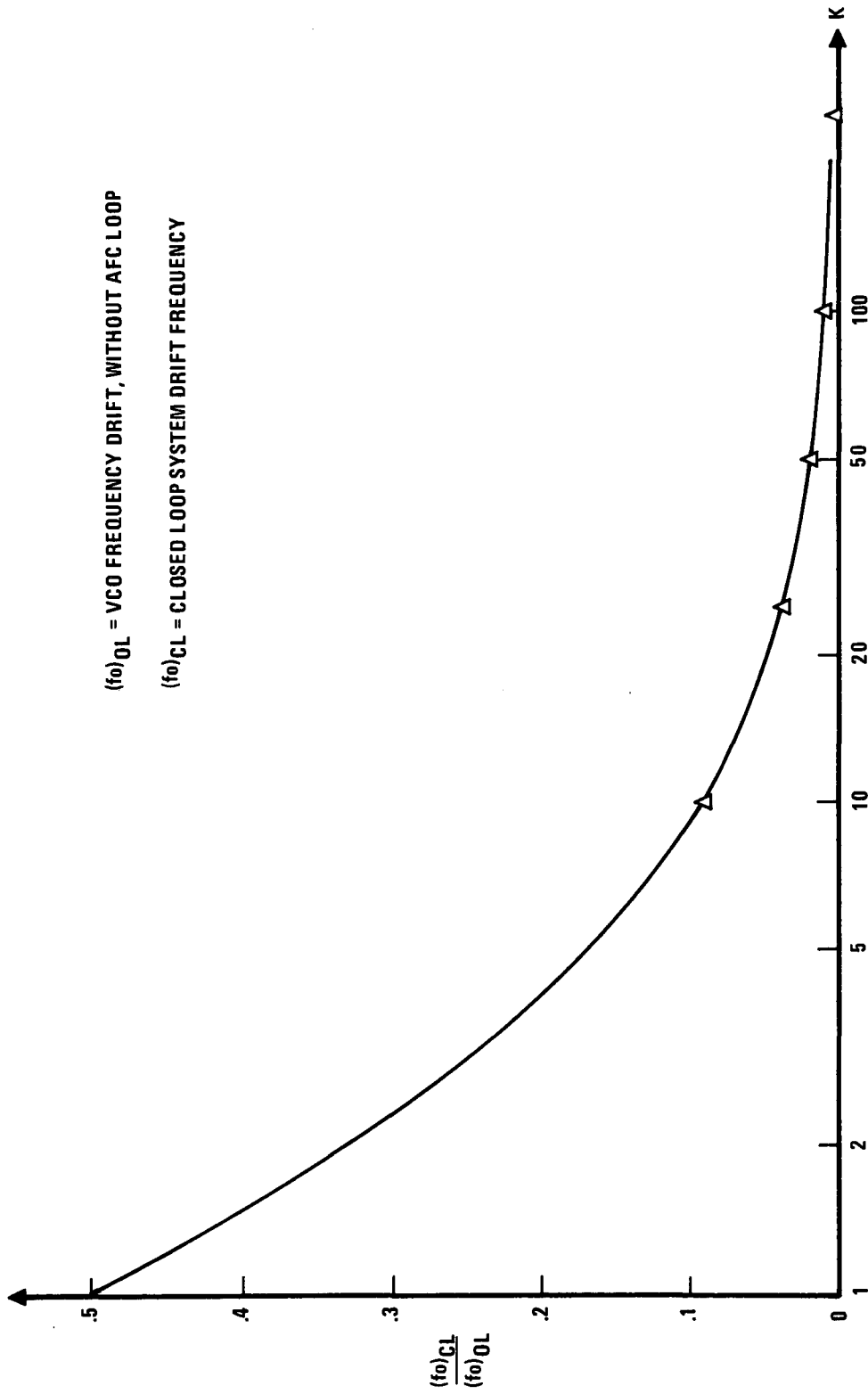


Figure 30. Steady-state frequency error.

or expected values. The data continues to be that for an AFC loop with sampler parameters such that the characteristic of the sampler is described by $C_1 = -.00075$. For the comparisons, loop gains of 10, 25, 50, and 100 will be used.

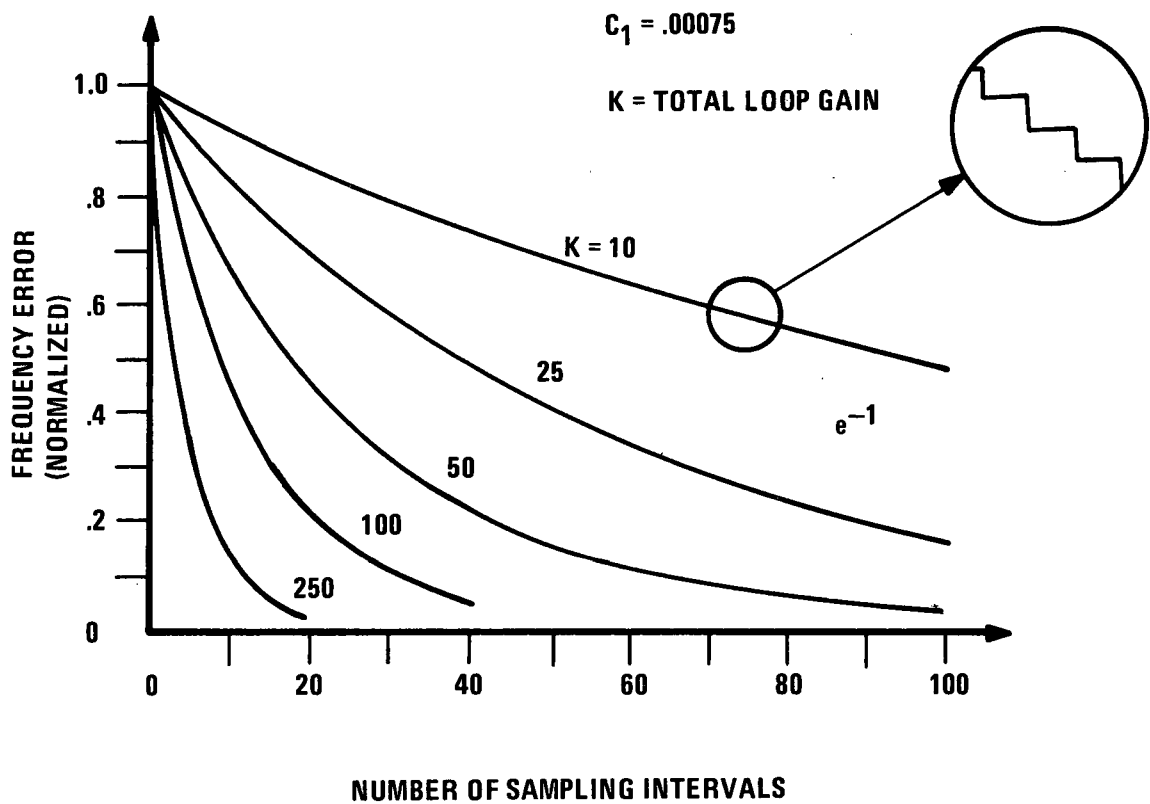
From the simulation runs from which the transient responses plotted in Figure 31 were obtained, the simulation "final" values of frequency error (approximate since settling was not complete) shown in Table II were read. These errors are to be compared with an initial error of 1.4×10^6 Hz; i.e., the ordinate of Figure 30 is to be multiplied by this initial error before comparing. The simulation final errors are seen to be essentially in agreement with the predicted values; the small differences are a result of ending the simulation at a finite time.

Having verified the steady state performance of the simulation program, one next investigates the transient behavior. In using the plot of the system time constant versus gain, note that this time constant is for the decay from the initial error frequency to the steady-state frequency error. That is,

$$\Delta f(\tau) = (\Delta f)_{ss} + e^{-1} [(\Delta f)_{t_0} - (\Delta f)_{ss}] \quad (44)$$

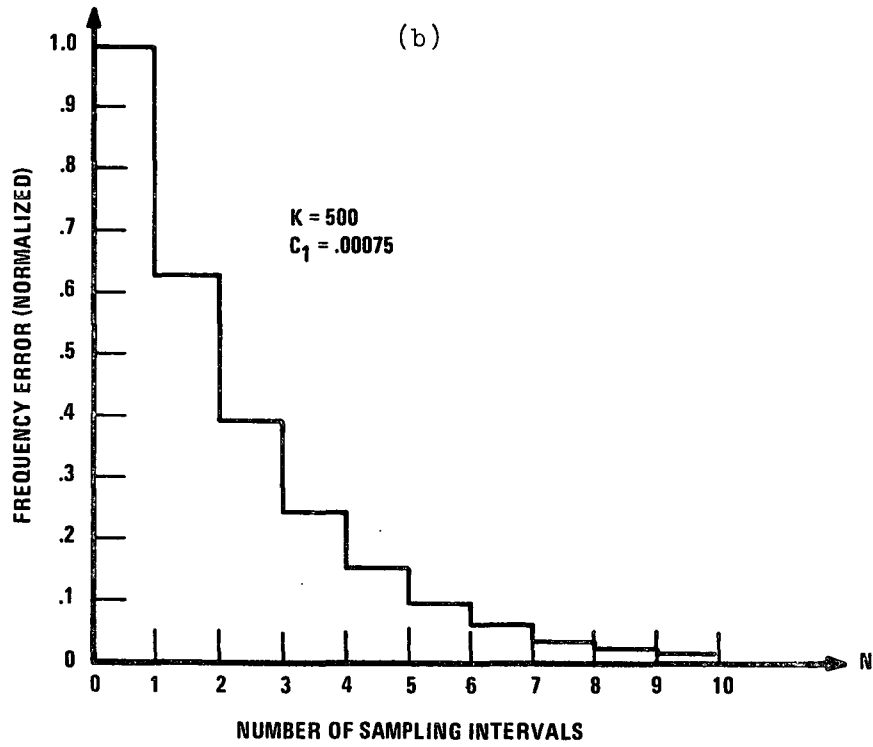
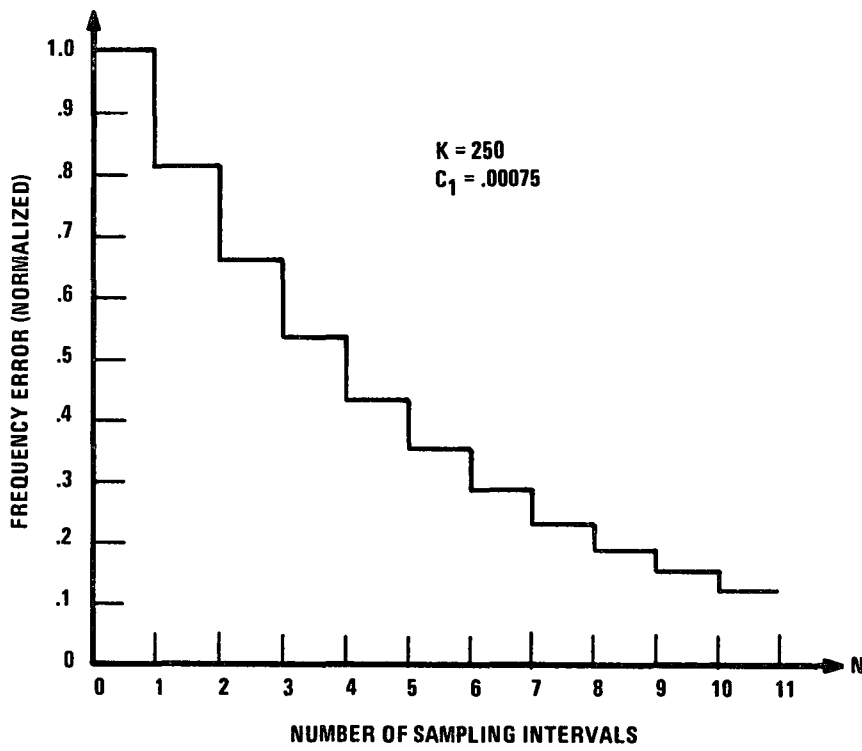
TABLE II
COMPARISON OF THEORETICAL AND SIMULATED FREQUENCY ERRORS

k	$(\Delta f)_{ss}$	
	<u>Simulation</u>	<u>Predicted</u>
10	127596	127272
25	54358	53846
50	28014	27451
100	14388	13861
500	2796	2794



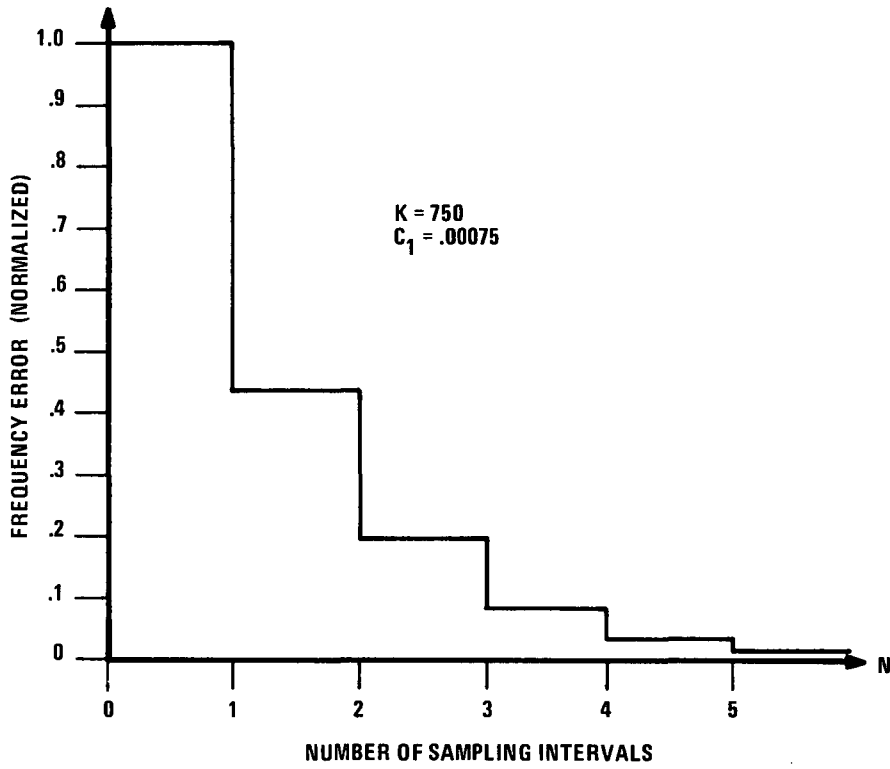
(a)

Figure 31. Step response of the VCO frequency in a sampling AFC loop for various values of loop gain in the linear simulation.

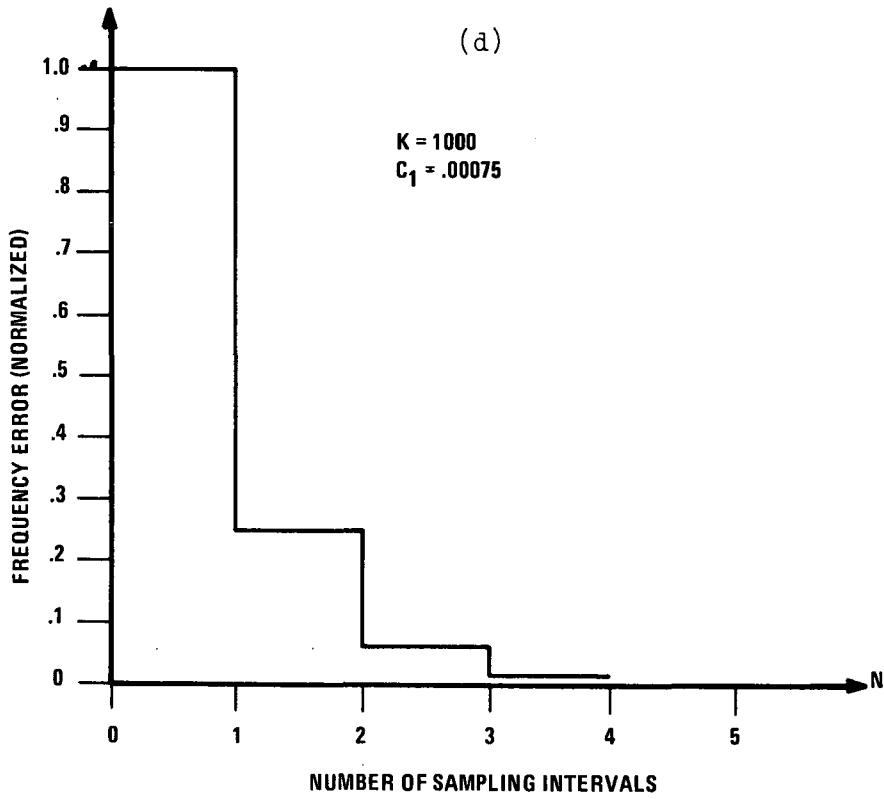


(c)

Figure 31 (Continued).



(d)



(e)

Figure 31 (Continued).

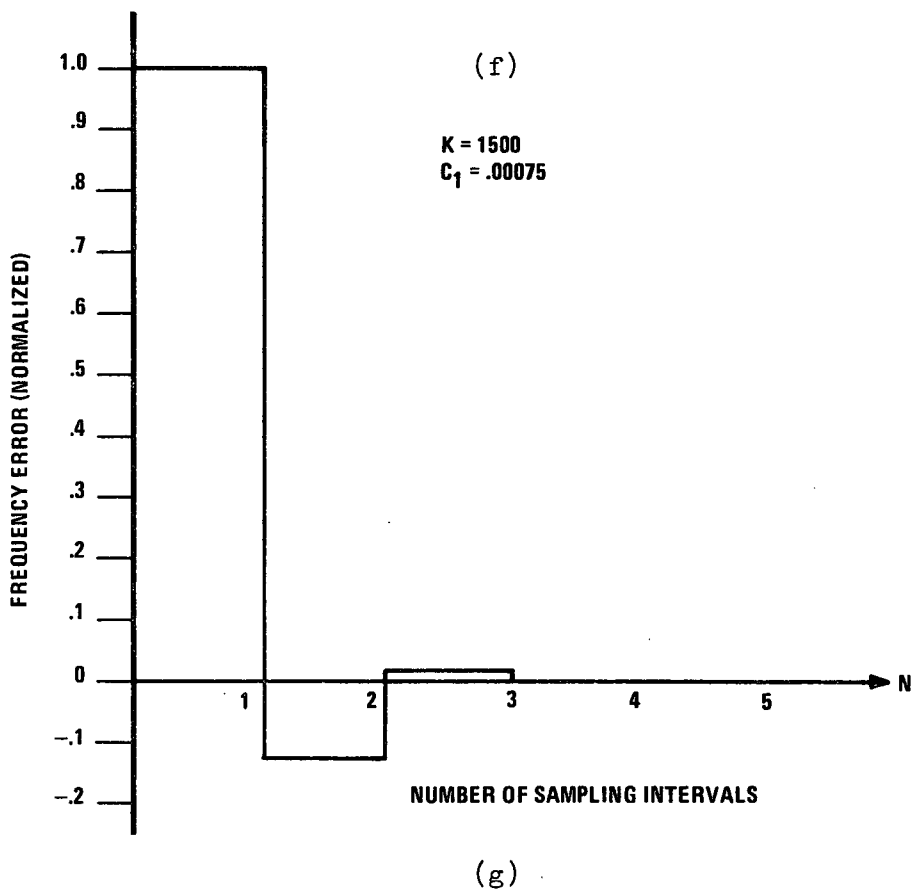
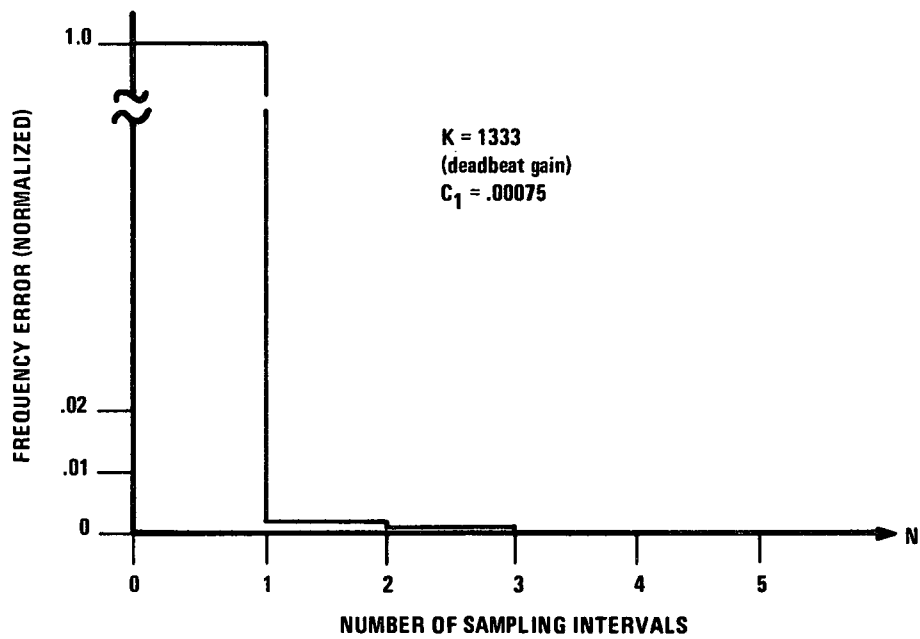
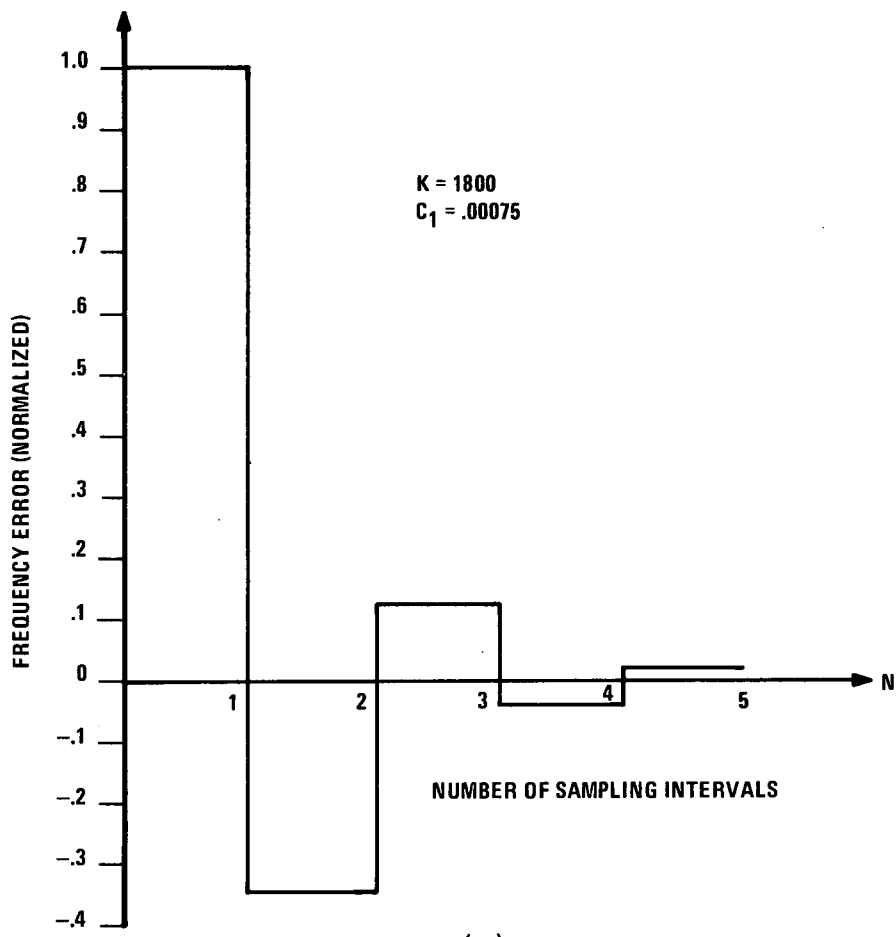
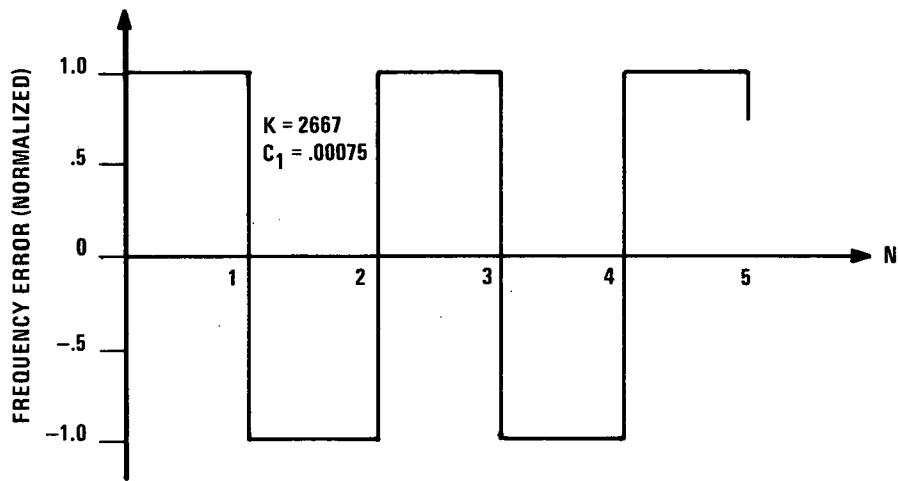


Figure 31 (Continued).

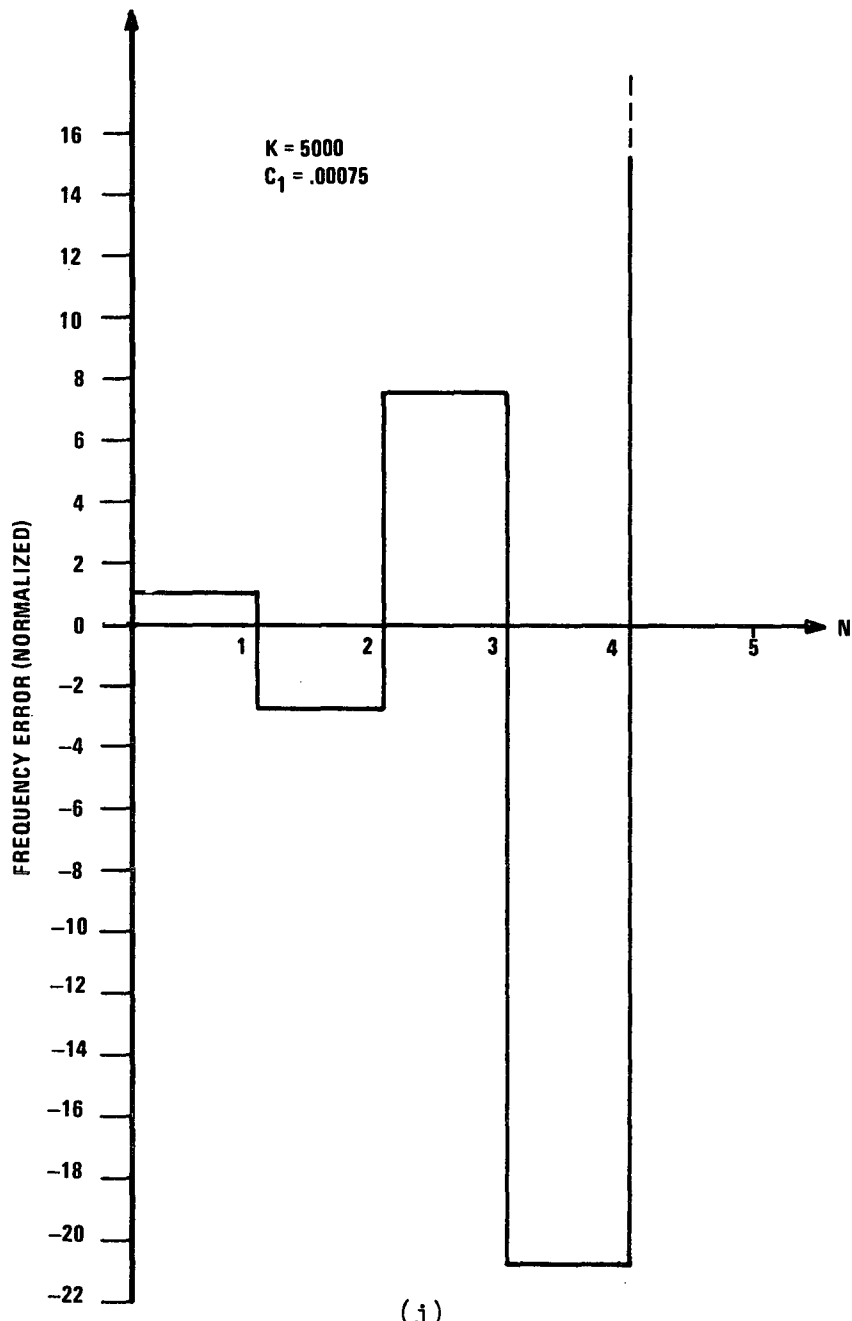


(h)



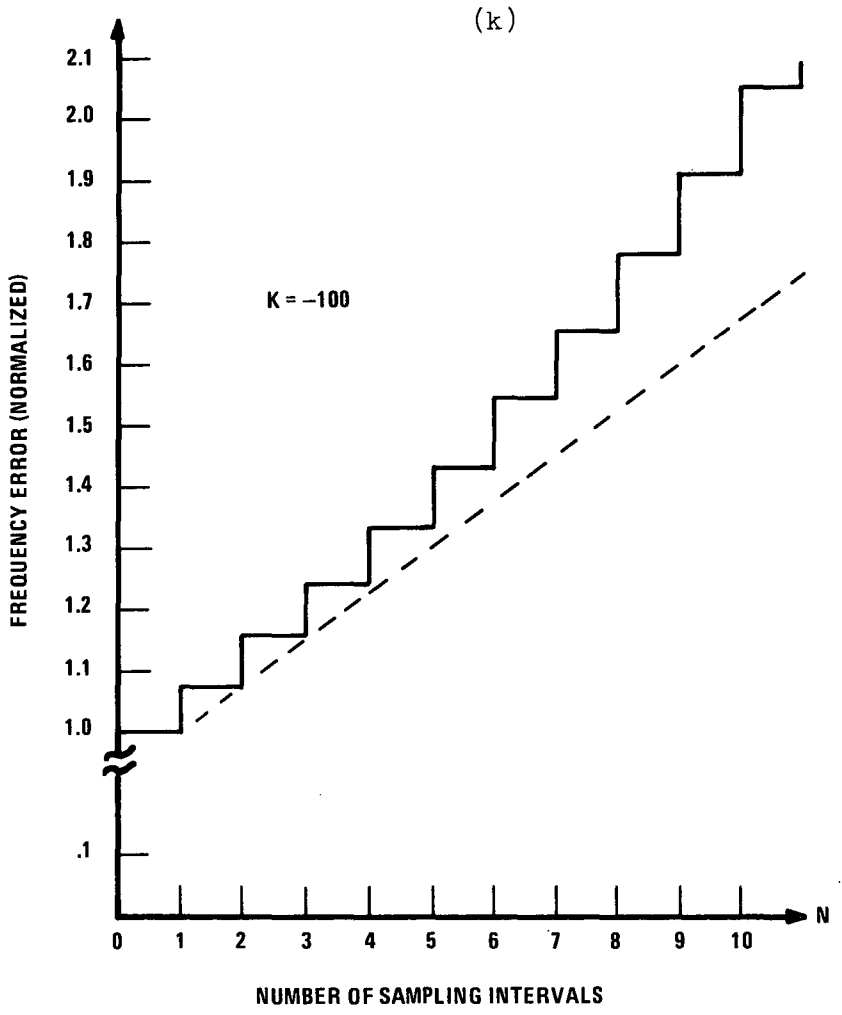
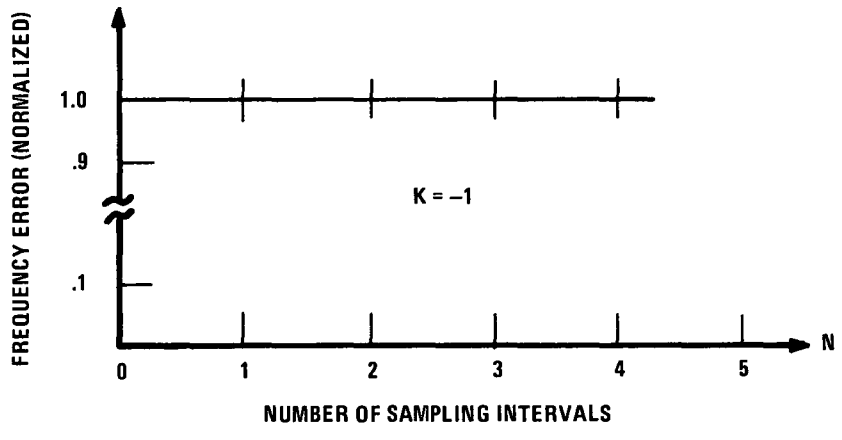
(i)

Figure 31. (Continued)



(j)

Figure 31 (Continued).



(1)

Figure 31 (Continued).

where $t = \tau$, the system time constant,

$(\Delta f)_{ss}$ = steady state frequency error,

$(\Delta f)_{t_0}$ = initial frequency error from which the system is recovering.

To verify the simulation transient response, the above expression for the frequency error at one time-constant, $\Delta f(\tau)$, is evaluated for each of several values of loop gain. (The predicted value of $(\Delta f)_{ss}$ can be used.) The calculated values of $\Delta f(\tau)$ for $k = 10, 25, 50,$ and 100 are tabulated in the second column of Table III. Referring then to the individual simulation runs, the time at which Δf has the value $\Delta f(\tau)$ is noted and the elapsed time since the start of the decay, normalized by dividing by the sample period, is recorded in Column 3 of the table. Finally, the predicted value of τ/T is calculated from Equation (34) for each gain and is recorded in the fourth column of Table III. Note that the differences between the simulation and predicted values of τ/T are less than one (step) and result from the use of a continuous expression, Equation (34), to approximate the discrete system.

TABLE III

COMPARISON OF THEORETICAL AND SIMULATED TIME CONSTANTS

k	$\Delta f(\tau)$	τ/T	
		Simulation	Predicted
10	595482	121	120.8
25	549068	51	50.8
50	532384	26	25.7
100	523793	13	12.7

As with the steady-state comparisons, the transient comparisons verify the correctness of the simulation. Now that the total AFC system is known to be correctly simulated, individual subsystems, or blocks, will be modeled in more detail in the simulation. Unlike the linear simulation, the later version will give results not available analytically. Specifically, the effects on the system performance of a limiter in the feedback path or a nonlinear VCO characteristic will be determined by simulation.

F. Simulation - Nonlinear

The linear simulation results show that as the loop gain is increased, both the transient response time and the steady-state frequency error go down, with the response time even reaching one sampling period for the gain referred to as "deadbeat gain." However, for reasonable sized frequency errors, these larger gains would result in very high voltages in the AFC loop, and the linear model of the AFC loop is not applicable for high voltages. It still may be desirable to use high gains so that the frequency error will be small and the small perturbations will disappear rapidly, if the system nonlinearities do not introduce stability problems at the higher signal levels; to investigate this area, the simulation will be modified to include the two predominant nonlinearities.

1. Limiter

The saturation of the feedback signal processing stages will be modeled as a single limiter located between the output of the error signal amplifier and the input to the sample-and-hold circuit, at a point after the summing of V_{bias} with the error signal. The large-signal nonlinearity of the oscillator (VCO) input-output curve can be modeled in the simulation by replacing the linear VCO model with either a nonlinear analytic function fitted to actual VCO characteristics, or by using a table-look-up and

interpolation scheme on data points from an actual VCO characteristic curve.

The saturation effect will be modeled by an ideal limiter. As long as the input signal has a magnitude less than the limit, L , the limiter has no effect on the signal; if, however, the input signal magnitude exceeds L , the output has the sign of the input signal but has magnitude L .

Simulation runs with the limiter in the program with several values of loop gain, k , have been made and plots of the error frequency versus time are given in Figure 32. These responses should be compared with those for the linear model which have been given in Figure 31. The responses show that the effect of the limiter is to slow the recovery process to a rate determined by the limiter, until the error signal becomes small enough to be within the linear region of the limiter. Thus the shape of the response curve depends upon the amplitude of the disturbance. Since the (stability) effect of the limiter is similar to that of reduced gain, and since the AFC system does not become unstable for decreased positive gains, the addition of the limiter would not be expected to introduce stability problems. This is born out by the simulation results. On the other hand, the limiting voltage must be set high enough so that expected variations in the reference value of the modulating signal, $(V_m)_{ref}$, do not bias the system so much that the sampler cannot supply the voltage required to offset V_m and keep the VCO frequency near nominal.

Figure 32 shows that the effect of including the limiter in the AFC loop simulation is to limit the slope of the response curve. Once the error signal is reduced below the saturation level, the response rate is determined by the time constant derived earlier; while still in saturation, the response rate is independent of the feedback gain. Note, however, that the value of Δf at which the system saturates depends upon the loop gain.

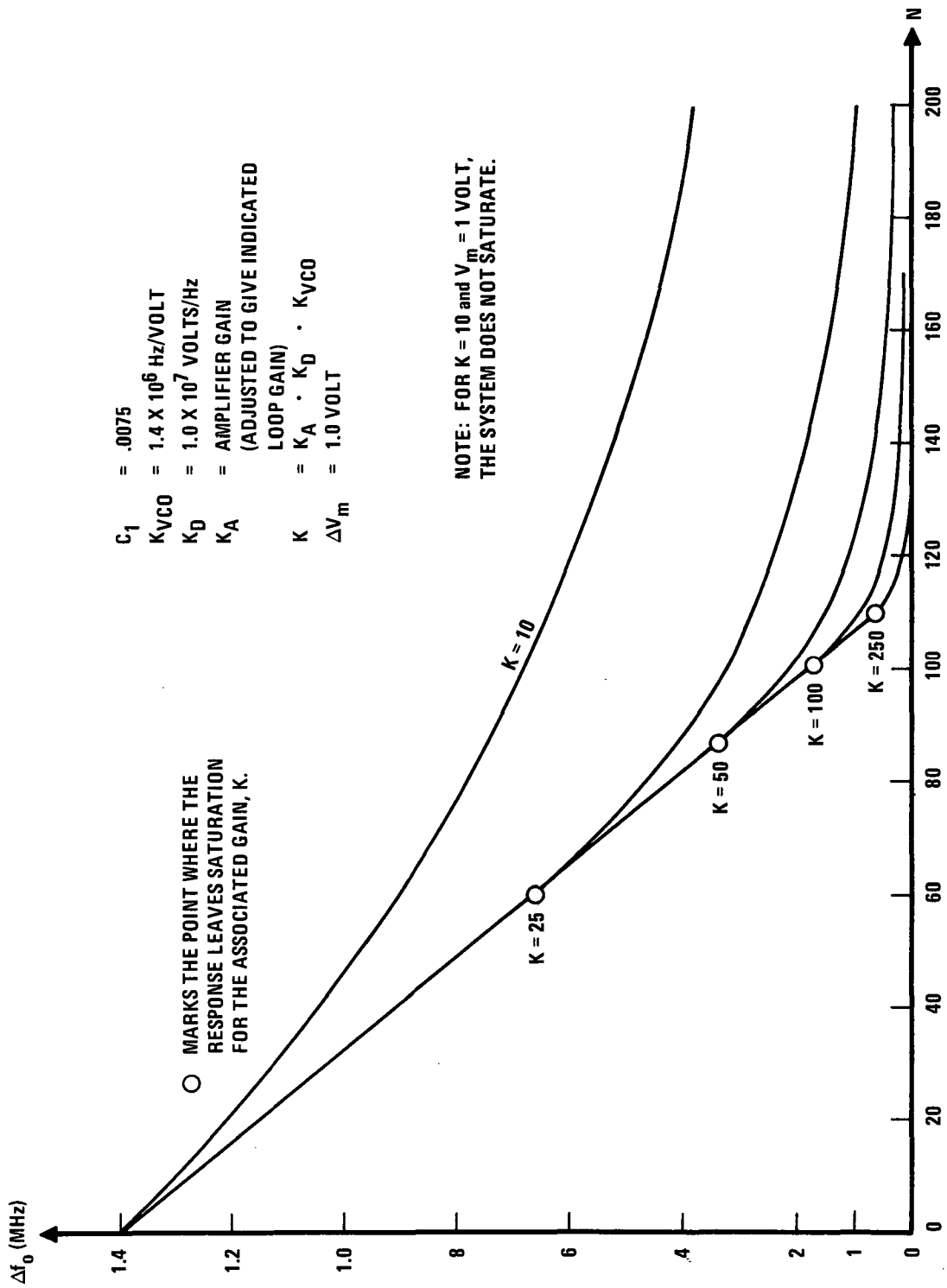


Figure 32. AFC loop simulation response with limiter set at 12 volts.

Thus the advantages of short transient time and low steady state frequency error associated with the higher loop gains in the linear model still apply. The only change in performance is the limiting of the response slope when the error frequency is large. Of course, the idea of a "deadbeat gain" is only applicable for the small frequency errors.

2. Nonlinear VCO

The Voltage Controlled Oscillator (VCO) characteristic curve (output frequency versus input voltage) was shown in Figure 22 as nonlinear but has been approximated for analysis and simulation thus far by a linear model. The VCO characteristic shown in Figure 33, which has an exaggerated nonlinearity, has been simulated in the AFC simulation to study the effects of the nonlinearity on the AFC system response. A listing of the AFC simulation program including the nonlinear VCO model and saturation is given in Appendix F. A typical simulation run is included. To simulate a particular VCO characteristic, one would simply replace the nonlinear equation with a curve-fit of the desired VCO characteristic.

Figure 34 shows the frequency-error transient response curves for the nonlinear VCO model. Note that the system remains stable and that the form of the response is changed very little by the inclusion of the nonlinearity. As would be expected from the sketch of the VCO nonlinearity (Figure 33), the VCO "gain" decreases as the input voltage increases above its nominal value and the gain increases as V drops below its nominal value. At the nominal point, the VCO "gain" is that used in the linear simulation. In the simulation runs, the input reference modulating voltage is stepped by one volt from $V = 7$ to $V = 8$ volts. In the linear model this produces an initial frequency error of 1.4 MHz; for the nonlinear VCO of Figure 33 the frequency shift is only 0.8 MHz. Note that if the voltage shift had been of the opposite polarity the nonlinear VCO frequency shift would have

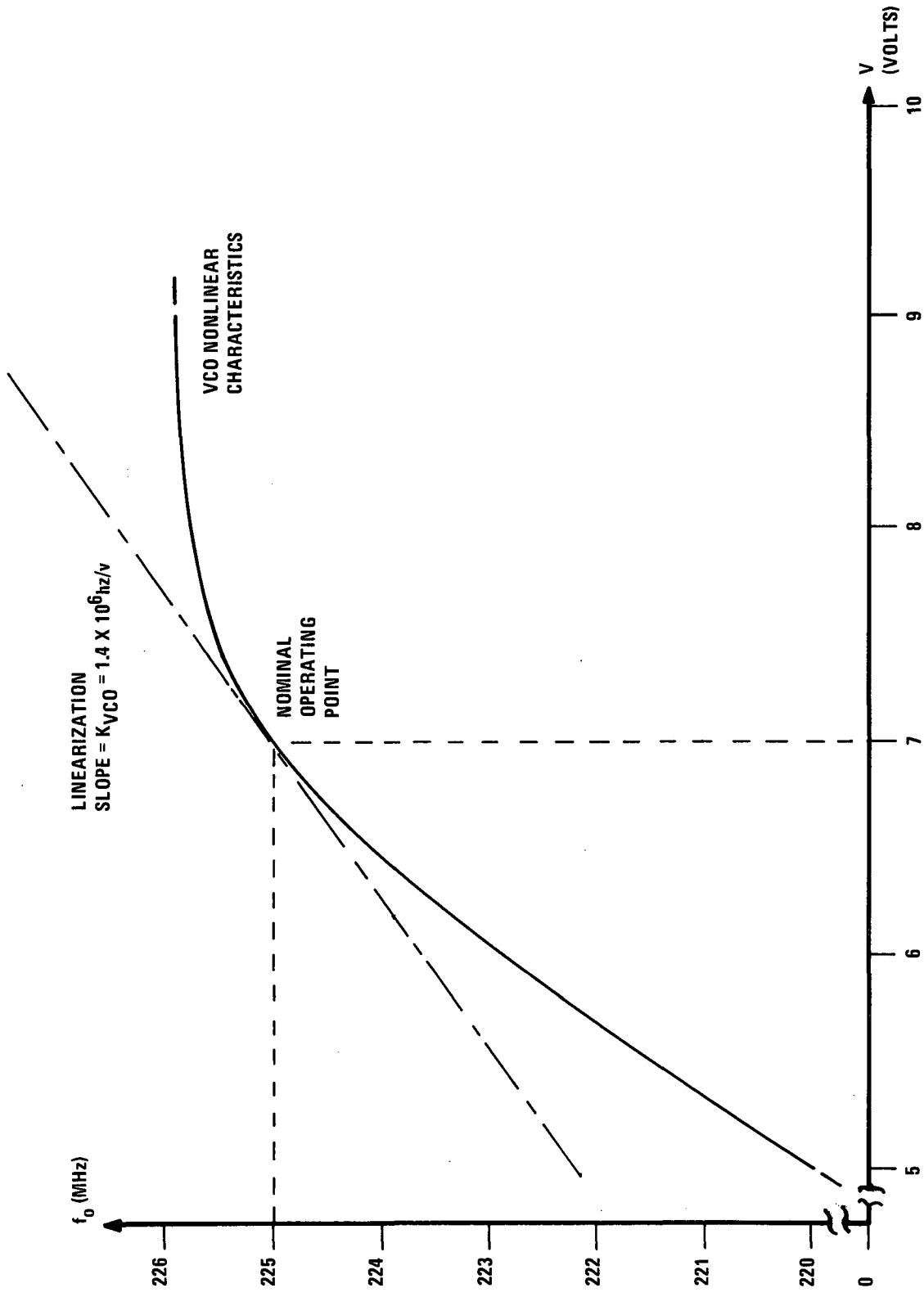


Figure 33. VCO characteristic (exaggerated).

AFC SIMULATION TRANSIENT RESPONSE
WITH NONLINEAR VCO AS IN FIGURE -

GAIN, K, IS EVALUATED AT OPERATING
POINT ON VCO CHARACTERISTIC

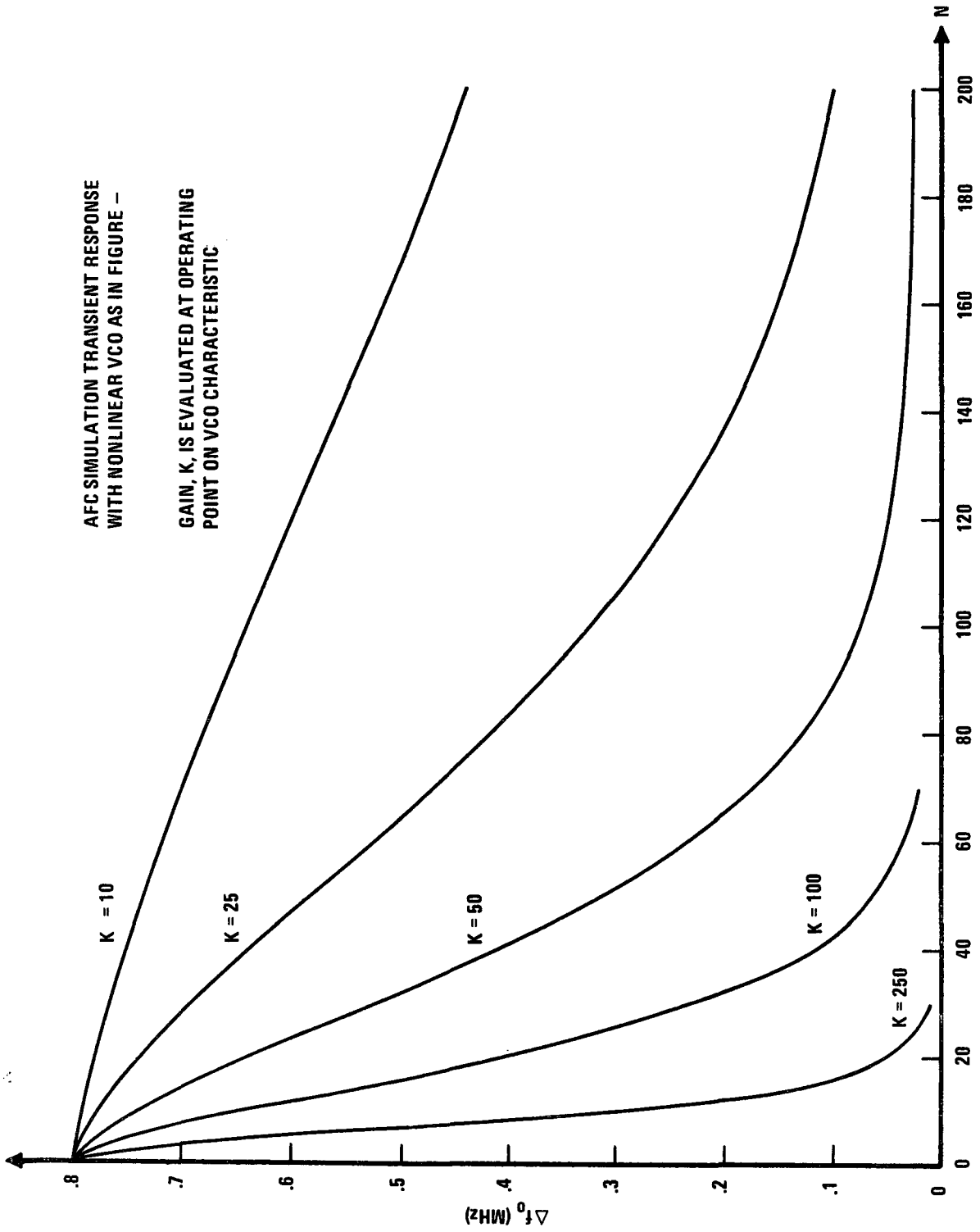


Figure 34. AFC simulation transient response with nonlinear VCO

been -2.0 MHz while that for the linear one would have been only -1.4 MHz.

From the transient responses in Figure 34 the effective gain reduction due to the VCO nonlinearity can be seen to decrease the magnitude of the initial slope. The effect is most easily seen for $k = 25$, but is present for all gains. In the linear model, the transient responses (when smoothed) were exponential decay curves (see Figure 31).

3. Limiter and Nonlinear VCO

Figure 35 gives the transient responses computed when both the nonlinear VCO model and the saturation effect were in the simulation program. Note that (1) the saturation portion of the curve is no longer a straight line, (2) the form of the response for (a) the linear AFC model, (b) the limiter, (c) the nonlinear VCO, or (d) the nonlinear VCO and the limiter are basically the same (Figures 31, 32, 34, and 35) and (3) the steady state frequency error for a given shift in $(V_{m \text{ ref}})$ is essentially the same for all the simulation models. The "final" frequency errors arrived at by the simulation model containing the nonlinear VCO and the limiter are tabulated for nominal loop gains ranging from 10 to 500 in Table IV.

TABLE IV
STEADY STATE FREQUENCY ERRORS WITH
NONLINEAR VCO AND LIMITER IN THE AFC SYSTEM

<u>Gain</u> (k)	<u>$(\Delta f_{o \text{ ss}})$</u> (MHz)
10	.128
25	.054
50	.029
100	.014
250	.006
500	.003

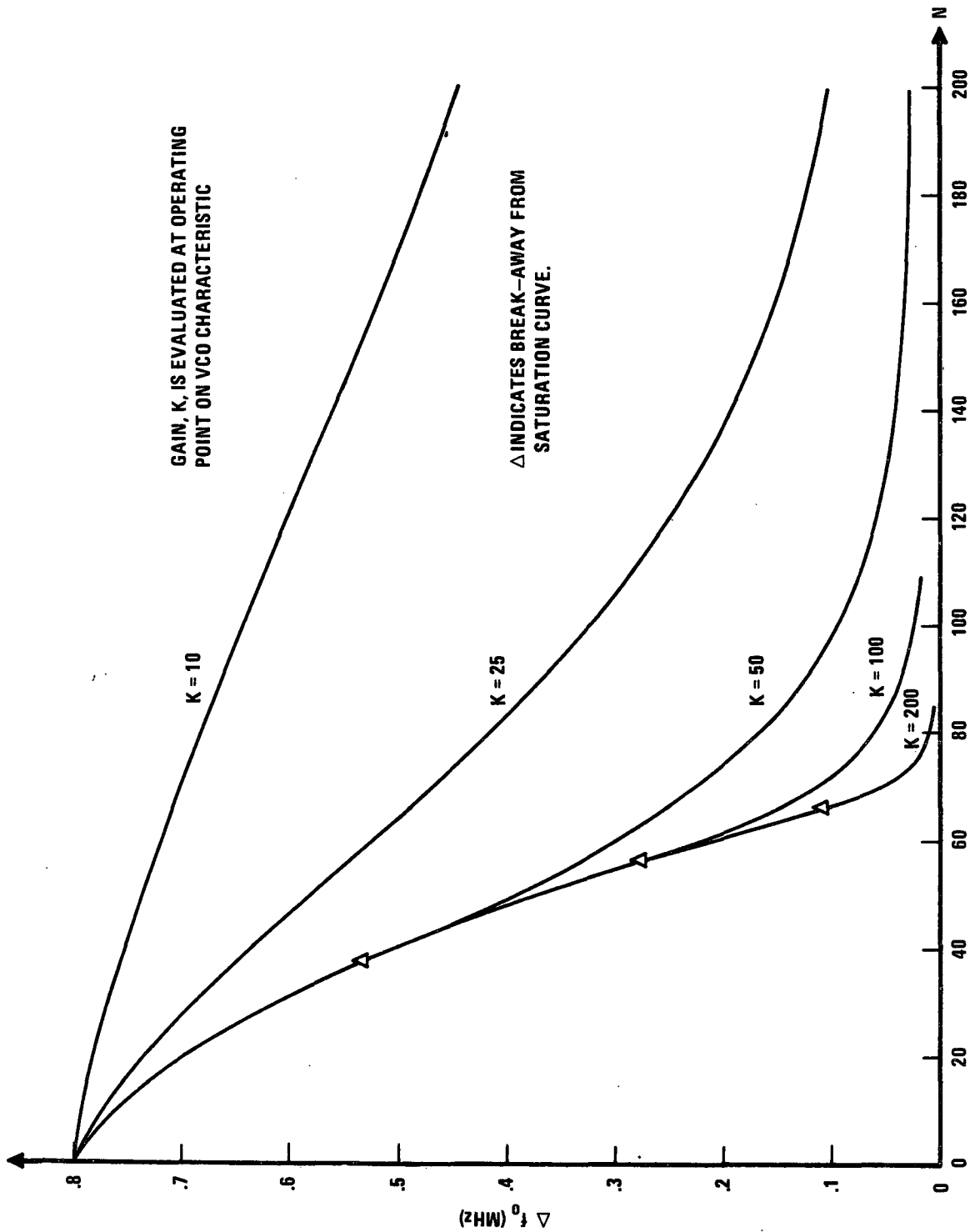


Figure 35. AFC simulation transient response with nonlinear VCO and with ± 12 volt limiter.

The table lists the steady state frequency error as a function of AFC loop gain for an open loop frequency shift of 0.8 MHz. In each case k is measured at the nominal VCO operating point.

G. An Alternate Sampling System

The feedback signal sampling circuit discussed thus far can be replaced by a simpler one with only a small loss in versatility. Deletion of the hold device in front of the RC charging circuit results in an AFC system that is somewhat slower in response at the higher gains, but is simpler to implement and is stable for all loop gains. The simplified system is not capable of "deadbeat" response, however. Consider the sampling scheme depicted in Figure 36.

1. Analysis

The differential equation describing the linearized AFC system with the simplified sampler will be derived using Figures 26 and 36. An algebraic expression relating the sampler input, V_3 , to the sample-and-hold output, V_4 , and the system parameters derived from Figure 26 is

$$V_3 = -kV_4 + D, \quad (45)$$

where the constants are

$$k = k_A k_{D1} k_v, \text{ and}$$

$$D = V_{\text{bias}} + k_A (k_{D1} [f_C - nf_R - f_D + k_v (V_m - V_c)] - k_{D2} [f_R - f_D]) . \quad (46)$$

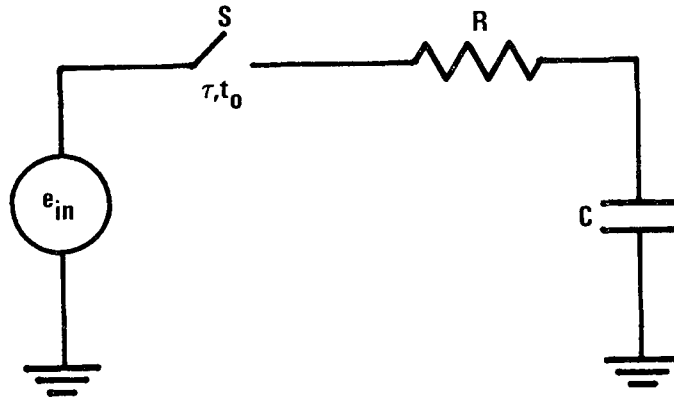


Figure 36. Alternate Sampler Model.

Combining this result with a description of the sampler, the closed-loop AFC system differential equation can be written. The simplified sampler (Figure 36) is a charging RC circuit whose response is governed by

$$(RC) \frac{de_o(t)}{dt} + e_o(t) = e_1(t) \quad (47)$$

where $e_1(t)$ and $e_o(t)$ are the (sampled) input and output voltage, respectively. Thus

$$(RC) \dot{V}_4 + V_4 = V_3 \quad (48)$$

From consideration of the upper portion of Figure 26,

$$V_4 = (f_c - f_o)/K_v + V_m - V_c \quad (49)$$

so that

$$\dot{V}_4 = -\dot{f}_o/K_v \quad (50)$$

Similarly, from the lower portion of Figure 26 one can deduce that

$$V_3 = k_A k_{D1} f_o + V_{bias} + k_A [k_{D1} (-nf_R - f_D) - k_{D2} (f_R - f_o)] \quad (51)$$

Substituting Equations (49), (50), and (51) into Equation (25), and recognizing that V_m is constant during the sampling interval, the differential equation governing the AFC system response during the sampling interval is

$$(RC) \dot{f}_o + (k + 1) f_o = k_v \left\{ V_m - V_c + \frac{f_c}{k_v} - V_{bias} + k_A \left[k_{D1} (nf_R + f_D) + k_{D2} (f_R - f_D) \right] \right\} . \quad (52)$$

The system is seen to be stable for all positive values of gain, k , with the sampling-interval time constant being inversely proportional to the open loop gain for large gains, i.e., $\tau_{SI} = RC/(k+1)$. The step response is always underdamped. Assuming that the sampling duration is t_o and that the sampling period is given by T , the effective time constant* is given by

$$\tau = \left(\frac{T}{t_o} \right) RC / (k + 1) . \quad (53)$$

For the typical parameter values used with the earlier sampler, the difference between the effective time constants for the two sampling schemes is negligible for loop gains below 500; that is, only when the deadbeat gain is approached does the earlier system show any advantage. Table V gives a comparison of the AFC system effective time constants for the two sampling schemes. The transient responses of the two systems are essentially identical for normal AFC loop gains. The steady state responses (sensitivities) of the two are also identical [see Equation (41)].

2. Simulation

A simulation using the alternate sampler AFC system

*The "effective time constant" has significance when the loop gain is low enough that "several" sampling intervals are required for recovery from a disturbance.

TABLE V

COMPARISON OF AFC EFFECTIVE TIME CONSTANTS OF
 TWO SAMPLING SCHEMES FOR $R = 20,000$ OHMS
 $C = 1 \times 10^{-7}$ FARADS, and $t_o = 1.5 \times 10^{-6}$ SECONDS

<u>Gain</u> (k)	<u>τ</u> <u>Alternate</u> <u>Sampler</u>	<u>Percent</u> <u>Difference</u>	<u>τ</u> <u>Flat-Top</u> <u>Pulse Sampler</u>
-1	∞		∞
-0.5	2666.6667	-.019	2667.1667
0	1333.3333	0	1333.3333
1	666.6666	.038	666.466
10	121.2121	.377	120.7569
25	51.2821	.950	50.7996
50	26.1438	1.924	25.6503
100	13.2013	3.950	12.6997
250	5.3121	10.745	4.7967

500	2.6613	25.344	2.1232
750	1.7754	46.982	1.2079
1000	1.3320	84.897	.7204
1250	1.0658	190.220	.3598
1333	1.0002		0

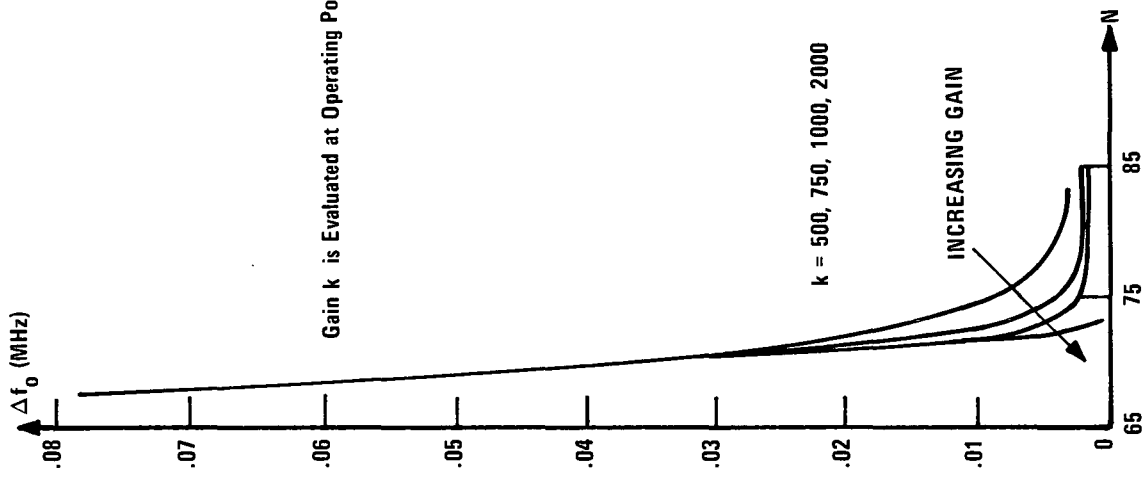
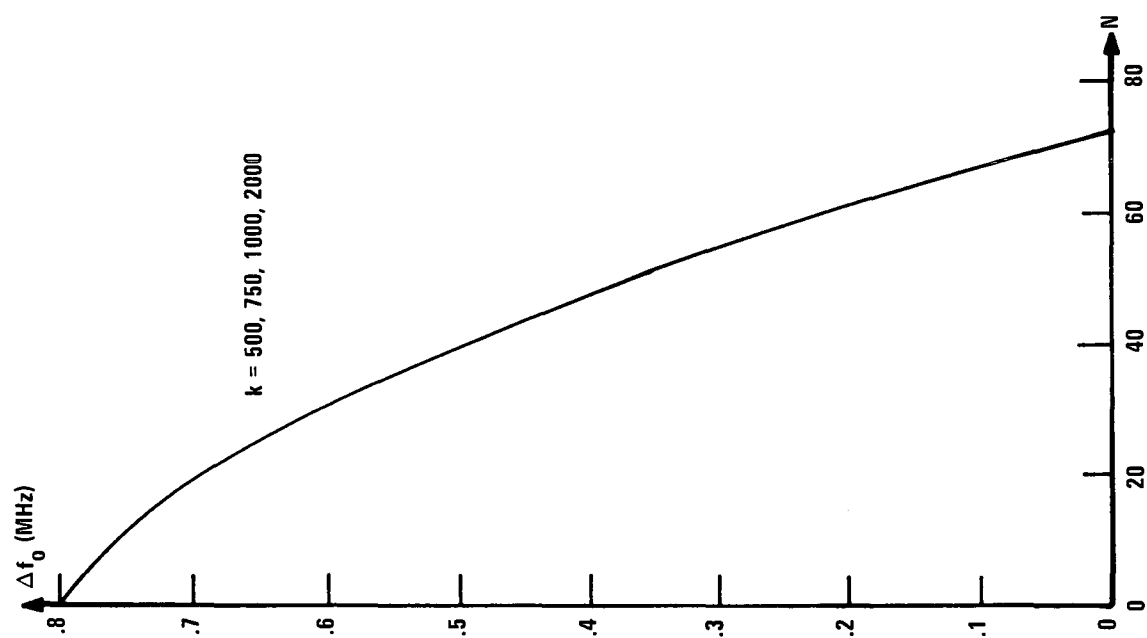
along with the nonlinear VCO and limiter models was constructed. A listing of the simulation is included along with one simulation run ($k = 250$) in Appendix G. The response is not significantly different from that obtained with the flat-top pulse sample scheme (see Figure 35) for the lower gains ($k = 10, 25, 50, 100$). Figure 37 shows the response for AFC loop gains of $k = 500, 750, 1000, \text{ and } 2000$; for these gains the alternate sampler system is somewhat more sluggish than the sample-and-hold system when the error signal is below the limiting value.

H. Conclusions

A sample-data AFC system for direct FM transmitters has been modeled, analyzed, and simulated to establish the relationships between AFC system performance and the parameters of subsystems such as the VCO, the reference oscillator, the discriminator, and the sampling system. The analytic results obtained with the linearized closed loop difference equation include the following:

- (1) the range of loop gain, k , for which the system is stable and the form of the response as a function of the sampler characteristic parameter, C_1 , (Table I and Figure 28),
- (2) the time constant of the continuous envelope of the (discrete) transient response as a function of loop gain, k , and sampler parameter, C_1 [Equation (34) and Figure 29],
- (3) frequency sensitivity; that is, the steady state frequency error as a function of shifts in the VCO center frequency, the input signal reference voltage, the reference oscillator frequency, and the amplitude dependence in the discriminator [Equation (41)],
- (4) a comparison of two sample-and-hold schemes.

The linear version of the simulation was verified using the analytic results and was used to establish transient responses for various values of loop gain. Nonlinear models were then introduced



Gain k is Evaluated at Operating Point on VCO Characteristic.

Figure 37. Alternate sampler AFC simulation transient response with nonlinear VCO and with ± 12 volt limiter.

into the appropriate program blocks to simulate signal saturation in the feedback loop and to model the VCO characteristics more accurately.

The nonlinear simulations indicate that the limiter does not destabilize the AFC loop, but only slows down the transient response until the error becomes small. This result is compatible with that obtained with the method of "describing functions" used in nonlinear control system analysis [8]. The latter treats a limiter as a variable gain which decreases as necessary to keep the output magnitude from exceeding a limiting value. The linear analysis shows that the AFC loop remains stable for decreasing positive values of loop gain.

The simulation with a nonlinear VCO input-output characteristic similarly yielded a stable system. Action of the nonlinear VCO can be visualized as a variable gain. Note, however, that the apparent VCO gain increases for large negative perturbations in the VCO input voltage. Consequently, the system stability for high nominal loop gains is marginal. The simulation run made with both nonlinearities (VCO and limiter) included is also stable and well behaved.

The two sample-and-hold schemes for feedback of the frequency error term yielded essentially equivalent performance for all except the highest AFC loop gains. Although the alternate scheme (instantaneous error term driving the RC network) is theoretically more sluggish, the difference in response is negligible until the gain approaches that for deadbeat operation. The existence of a deadbeat gain seems to be the only advantage of the first scheme. The alternate scheme is much simpler to implement.

Even with a limiter in the feedback path, the use of a relatively large loop gain seems desirable from a signal (as opposed to noise) point of view. The system still has high effective gain for low frequency errors producing small steady-state frequency errors. The transient response for small perturbations of parameter values

is also much faster with high gains. From a noise point of view, on the other hand, increased gain is detrimental. Noise effects should be studied using simulation and/or analytic results before raising the loop gain of any existing AFC systems to obtain the faster response and smaller steady state errors.

IV. DETAILED CIRCUIT SIMULATION: STIFF SYSTEMS

A. Introduction

The digital simulation of a linear dynamic system is often complicated by the existence of a large spread in the eigenvalues of the system. Since the step size in the numerical integration needs to be small with respect to the shortest time constant of the system while the range of time over which integration is desired is usually greater than the largest time constant of the system, a large spread in eigenvalues leads to an excessive number of steps in the numerical integration. Simulations of such stiff systems suffer from large round-off errors and excessive computer time requirements. In those cases where the transient response associated with the short time constant modes is of no interest (having decayed to an insignificant level almost immediately), one would like to "remove" those fast modes from the system model. This section describes the development and application of a method for removing such roots from the equations comprising the model. This permits approximating a linear dynamic system by a set of differential equations of lower order not containing the fast eigenvalue(s).

Following the development of the theory of "root removal," a simulation program was developed which uses the root removal technique to efficiently simulate linear stiff systems. The simulation, known as the "Approximate Linear System Analysis Program" (ALSAP), accepts the system differential equations in state variable form, approximates them by a lower order system of equations without the fast eigenvalues, and predicts the system response by numerically integrating the approximate system equations. The construction of ALSAP is described, along with its application to a thirteenth order system representing an RLC bandpass filter. The system response predicted by ALSAP compared favorably with the response of the actual filter as obtained in laboratory measurements.

B. Derivation of Root Removal Technique

Assume that a linear, time-invariant system is described in the usual state variable form,

$$\dot{\underline{x}} = \underline{A}\underline{x} + \underline{B}\underline{u} \quad . \quad (54)$$

One approach for "removing" a particular mode would be to first transform the system so that the matrix A is in Jordan canonical form. The scalar differential equation corresponding to the fast mode could then be assumed to have an approximate solution equivalent to an instantaneous response. The remainder of the scalar differential equations would not contain the fast root and could be numerically integrated if desired. The solution vector would then be transformed back from the canonical frame to the original coordinate frame. Note that the matrix required for the transformation has all of the system eigenvectors as its columns and that the inverse of this matrix is required [7].

The above procedure is not practical. However, a related procedure has been developed which requires only the fast eigenvalue and its single associated eigenvector in order to remove a fast root. The procedure does not require matrix inversion. The resulting approximation is analogous to replacing the transfer function $[1/(s+a)]$ by the gain $[1/a]$ in a system for which the time constant $(-1/a)$ is much faster than any of the other time constants of the system or components of the system input signal. The resulting approximate system is related to that which Chidambara [9] developed for control system synthesis. The digital simulation application is not sensitive to the points of criticism of Davison [10].

Let the matrices in Equation (54) be partitioned to isolate the last element of the state vector:

where I_{n-1} is an $(n-1)$ by $(n-1)$ identity matrix and $\underline{0}^T$ is a 1 by $(n-1)$ matrix of zeros. Note that one of the features of this particular transformation matrix is that its inverse can be formed by simply reversing the signs of the top $(n-1)$ elements in the n^{th} column of the matrix P ; that is,

$$P^{-1} = \left[\begin{array}{c|c} I_{n-1} & -P \\ \hline \underline{0}^T & 1 \end{array} \right]. \quad (60)$$

The term $(P^{-1}AP)$ which appears in the transformed state equation [Equation (57)] can best be evaluated by multiplication of the partitioned matrices:

$$\begin{aligned} P^{-1}AP &= \left[\begin{array}{c|c} I & -P \\ \hline \underline{0}^T & 1 \end{array} \right] \cdot \left[\begin{array}{c|c} A_{11} & A_{12} \\ \hline A_{21} & a_{nn} \end{array} \right] \cdot \left[\begin{array}{c|c} I & -P \\ \hline \underline{0}^T & 1 \end{array} \right] \\ &= \left[\begin{array}{c|c} I & -P \\ \hline \underline{0}^T & 1 \end{array} \right] \cdot \left[\begin{array}{c|c} A_{11} & A_{11}P + A_{12} \\ \hline A_{21} & A_{21}P + a_{nn} \end{array} \right] \\ &= \left[\begin{array}{c|c} A_{11} - P A_{21} & A_{11}P + A_{12} - P A_{21}P - P a_{nn} \\ \hline A_{21} & A_{21}P + a_{nn} \end{array} \right]. \end{aligned} \quad (61)$$

It is desired to show that the upper-right-hand submatrix of $P^{-1}AP$ is zero and that the lower-right-hand submatrix is the fast eigenvalue, λ . To show this, recall the definition of eigenvalue and eigenvector:

$$A\underline{v} = \lambda\underline{v} \quad (62)$$

Writing this definition in partitioned form, one has

$$\begin{bmatrix} A_{11} & | & A_{12} \\ \hline A_{21} & | & a_{nn} \end{bmatrix} \begin{bmatrix} p \\ 1 \end{bmatrix} = \lambda \begin{bmatrix} p \\ 1 \end{bmatrix} \quad (63)$$

which can be separated into two equations as follows:

$$A_{11} p + A_{12} = \lambda p \quad (64)$$

and

$$A_{21} p + a_{nn} = \lambda . \quad (65)$$

Substitution for λ from Equation (65) into Equation (64) gives (since $\lambda p = p\lambda$)

$$A_{11} p + A_{12} = p (A_{21} p + a_{nn}) , \quad (66)$$

or

$$A_{11} p + A_{12} - p A_{21} p - p a_{nn} = \underline{0} . \quad (67)$$

Thus the upper right submatrix of $P^{-1}AP$ is indeed zero. Furthermore, Equation (65) shows that the lower right element of $P^{-1}AP$ is equal to the fast eigenvalue, λ . Thus

$$P^{-1}AP = \begin{bmatrix} A_{11} - p A_{21} p & | & \underline{0} \\ \hline A_{21} & | & \lambda \end{bmatrix} . \quad (68)$$

Note that this matrix is easily constructed from the matrix A , the fast eigenvalue λ , and the upper portion of the associated eigenvector; note further that matrix inversion is not required.

The matrix $(P^{-1}B)$ is also required in Equation (57):

$$P^{-1}B = \begin{bmatrix} I & | & -p \\ \hline \underline{0}^T & | & 1 \end{bmatrix} \begin{bmatrix} B_1 \\ B_2 \end{bmatrix} = \begin{bmatrix} B_1 - p B_2 \\ B_2 \end{bmatrix} . \quad (69)$$

Before substituting the expressions for $P^{-1}AP$ and $P^{-1}B$ into Equation (57) partition the new state vector, \underline{y} , into two sub-vectors with the second being a scalar. That is,

$$\underline{y} = \begin{bmatrix} \underline{r} \\ y_n \end{bmatrix} . \quad (70)$$

Substitution of Equations (68), (69), and (70) into Equation (57) allows the transformed state equation to be written in the following form:

$$\begin{bmatrix} \dot{\underline{r}} \\ \dot{y}_n \end{bmatrix} = \begin{bmatrix} A_{11} - p A_{21} & 0 \\ A_{21} & \lambda \end{bmatrix} \cdot \begin{bmatrix} \underline{r} \\ y_n \end{bmatrix} + \begin{bmatrix} B_1 - p B_2 \\ B_2 \end{bmatrix} \underline{u} . \quad (71)$$

Note that the variable, y_n , does not enter into the $\dot{\underline{r}}$ equation; the upper (n-1) scalar differential equations can be solved independently of the y_n equation. It can be shown that the fast root isolated in the y_n equation does not appear in the \underline{r} equation.

The transformed state equation can be separated into two state equations:

$$\dot{\underline{r}} = (A_{11} - p A_{21}) \underline{r} + (B_1 - p B_2) \underline{u} \quad (72)$$

and

$$\dot{y}_n = A_{21} \underline{r} + \lambda y_n + B_2 \underline{u} . \quad (73)$$

Equation (72) is a state equation of order (n-1) whose eigenvalues are those of the original system [Equation (54)] except that the fast eigenvalue, λ , is absent. Thus Equation (72) can be numerically integrated with reasonable simulation time requirements. To reconstruct the original state vector, the value of $y_n(t)$ as well as $\underline{r}(t)$ is required. Keeping in mind that $\underline{r}(t)$ can be evaluated independently of $y_n(t)$, rewrite Equation (73) with $\underline{r}(t)$ considered as an additional input.

$$\dot{y}_n = \lambda y_n + (A_{21} \underline{r} + B_2 \underline{u}) . \quad (74)$$

While this differential equation could be solved explicitly, it is useful to approximate its solution by assuming that $|\lambda|$ is sufficiently large (fast) that the response in $y_n(t)$ to a change in $\underline{r}(t)$ or $\underline{u}(t)$ is essentially instantaneous. This is equivalent to replacing the transfer function $[1/(s+a)]$ by the gain $[1/a]$; this is often done in frequency domain studies when the root is much faster than input variations or other roots of the system. The resulting approximation is

$$y_n \approx \frac{-1}{\lambda} (A_{21} \underline{r} + B_2 \underline{u}) . \quad (75)$$

C. Reconstructing the Original State Vector

Assuming that the $\dot{\underline{r}}$ equation has been successfully integrated and that the \dot{y}_n equation has been approximated as above, the original state vector, \underline{x} , can be reconstructed as

$$\underline{x} = P\underline{y} = \begin{bmatrix} I_{n-1} & \vdots & \underline{p} \\ \hline 0^T & \vdots & 1 \end{bmatrix} \cdot \begin{bmatrix} \underline{r} \\ \hline y_n \end{bmatrix} = \begin{bmatrix} \underline{r} + \underline{p}y_n \\ \hline y_n \end{bmatrix} . \quad (76)$$

Substitution of Equation (75) into Equation (76) gives

$$\underline{x} = \begin{bmatrix} I_{n-1} & -\underline{p} A_{21}/\lambda \\ \hline & -A_{21}/\lambda \end{bmatrix} \underline{r} - \begin{bmatrix} \underline{p} B_2/\lambda \\ \hline B_2/\lambda \end{bmatrix} \underline{u} . \quad (77)$$

The initial conditions for the components of \underline{r} can be expressed in terms of the initial conditions of the components of \underline{x} as follows:

$$r_i(o) = x_i(o) - p_i x_n(o) . \quad (78)$$

Recapitulating, for a set of state equations as in Equation (54) containing one* fast root, a lower order system [Equation (72)] which does not contain the fast root can be numerically integrated using the initial conditions as given by Equation (78); the original state vector, $\underline{x}(t)$, can then be determined by applying Equation (77). These steps are well-suited for inclusion in a simulation and the computer time required for the transformation will be small in comparison with the savings in integration time.

Example:

Consider the following 3rd order system with scalar control:

$$\begin{bmatrix} \dot{x}_1 \\ \dot{x}_2 \\ \dot{x}_3 \end{bmatrix} = \begin{bmatrix} -3 & 9 & 8 \\ 1 & -11 & -8 \\ -1 & -9 & -12 \end{bmatrix} \begin{bmatrix} x_1 \\ x_2 \\ x_3 \end{bmatrix} + \begin{bmatrix} 0 \\ 0 \\ 1 \end{bmatrix} u. \quad (79)$$

The roots of the system are -2, -4, and -20; assume that the "fast" root, $\lambda = -20$, is to be removed. The corresponding eigenvector is found to be $\underline{v} = (-1, 1, 1)^T$ so that

$$P = \begin{bmatrix} -1 \\ 1 \\ 1 \end{bmatrix}. \quad (80)$$

The necessary terms in Equation (72) are evaluated as follows:

$$(A_{11} - P A_{21}) = \begin{bmatrix} -3 & 9 \\ 1 & -11 \end{bmatrix} - \begin{bmatrix} -1 \\ 1 \end{bmatrix} \begin{bmatrix} -1 & -9 \end{bmatrix} = \begin{bmatrix} -4 & 0 \\ 2 & -2 \end{bmatrix} \quad (81)$$

$$(B_1 - P B_2) = \begin{bmatrix} 0 \\ 0 \end{bmatrix} - \begin{bmatrix} -1 \\ 1 \end{bmatrix} [1] = \begin{bmatrix} 1 \\ -1 \end{bmatrix}. \quad (82)$$

* Repeated application is required when more than one fast mode is to be removed.

The reduced-order system then is

$$\begin{bmatrix} \dot{r}_1 \\ \dot{r}_2 \end{bmatrix} = \begin{bmatrix} -4 & 0 \\ 2 & -2 \end{bmatrix} \begin{bmatrix} r_1 \\ r_2 \end{bmatrix} + \begin{bmatrix} 1 \\ -1 \end{bmatrix} u. \quad (83)$$

The initial conditions are found from Equation (78) to be

$$r_1(0) = x_1(0) + x_3(0)$$

and

$$r_2(0) = x_2(0) - x_3(0), \quad (84)$$

and the original state variables are expressed in terms of the reduced system variables by applying Equation (77).

$$\begin{bmatrix} x_1 \\ x_2 \\ x_3 \end{bmatrix} = \begin{bmatrix} 1.05 & .45 \\ -.05 & .55 \\ -.05 & -.45 \end{bmatrix} \begin{bmatrix} r_1 \\ r_2 \end{bmatrix} + \begin{bmatrix} -.05 \\ .05 \\ .05 \end{bmatrix} u. \quad (85)$$

Thus the solution to Equation (79) can be approximated by simulating the reduced system described by Equations (83) and (84) and substituting the results into Equation (85). This procedure is straightforward to implement in a digital simulation.

D. Practical Application: RLC Bandpass Filter

The CCS telemetry bandpass filter which was analyzed earlier in this report from a frequency domain point of view and whose schematic is given in Figures 1 and 2 has been simulated using ALSAP. The state variables were chosen as the capacitor voltages and inductor currents, except that the (excess) current through the mutual inductance was not included. The specific relationships between the state variables and the circuit voltages and currents are specified in Table VI.

TABLE VI
 PHYSICAL INTERPRETATION OF THE BANDPASS FILTER
 STATE VARIABLES

<u>State Variable</u>	<u>Physical Interpretation</u> (volts, amps)	
X_1	Voltage across	C_1
X_2	" "	C_2
X_3	" "	C_3
X_4	" "	C_4
X_5	" "	C_5
X_6	" "	C_6
X_7	" "	C_7
X_8	Current through	L_{T1}
X_9	" "	L_{T2}
X_{10}	" "	L_2
X_{11}	" "	L_3
X_{12}	" "	L_4
X_{13}	" "	L_5

Note: The circuit elements referred to here are shown in Figures 1 and 2. Positive currents are assumed flowing to the right or down and voltages are considered positive at the left or at the top of the element.

Also, the component nomenclature for the ALSAP simulation is related to the component nomenclature shown in Figure 2 by the following: $LT1 = L11$, $LT2 = L13$, $LM = L12$, $RT2 = R13$, $RL2 = R4$, $RL3 = R5$, $RL4 = R6$, $RL5 = R7$, and the double subscripted C values shown in Figure 2 were not used in the ALSAP simulation

The state equation was written using Bashkow's A matrix method [11] and is of the form $\dot{\underline{x}} = A\underline{x} + Bu$, where \underline{x} is the thirteenth order state vector, u is the input voltage, A is the thirteen-by-thirteen state distribution matrix and B is the thirteen-by-one control distribution matrix. The resulting A and B matrices are specified in terms of the circuit elements in Table VII. The thirteen eigenvalues of the matrix A are given in Table VIII.

The nominal operating frequency of the filter is 1.024 MHz. It can be seen from the system eigenvalues in Table VIII that two of the eigenvalues, λ_{12} and λ_{13} , are trivially fast with respect to the other eigenvalues. Using ALSAP, these two fast roots were removed; the simplified eleventh order system was numerically integrated; and the original state variables were reconstructed for printout. While numerical integration of the original state equations would have required a prohibitive amount of machine time, the time required for ALSAP to transform and integrate the system equations for a reasonable response time was under one minute. Figure 38 shows the filter response to a one MHz input as determined by ALSAP. Laboratory tests on the actual filter confirmed the simulation results, showing that the root removal approximations were valid. Appendix H gives a listing of ALSAP.

E. Complex Pairs of Fast Roots

When the fast root to be removed is complex, the same procedure as used for removal of a real root can be used provided the simulation uses complex arithmetic. However, complex roots always appear in complex conjugate pairs and any complex roots that are "fast" must be removed in pairs. The necessary equations have been derived for removing a fast complex pair of roots in one step without using complex arithmetic in the simulation. These equations, which are somewhat more complicated than those for single root removal, are given in Appendix I.

TABLE VII

NON-ZERO ELEMENTS OF STATE AND CONTROL DISTRIBUTION MATRICES
FOR BANDPASS FILTER SHOWN IN FIGURES 1 and 2

All elements of the A and B matrices are zero except for the following elements:

$$\begin{aligned}
 A(1,10) &= 1/C1 \\
 A(1,11) &= 1/C1 \\
 A(2,10) &= 1/C2 \\
 A(3,11) &= 1/C3 \\
 A(4,11) &= 1/C4 \\
 A(4,13) &= -1/C4 \\
 A(5,11) &= 1/C5 \\
 A(5,12) &= -1/C5 \\
 A(5,13) &= -1/C5 \\
 A(6,6) &= -1/(R3 \cdot C6) \\
 A(6,13) &= 1/C6 \\
 A(7,7) &= -1/(RL \cdot C7) \\
 A(7,13) &= 1/C7 \\
 K1 &= (LT2 + LM)/(LM \cdot [LT1 \cdot LT2 + LM \cdot (LT1 + LT2)]) \\
 K2 &= 1/(LT1 \cdot LT2 + LM \cdot [LT1 + LT2]) \\
 A(8,8) &= -LM \cdot R1 \cdot K1 \\
 A(8,9) &= -(RT2 + R2) \cdot (LT1 + LM) \cdot K1 + (R2 + RT2)/LM \\
 A(8,10) &= R2 \cdot (LT1 + LM) \cdot K1 - R2/LM \\
 A(8,11) &= R2 \cdot (LT1 + LM) \cdot K1 - R2/LM \\
 A(9,8) &= -LM \cdot R1 \cdot K2 \\
 A(9,9) &= -(RT2 + R2) \cdot (LT1 + LM) \cdot K2 \\
 A(9,10) &= R2 \cdot (LT1 + LM) \cdot K2 \\
 A(9,11) &= R2 \cdot (LT1 + LM) \cdot K2 \\
 A(10,1) &= -1/L2 \\
 A(10,2) &= -1/L2 \\
 A(10,9) &= R2/L2 \\
 A(10,10) &= -(R2 + RL2)/L2
 \end{aligned}$$

(CONTINUED)

TABLE VII (CONTINUED)

NON-ZERO ELEMENTS OF STATE AND CONTROL DISTRIBUTION MATRICES
FOR BANDPASS FILTER SHOWN IN FIGURES 1 and 2

$$A(10,11) = -R2/L2$$

$$A(11,1) = -1/L3$$

$$A(11,3) = -1/L3$$

$$A(11,4) = -1/L3$$

$$A(11,5) = -1/L3$$

$$A(11,9) = R2/L3$$

$$A(11,10) = -R2/L3$$

$$A(11,11) = -(R2 + RL3)/L3$$

$$A(12,5) = 1/L4$$

$$A(12,12) = -RL4/L4$$

$$A(13,4) = 1/L5$$

$$A(13,5) = 1/L5$$

$$A(13,6) = -1/L5$$

$$A(13,7) = -1/L5$$

$$A(13,13) = -RL5/L5$$

$$B(8) = LM \cdot K1$$

$$B(9) = LM \cdot K2$$

TABLE VIII

EIGENVALUES OF THE BANDPASS FILTER A-MATRIX

$$\lambda_1 = 0$$

$$\lambda_2 = (-6.11 \times 10^4) + j(0)$$

$$\lambda_3 = (-4.18 \times 10^5) + j(-6.31 \times 10^6)$$

$$\lambda_4 = (-4.18 \times 10^5) + j(6.31 \times 10^6)$$

$$\lambda_5 = (-1.87 \times 10^5) + j(-5.84 \times 10^6)$$

$$\lambda_6 = (-1.87 \times 10^5) + j(5.84 \times 10^6)$$

$$\lambda_7 = (-7.81 \times 10^5) + j(0)$$

$$\lambda_8 = (-2.44 \times 10^5) + j(-6.74 \times 10^6)$$

$$\lambda_9 = (-2.44 \times 10^5) + j(6.74 \times 10^6)$$

$$\lambda_{10} = (-1.03 \times 10^5) + j(-1.77 \times 10^7)$$

$$\lambda_{11} = (-1.03 \times 10^5) + j(1.77 \times 10^7)$$

$$\lambda_{12} = (-2.49 \times 10^8) + j(0)$$

$$\lambda_{13} = (-1.96 \times 10^9) + j(0)$$

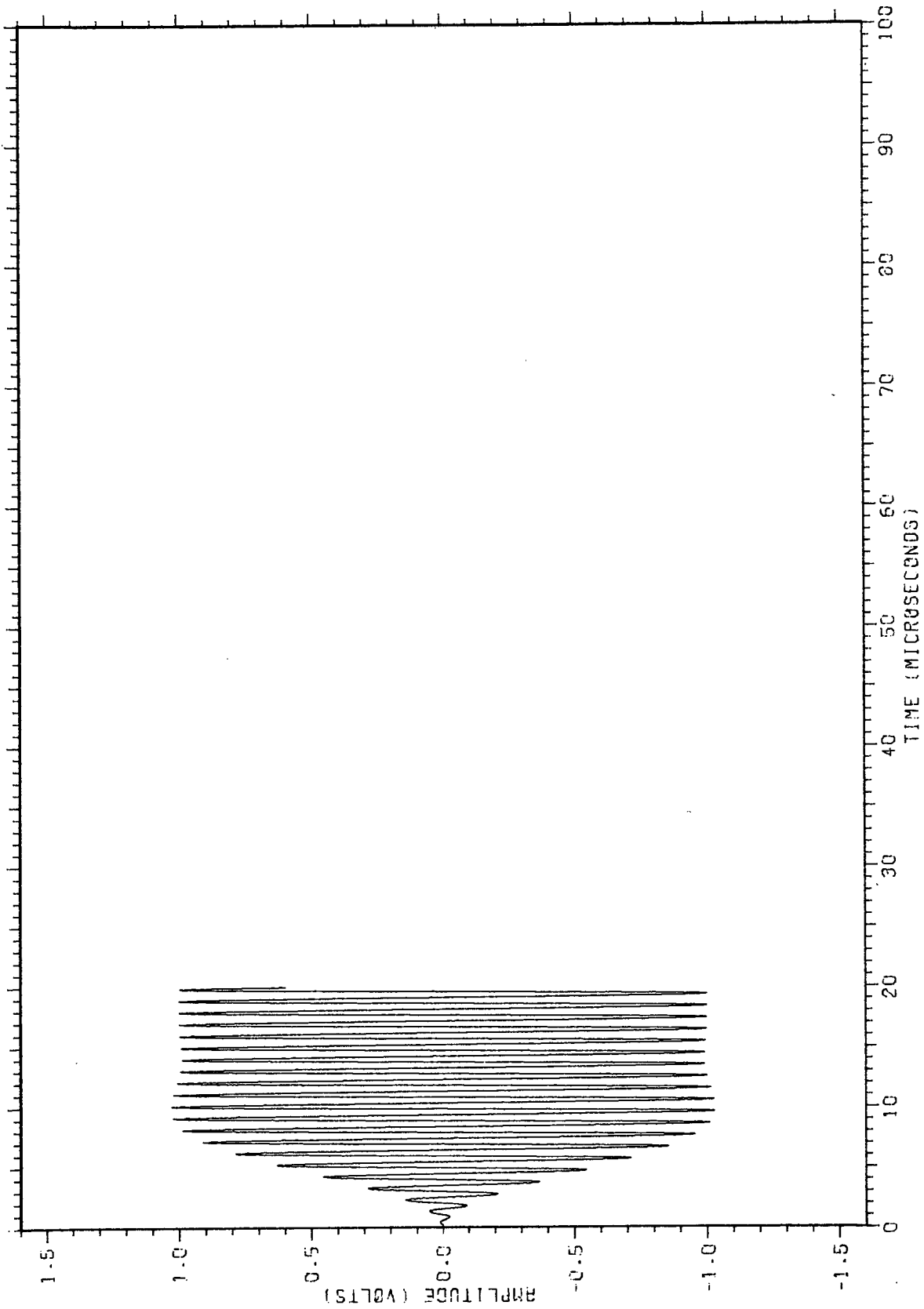


Figure 38. Transient response of the CCS telemetry bandpass filter obtained by using state variable techniques.

F. Conclusions

A method has been developed for efficient digital simulation of stiff linear dynamic systems by the "removal" of insignificant eigenvalues. The method has been implemented in the digital simulation ALSAP and has been successfully applied to the simulation of both passive and active networks. The computer time required for the simulation of a typical linear network using ALSAP is significantly less than that required for available general circuit analysis programs. The general programs, however, are capable of generating internally the governing differential equations from a topological description of the network while ALSAP currently requires that the engineer write the network state equations. The inclusion of an option allowing the use of the ALSAP technique with stiff linear systems in a general computer aided design program would result in a more useful simulation facility.

V. REFERENCES

1. Walsh, J. R. and R. D. Wetherington, Down Link Spectral Investigation, Special Technical Memorandum, Project A-852, Contract NAS8-20054, Georgia Institute of Technology, Engineering Experiment Station, 9 March 1971.
2. Wetherington, R. D. and J. R. Walsh, Spectral Studies of Signals Present in the Command and Communications System Up-Link Transmitter, Technical Report No. 3, Project A-852, Contract NAS8-20054, Georgia Institute of Technology, Engineering Experiment Station, 1 July 1967.
3. Walsh, J. R. and R. D. Wetherington, CCS Down-Link Spectral Studies, Technical Report No. 7, Project A-852, Contract NAS8-20054, Georgia Institute of Technology, Engineering Experiment Station, May 1970.
4. Reed, B., "Command and Communication System," Proceedings of the Apollo Unified S-Band Technical Conference, National Aeronautics and Space Administration, Goddard Space Flight Center, July 14-15, 1965, NASA SP-87.
5. Final Report Generalized Concept Receiving System, The Engineering Staff, Interstate Electronics Corporation, Anaheim, California, Contract NAS8-11650.
6. Kuo, B. C., Automatic Control Systems, Prentice-Hall, Inc., Englewood Cliffs, N. J., 1962, page 405.
7. Ogata, K., State Space Analysis of Control Systems, Prentice-Hall, Inc., Englewood Cliffs, N. J., 1967, page 339.
8. Thaler, G. J., and M. P. Pastel, Analysis and Design of Nonlinear Feedback Control Systems, McGraw Hill, Inc., New York, 1962, Chapter 4.
9. Chidambara, M. R., "On a Method for Simplifying Linear Dynamic Systems," IEEE Transactions on Automatic Controls, February 1967, pp 119,120.
10. Davison, E. J., "Author's Reply," in Reference 9 above.
11. Kuo, F. F., Linear Networks and Systems, John Wiley and Sons, 1967, Chapter 6.

PRECEDING PAGE BLANK NOT FILMED

APPENDIX A.

Subroutine FOFT - for evaluation of
the complex time function $e^{j\beta\psi(t)}$.

APPENDIX B

Subroutine TLMFLT - the evaluation of the CCS telemetry bandpass filter transfer function.

```

SUBROUTINE TLMFLT(A,N,NBIT)
C THIS SUBROUTINE CALCULATES THE TRANSFER FUNCTION OF THE CCS TELEMETRY
C BANDPASS FILTER, NORMALIZED IT TO UNITY AT ITS PEAK VALUE, AND APPLIES
C IT TO THE INPUT FREQUENCY ARRAY A.
C * * * * *
COMPLEX Z11,Z12,Z13,Z2,Z3,Z4,Z5,Z6,Z7,Z8,Z9,Z10,ZA1,ZA2,ZB,ZC,ZDD,
1ZE,ZF,ZN,ZD,ZD1,ZD2,ZD3,ZD4,ZD5,ZD6,ZD7,ZD8,ZD9,H,A,(56),B,(256)
REAL L11,L12,L13,L2,L3,L4,L5
N2 = N / 2
N4 = N - 1
T2 = 0.
C THE FOLLOWING INSTRUCTIONS SET THE FILTER ELEMENT VALUES
R2 = 5.1E3
R3 = 4.7E3
RL = 6.2E2
C1 = 4.80E-10
C2 = 1.368E-9
C3 = 5.10E-10
C4 = 2.2E-9
C5 = 3.42E-10
C6 = 5.7E-10
C7 = 1.8E-9
C22 = 2.07E-11
C33 = 1.65E-11
C55 = 1.65E-11
L11 = -5.358E-6
L12 = 6.06E-6
L13 = 5.194E-5
L2 = 1.08E-5
L3 = 5.1E-5
L4 = 1.6E-5
L5 = 5.1E-5
C DO LOOP 10 CALCULATES THE FILTER TRANSFER FUNCTION
DO 10 I = 2,N
II = I - 1
F1 = 1. / (NBIT * 1.E-6)
F = F1 * II
W = 6.2831853 * F
WSQ = W ** 2
Z11 = CMPLX(51., W * L11)
Z12 = CMPLX(10., W * L12)
Z13 = CMPLX(7.78, W * L13)
Z2 = CMPLX(R2, 0.) / CMPLX(1., W * R2 * C22)
Z3 = CMPLX(10., -1. / (W * C1))
Z4 = CMPLX(1.70, (W * L2 - 1. / (W * C2)))
Z5 = CMPLX(8.01, W * L3) / CMPLX(1. - WSQ * L3 * C33),
1(W * 8.01 * C33) + CMPLX(10., - 1. / (W * C3))
Z6 = CMPLX(2.51, W * L4) / CMPLX(1. - WSQ * L4 * C51,
1(2.51 * W * C51) + CMPLX(10., - 1. / (W * C4)))
Z7 = CMPLX(8.01, W * L5) / CMPLX(1. - WSQ * L5 * C55),
1(W * 8.01 * C55)
Z8 = CMPLX(1.E7, 0.)
Z9 = CMPLX(R3, 0.) / CMPLX(1., W * R3 * C6)
Z10 = CMPLX(RL, 0.) / CMPLX(1., W * RL * C7)
ZA1 = Z11 + Z12
ZA2 = Z12 + Z13 + Z2
ZB = Z2 + Z3 + Z4
ZC = Z4 + Z5 + Z6
ZD = Z6 + Z7 + Z8
ZE = Z8 + Z9 + Z10
ZF = ZA1 * ZA2 - (Z12 ** 2.)
ZN = Z12 * Z2 * Z4 * Z6 * Z8 * Z10
ZD1 = ZD * ZE * (Z4 ** 2.)
ZD2 = ZB * ZE * (Z6 ** 2.)
ZD3 = (Z4 ** 2.) * (Z8 ** 2.)
ZD4 = ZB * ZC * ZD * ZE
ZD5 = ZB * ZC * (Z8 ** 2.)
ZD6 = ZA1 * (Z2 ** 2.)
ZD7 = ZC * ZD * ZE
ZD8 = ZC * (Z8 ** 2.)
ZD9 = ZE * (Z6 ** 2.)
ZDD = ZF * (-ZD1 - ZD2 + ZD3 + ZD4 - ZD5)
1 + ZD6 * (-ZD7 + ZD8 + ZD9)
H = ZN / ZDD
T1 = CABS(H)
IF(T1 .LT. T2) GO TO 15
T2 = T1
15 CONTINUE
10 B(I) = H
WRITE(6,1002)
1002 FORMAT(1H1)
WRITE(6,1001) ((I,B(I)), I = 2,N)
1001 FORMAT(1H ,16.2E20.6)
COR = 1. / T2
C DO LOOP 25 NORMALIZES THE PEAK VALUE OF THE TRANSFER FUNCTION TO 1.0 AND
C APPLIES IT TO THE INPUT ARRAY A
DO 25 I = 1,N
B(I) = COR * B(I)
25 A(I) = A(I) * B(I)
WRITE(6,1020)
1020 FORMAT(1H0,2X,2CHNORMALIZATION FACTOR)
WRITE(6,1015) COR
1015 FORMAT(1H*,23X,L20.8)
RETURN
END

```

APPENDIX C.
Main program S-band calculations.

```
COMPLEX A(8192)
DIMENSION IBUF(10000)
CALL PLOTS(IBUF(1),10000,2)
```

C

```
IGAM = 13
BETA = 1.0
FC = 1.0E6
FMOD = 1.3653333E4
FPCM = 4.9834666E5
FSC = 1.024E6
PI = 3.1415927
PI2 = 6.2831853
NBIT = 146
```

C

```
N = 2 ** IGAM
W = PI2 * FSC
WM = PI2 * FMOD
WPCM = PI2 * FPCM
DELT = (2. / (FMOD * N))
DELF = FMOD / 2.
DO 1 I = 1,NBIT
  C(I) = 1
1 CONTINUE
DO 2 I = 2,NBIT,2
2 C(I) = -1
  CALL TIMFCN(A,C,N,DELT,W,WM,WPCM)
  CALL FOFT(A,IGAM,BETA)
  CALL FFT(A,IGAM,-1)
  CALL LFOLD(A,N)
  CALL FFTPLT(A,N,DELF)
  CALL PLOT(0.,0.,999)
  STOP
END
```

APPENDIX D

Subroutine TIMPLT - Calcomp plot routine for
plotting baseband time functions.

```

SUBROUTINE TIMPLT(A,N,PRD)
C * * * * *
COMPLEX A(1)
CALL FACTOR(0.4)
CALL PLOT(0.,-20.,3)
CALL PLOT(12.,0.,-3)
CALL PLOT(-10.,-14.,3)
C * * * * *
C DO LOOP 3 DRAWS THE BORDER OF THE PLOTTING AREA
C * * * * *
DO 3 I = 1,2
CALL PLOT(-10.,0.,2)
CALL PLOT(10.,0.,2)
CALL PLOT(10.,-14.,2)
CALL PLOT(-10.01,-14.,2)
CALL PLOT(-10.01,0.01,2)
CALL PLOT(10.01,0.01,2)
CALL PLOT(10.01,-14.01,2)
3 CALL PLOT(-10.,-14.01,2)
C * * * * *
C DO LOOP 10 TICKS THE POSITIVE HALF OF THE LEFT HAND BORDER
C * * * * *
DO 10 I = 0,16
Y = - 7. + 0.4375 * I
IF (MOD(I,5) .EQ. 0) GO TO 6
CALL PLOT(-10.1,Y,3)
GO TO 8
6 CALL PLOT(-10.2,Y,3)
8 CALL PLOT(-10.,Y,2)
10 CONTINUE
C * * * * *
C DO LOOP 11 TICKS THE NEGATIVE HALF OF THE LEFT HAND BORDER
C * * * * *
DO 11 I = 1,15
Y = - 7. - 0.4375 * I
IF(MOD(I,5) .EQ. 0) GO TO 7
CALL PLOT(-10.1,Y,3)
GO TO 9
7 CALL PLOT(-10.2,Y,3)
9 CALL PLOT(-10.,Y,2)
11 CONTINUE
C * * * * *
C DO LOOPS 12 AND 13 AND THE FOLLOWING INSTRUCTIONS PROVIDE THE CALIBRATION
C AND LABELING OF THE LEFT HAND BORDER
C * * * * *
DO 12 I = 0,3
Y = -7.105 + I * 2.188
12 CALL NUMBER(-10.88,Y,.21,1.0*I,0.,1)
DO 13 I = 1,3
Y = -7.105 - I * 2.188
13 CALL NUMBER(-11.09,Y,.21,-1.0*I,0.,1)
CALL SYMBOL(-11.03,-8.5,.21,17AMPLITUDE (VOLTS),90.,17)
C * * * * *
C DO LOOP 25 PROVIDES THE TICK MARKS ALONG THE BOTTOM BORDER
C * * * * *
DO 25 I = 0,100
X = -10. + 0.2 * I
IF(MOD(I,5) .EQ. 0) GO TO 26
CALL PLOT(X,-14.1,3)
GO TO 28
26 IF(MOD(I,10) .EQ. 0) GO TO 27
CALL PLOT(X,-14.16,3)
GO TO 28
27 CALL PLOT(X,-14.2,3)
28 CALL PLOT(X,-14.,2)
25 CONTINUE
C * * * * *
C DO LOOP 20 PROVIDES THE TICK MARKS ALONG THE TOP BORDER
C * * * * *
DO 20 I = 0,100
X = -10. + 0.2 * I
IF(MOD(I,5) .EQ. 0) GO TO 21
CALL PLOT(X,0.1,3)
GO TO 22
21 IF(MOD(I,10) .EQ. 0) GO TO 23
CALL PLOT(X,0.16,3)
GO TO 22
23 CALL PLOT(X,0.2,3)
22 CALL PLOT(X,0.0,2)
20 CONTINUE

```

```

C * * * * *
C DO LOOP 35 TICKS THE POSITIVE HALF OF THE RIGHT HAND BORDER
C * * * * *
DO 35 I = 0,16
  Y = - 7. + I * 0.4375
  IF(MOD(I,5) .EQ. 0) GO TO 36
  CALL PLOT(10.1,Y,3)
  GO TO 37
36 CALL PLOT(10.2,Y,3)
37 CALL PLOT(10.,Y,2)
35 CONTINUE
C * * * * *
C DO LOOP 40 TICKS THE NEGATIVE HALF OF THE RIGHT HAND BORDER
C * * * * *
DO 40 I = 1,15
  Y = - 7. - I * 0.4375
  IF(MOD(I,5) .EQ. 0) GO TO 41
  CALL PLOT(10.1,Y,3)
  GO TO 42
41 CALL PLOT(10.2,Y,3)
42 CALL PLOT(10.,Y,2)
40 CONTINUE
C
C THE FOLLOWING INSTRUCTION , DO LOOP 50, AND THE INSTRUCTION FOLLOWING
C DO LOOP 50 PROVIDE THE CALIBRATION OF THE LOWER BORDER.
C
CALL NUMBER(-10.105,-14.5,.21,0.,0.,-1)
DO 50 I = 1,9
  X = -10.21 + I * 2.
50 CALL NUMBER(X,-14.5,.21,20.*I,0.,-1)
CALL NUMBER(9.685,-14.5,.21,200.,0.,-1)
C
CALL SYMBOL(-2.,-14.9,.21,19HTIME (MICROSECONDS),0.,19)
C
CHANGE OF ORIGIN
C
CALL PLOT(-10.,-7.,-3)
C * * * * *
C PLOTTING THE DATA WITH A STRAIGHT LINE BETWEEN POINTS
C * * * * *
DO 60 I = 1,N
  II = I - 1
  X = (II * PRD* (0.2E6)) / N
  IF(X .GE. 20.) GO TO 71
  Y = 2.1875 * REAL(A(II))
60 CALL PLOT(X,Y,2)
DO 70 I = 1,N
  II = I - 1
  X = (II * PRD* (0.2E6)) / N + PRD * 0.2E6
  IF(X .GT. 20.) GO TO 71
  Y = 2.1875 * REAL(A(II))
70 CALL PLOT(X,Y,2)
C * * * * *
C RETURNING THE PEN TO THE LOWER EDGE OF THE PAPER
C * * * * *
71 CALL PLOT(26.,-13.,-3)
C
WRITE(6,1035)
1035 FORMAT(1H1,2X,14HPLOT COMPLETED)
RETURN
END
C * * * * *

```

PRECEDING PAGE BLANK NOT SHOWN

APPENDIX E

FORTRAN program for linearized AFC system simulation.


```

00143 29* C COMMENT***UPDATE INPUT SIGNAL***
00143 30* C
00143 31* C IP(I*STEP,EG,10) VM = ARUM(I)
00144 32* C
00144 33* C COMMENT***INPUT AND FEEDBACK SUMMATION***
00144 34* C
00144 35* C V = VM - V4
00146 36* C
00146 37* C COMMENT***VOLTAGE CONTROLLED OSCILLATOR SIMULATION***
00146 38* C
00146 39* C F0 = FC + KYCO*(V-VC)
00147 40* C
00147 41* C COMMENT***MIXER***
00147 42* C
00147 43* C FI = F0 - CN*FR
00150 44* C
00150 45* C COMMENT***DISCRIMINATOR***
00150 46* C
00150 47* C V1 = KD1*(FI - FD)
00151 48* C V2 = KD2*(FR-FD)
00152 49* C DELF = FI - FR
00153 50* C
00153 51* C COMMENT***DEVELOP ERROR SIGNAL***
00153 52* C
00153 53* C V5 = V1 - V2
00154 54* C
00154 55* C COMMENT***PULSE AMPLIFIER AND VCO BIAS***
00154 56* C
00154 57* C V6 = VBIAS + KA*V5
00155 58* C
00155 59* C COMMENT***INSERT LIMITER HERE***
00155 60* C
00155 61* C V3 = V6
00156 62* C
00156 63* C COMMENT***SWITCHED RC NETWORK--SAMPLER***
00156 64* C
00156 65* C V4 = V4 + (V3 - V4)*C1
00157 66* C
00157 67* C COMMENT***PRINT***
00157 68* C
00157 69* C
00160 70* C L1 = MOD(LINE,40)
00161 71* C L2 = MOD(LINE,5)
00162 72* C IF (L1) 52,50,52
00163 73* C 50 CONTINUE
00165 74* C WRITE(6,110) GAIN
00166 75* C FOR:AT(1,1,20X,100) LOOP GAIN ,16,0)
00171 76* C
00172 77* C 120 FOR:AT(10 STEP,7X,1T,7X,VM,8X,V3,11X,V0,15X,DELF,
00174 78* C 1 11X,MCSEC,4X,VOLTS,5X,VOLTS,9X,4Z,16X,4Z)
00175 79* C 52 IF (L2 .EQ. 0) WRITE(6,125)
00200 80* C
00201 81* C LINE = LINE + 1
00202 82* C WRITE(6,130) ISTEP,T,VM,V3,F0,DELF
00212 83* C FOR:AT(1,15,F10,0,2F10,4,E15,6,2X,F12,0)
00212 84* C
00212 85* C COMMENT***REPEAT FOR NEXT SAMPLING INTERVAL***
00212 86* C
00213 87* C 990 CONTINUE
00216 88* C STOP
00217 89* C END

```

END OF COMPILATION: NO DIAGNOSTICS.

FREQUENCY CONTROL SIMULATION

LOOP GAIN 100.

STEP	T MCSEC	V1 VOLTS	V3 VOLTS	F0 HZ	DELTA HZ
1	03.	.0000	-7.0000	.225000+09	0.
2	120.	.0000	-7.0000	.225000+09	0.
3	189.	.0000	-7.0000	.225000+09	0.
4	252.	.0000	-7.0000	.225000+09	0.
5	315.	.0000	-7.0000	.225000+09	0.
6	378.	.0000	-7.0000	.225000+09	0.
7	441.	.0000	-7.0000	.225000+09	0.
8	504.	.0000	-7.0000	.225000+09	0.
9	567.	.0000	-7.0000	.225000+09	0.
10	630.	1.0000	93.0000	.226400+09	1400000.
11	643.	1.0000	85.5027	.226295+09	1295038.
12	750.	1.0000	78.5731	.226193+09	1198024.
13	819.	1.0000	72.1684	.226108+09	1108358.
14	882.	1.0000	66.2480	.226025+09	1025480.
15	945.	1.0000	60.7770	.225949+09	948878.
16	1008.	1.0000	55.7199	.225878+09	878078.
17	1071.	1.0000	51.0456	.225813+09	812638.
18	1134.	1.0000	46.7251	.225752+09	752152.
19	1197.	1.0000	42.7320	.225696+09	696248.
20	1260.	1.0000	39.0411	.225645+09	644576.
21	1323.	1.0000	35.6299	.225597+09	596818.
22	1386.	1.0000	32.4767	.225553+09	552674.
23	1449.	1.0000	29.5620	.225512+09	511876.
24	1512.	1.0000	26.8689	.225474+09	474164.
25	1575.	1.0000	24.3793	.225439+09	439310.
26	1638.	1.0000	22.0781	.225407+09	407094.
27	1701.	1.0000	19.9513	.225377+09	377318.
28	1764.	1.0000	17.9854	.225350+09	349796.
29	1827.	1.0000	16.1684	.225324+09	324358.
30	1890.	1.0000	14.4890	.225301+09	300846.
31	1953.	1.0000	12.9369	.225279+09	279116.
32	2016.	1.0000	11.5021	.225259+09	259030.
33	2079.	1.0000	10.1761	.225240+09	240466.
34	2142.	1.0000	8.9504	.225223+09	223306.
35	2205.	1.0000	7.8177	.225207+09	207448.
36	2268.	1.0000	6.7706	.225193+09	192788.
37	2331.	1.0000	5.8029	.225179+09	179240.
38	2394.	1.0000	4.9084	.225167+09	166718.
39	2457.	1.0000	4.0816	.225155+09	155142.
40	2520.	1.0000	3.3174	.225144+09	144444.

FREQUENCY CONTROL SIMULATION

LOOP GAIN 100.					
STEP	T MCSEC	VM VOLTS	V3 VOLTS	F0 HZ	UELF HZ
41	2563.	1.0000	2.6111	.225135+09	134556.
42	2640.	1.0000	1.9584	.225125+09	125418.
43	2709.	1.0000	1.3550	.225117+09	116970.
44	2772.	1.0000	.7973	.225109+09	109162.
45	2835.	1.0000	.2819	.225102+09	101946.
46	2898.	1.0000	-.1946	.225095+09	95276.
47	2961.	1.0000	-.6349	.225089+09	89112.
48	3024.	1.0000	-1.0419	.225083+09	83414.
49	3087.	1.0000	-1.4180	.225078+09	78148.
50	3150.	1.0000	-1.7657	.225073+09	73280.
51	3213.	1.0000	-2.0871	.225069+09	68780.
52	3276.	1.0000	-2.3841	.225065+09	64622.
53	3339.	1.0000	-2.6587	.225061+09	60778.
54	3402.	1.0000	-2.9124	.225057+09	57226.
55	3465.	1.0000	-3.1470	.225054+09	53942.
56	3528.	1.0000	-3.3639	.225051+09	50906.
57	3591.	1.0000	-3.5641	.225048+09	48102.
58	3654.	1.0000	-3.7493	.225046+09	45510.
59	3717.	1.0000	-3.9206	.225043+09	43112.
60	3780.	1.0000	-4.0787	.225041+09	40898.
61	3843.	1.0000	-4.2250	.225039+09	38850.
62	3906.	1.0000	-4.3601	.225037+09	36958.
63	3969.	1.0000	-4.4850	.225035+09	35210.
64	4032.	1.0000	-4.6004	.225034+09	33594.
65	4095.	1.0000	-4.7073	.225032+09	32098.
66	4158.	1.0000	-4.8059	.225031+09	30718.
67	4221.	1.0000	-4.8970	.225029+09	29442.
68	4284.	1.0000	-4.9813	.225028+09	28262.
69	4347.	1.0000	-5.0591	.225027+09	27172.
70	4410.	1.0000	-5.1311	.225026+09	26164.
71	4473.	1.0000	-5.1977	.225025+09	25232.
72	4536.	1.0000	-5.2591	.225024+09	24372.
73	4599.	1.0000	-5.3160	.225024+09	23576.
74	4662.	1.0000	-5.3686	.225023+09	22840.
75	4725.	1.0000	-5.4171	.225022+09	22160.
76	4788.	1.0000	-5.4620	.225022+09	21532.
77	4851.	1.0000	-5.5036	.225021+09	20950.
78	4914.	1.0000	-5.5419	.225020+09	20414.
79	4977.	1.0000	-5.5773	.225020+09	19918.
80	5040.	1.0000	-5.6100	.225019+09	19460.

FREQUENCY CONTROL SIMULATION

LOOP GAIN 100.

STEP	T MSEC	VM VOLTS	V3 VOLTS	F0 HZ	UELF HZ
81	5103.	1.0000	-5.6403	.225019+09	19036.
82	5100.	1.0000	-5.6683	.225019+09	18644.
83	5224.	1.0000	-5.6941	.225018+09	18282.
84	5292.	1.0000	-5.7181	.225018+09	17946.
85	5355.	1.0000	-5.7401	.225018+09	17638.
86	5418.	1.0000	-5.7606	.225017+09	17352.
87	5481.	1.0000	-5.7794	.225017+09	17088.
88	5544.	1.0000	-5.7969	.225017+09	16844.
89	5607.	1.0000	-5.8130	.225017+09	16618.
90	5670.	1.0000	-5.8280	.225016+09	16408.
91	5733.	1.0000	-5.8417	.225016+09	16216.
92	5790.	1.0000	-5.8544	.225016+09	16038.
93	5859.	1.0000	-5.8663	.225016+09	15872.
94	5922.	1.0000	-5.8771	.225016+09	15720.
95	5985.	1.0000	-5.8871	.225016+09	15580.
96	6048.	1.0000	-5.8964	.225015+09	15450.
97	6111.	1.0000	-5.9050	.225015+09	15330.
98	6174.	1.0000	-5.9130	.225015+09	15218.
99	6237.	1.0000	-5.9203	.225015+09	15116.
100	6300.	1.0000	-5.9271	.225015+09	15020.
101	6363.	1.0000	-5.9333	.225015+09	14934.
102	6420.	1.0000	-5.9391	.225015+09	14852.
103	6489.	1.0000	-5.9446	.225015+09	14776.
104	6552.	1.0000	-5.9494	.225015+09	14708.
105	6615.	1.0000	-5.9540	.225015+09	14644.
106	6678.	1.0000	-5.9583	.225015+09	14584.
107	6741.	1.0000	-5.9621	.225015+09	14530.
108	6804.	1.0000	-5.9657	.225014+09	14480.
109	6867.	1.0000	-5.9691	.225014+09	14432.
110	6930.	1.0000	-5.9721	.225014+09	14390.
111	6993.	1.0000	-5.9750	.225014+09	14350.
112	7050.	1.0000	-5.9777	.225014+09	14312.
113	7119.	1.0000	-5.9801	.225014+09	14278.
114	7182.	1.0000	-5.9824	.225014+09	14246.
115	7245.	1.0000	-5.9844	.225014+09	14218.
116	7308.	1.0000	-5.9864	.225014+09	14190.
117	7371.	1.0000	-5.9881	.225014+09	14166.
118	7434.	1.0000	-5.9899	.225014+09	14142.
119	7497.	1.0000	-5.9913	.225014+09	14122.
120	7560.	1.0000	-5.9927	.225014+09	14102.

FREQUENCY CONTROL SIMULATION

LOOP GAIN 100.

STEP	T MCSEC	V1 VOLTS	V3 VOLTS	F0 HZ	DELTA HZ
121	7623.	1.0000	-5.9940	.225014+09	14084.
122	7680.	1.0000	-5.9953	.225014+09	14066.
123	7749.	1.0000	-5.9963	.225014+09	14052.
124	7812.	1.0000	-5.9974	.225014+09	14036.
125	7875.	1.0000	-5.9983	.225014+09	14024.
126	7938.	1.0000	-5.9991	.225014+09	14012.
127	8001.	1.0000	-6.0000	.225014+09	14000.
128	8064.	1.0000	-6.0007	.225014+09	13990.
129	8127.	1.0000	-6.0014	.225014+09	13980.
130	8190.	1.0000	-6.0020	.225014+09	13972.
131	8253.	1.0000	-6.0027	.225014+09	13962.
132	8316.	1.0000	-6.0031	.225014+09	13956.
133	8379.	1.0000	-6.0037	.225014+09	13948.
134	8442.	1.0000	-6.0041	.225014+09	13942.
135	8505.	1.0000	-6.0046	.225014+09	13936.
136	8568.	1.0000	-6.0050	.225014+09	13930.
137	8631.	1.0000	-6.0054	.225014+09	13924.
138	8694.	1.0000	-6.0057	.225014+09	13920.
139	8757.	1.0000	-6.0060	.225014+09	13916.
140	8820.	1.0000	-6.0063	.225014+09	13912.
141	8883.	1.0000	-6.0066	.225014+09	13908.
142	8946.	1.0000	-6.0069	.225014+09	13904.
143	9009.	1.0000	-6.0070	.225014+09	13902.
144	9072.	1.0000	-6.0073	.225014+09	13898.
145	9135.	1.0000	-6.0074	.225014+09	13896.
146	9198.	1.0000	-6.0077	.225014+09	13892.
147	9261.	1.0000	-6.0079	.225014+09	13890.
148	9324.	1.0000	-6.0080	.225014+09	13888.
149	9387.	1.0000	-6.0081	.225014+09	13886.
150	9450.	1.0000	-6.0083	.225014+09	13884.
151	9513.	1.0000	-6.0084	.225014+09	13882.
152	9576.	1.0000	-6.0084	.225014+09	13882.
153	9639.	1.0000	-6.0086	.225014+09	13880.
154	9702.	1.0000	-6.0087	.225014+09	13878.
155	9765.	1.0000	-6.0087	.225014+09	13878.
156	9828.	1.0000	-6.0089	.225014+09	13876.
157	9891.	1.0000	-6.0090	.225014+09	13874.
158	9954.	1.0000	-6.0090	.225014+09	13874.
159	10017.	1.0000	-6.0090	.225014+09	13874.
160	10080.	1.0000	-6.0091	.225014+09	13872.

FREQUENCY CONTROL SIMULATION

LOOP GAIN 100.

STEP	T MCSEC	V1 VOLTS	V3 VOLTS	F0 HZ	UELF HZ
161	10143.	1.0000	-6.0091	.225014+09	13872.
162	10206.	1.0000	-6.0093	.225014+09	13870.
163	10269.	1.0000	-6.0093	.225014+09	13870.
164	10332.	1.0000	-6.0093	.225014+09	13870.
165	10395.	1.0000	-6.0094	.225014+09	13868.
166	10458.	1.0000	-6.0094	.225014+09	13868.
167	10521.	1.0000	-6.0094	.225014+09	13868.
168	10584.	1.0000	-6.0094	.225014+09	13868.
169	10647.	1.0000	-6.0096	.225014+09	13866.
170	10710.	1.0000	-6.0096	.225014+09	13866.
171	10773.	1.0000	-6.0096	.225014+09	13866.
172	10836.	1.0000	-6.0096	.225014+09	13866.
173	10899.	1.0000	-6.0096	.225014+09	13866.
174	10962.	1.0000	-6.0096	.225014+09	13866.
175	11025.	1.0000	-6.0097	.225014+09	13864.
176	11088.	1.0000	-6.0097	.225014+09	13864.
177	11151.	1.0000	-6.0097	.225014+09	13864.
178	11214.	1.0000	-6.0097	.225014+09	13864.
179	11277.	1.0000	-6.0097	.225014+09	13864.
180	11340.	1.0000	-6.0097	.225014+09	13864.
181	11403.	1.0000	-6.0097	.225014+09	13864.
182	11466.	1.0000	-6.0097	.225014+09	13864.
183	11529.	1.0000	-6.0097	.225014+09	13864.
184	11592.	1.0000	-6.0097	.225014+09	13864.
185	11655.	1.0000	-6.0097	.225014+09	13864.
186	11718.	1.0000	-6.0097	.225014+09	13864.
187	11781.	1.0000	-6.0099	.225014+09	13862.
188	11844.	1.0000	-6.0099	.225014+09	13862.
189	11907.	1.0000	-6.0099	.225014+09	13862.
190	11970.	1.0000	-6.0099	.225014+09	13862.
191	12033.	1.0000	-6.0099	.225014+09	13862.
192	12096.	1.0000	-6.0099	.225014+09	13862.
193	12159.	1.0000	-6.0099	.225014+09	13862.
194	12222.	1.0000	-6.0099	.225014+09	13862.
195	12285.	1.0000	-6.0099	.225014+09	13862.
196	12348.	1.0000	-6.0099	.225014+09	13862.
197	12411.	1.0000	-6.0099	.225014+09	13862.
198	12474.	1.0000	-6.0099	.225014+09	13862.
199	12537.	1.0000	-6.0099	.225014+09	13862.
200	12600.	1.0000	-6.0099	.225014+09	13862.

FIN

APPENDIX F

FORTRAN program for nonlinear AFC system.

FOR IS MAIN
FOR SBA-11/06-16:27 (.0)

MAIN PROGRAM

STORAGE USED: CODE(1) 000321; DATA(0) 000155; BLANK COMMON(2) 000000

EXTERNAL REFERENCES (BLOCK, NAME)

- 0003 NINTR\$
- 0004 EXP
- 0005 NMDU\$
- 0006 NIOZ\$
- 0007 NSTOP\$

STORAGE ASSIGNMENT (BLOCK, TYPE, RELATIVE LOCATION, NAME)

```

0000 000056 110F 0000 000064 120F 0000 000111 125F 0001 000056 126G 0000 000112 130F
0001 000112 141G 0001 000154 200L 0001 000163 201L 0001 000171 202L 0001 000231 300L
0001 000233 301L 0001 000226 302L 0001 000264 52L 0000 R 000020 C
0000 R 000044 FI 0000 R 000022 C1 0000 R 000047 DELF 0000 R 000027 FD
0000 R 000044 F1 0000 R 000026 FR 0000 R 000043 F0 0000 R 000033 GAIN 0000 I 000032 II
0000 I 000037 ILAST 0000 I 000040 ISTEP 0000 I 000016 IS 0000 R 000003 KA 0000 R 000000 KD1
0000 R 000001 KD2 0000 R 000002 KVCO 0000 R 000004 L 0000 I 000034 LINE 0000 I 000054 LI
0000 I 000055 L2 0000 I 000030 N 0000 R 000017 R 0000 R 000041 T 0000 R 000021 T0
0000 R 000042 V 0000 R 000025 VBIAS 0000 R 000024 VC 0000 R 000035 VM 0000 R 000045 V1
0000 R 000046 V2 0000 R 000053 V3 0000 R 000036 V4 0000 R 000050 V5 0000 R 000051 V6
0000 R 000052 V6ABS

```

```

00101 1* REAL KD1,KD2,KVCO,KA
00102 2* REAL L
00103 3* DIMENSION AR(9)/10.,25.,50.,100.,250.,500.,1000.,1333.,1800./
00104 4* L = 12.
00105 5* R = 2.0E4
00106 6* C = 1.0E-7
00107 7* T0 = 1.5E-6
00108 8* C1 = 1.0 - EXP(-T0/(R*C))
00109 9* KD1 = 1.0E-7
00110 10* KD2 = KD1
00111 11* KVCO = 1.4E6
00112 12* FC = 225.0E6
00113 13* VC = 7.
00114 14* VBIAS = -VC
00115 15* FR = 45.0E6
00116 16* FD = FR
00117 17* N = 4
00118 18* CN = N
00119 19* DO 990 II = 2,5
00120 20* GAIN = AR(II)
00121 21* LINE = 0
00122 22* VM = 0.0
00123 23* V4 = VBIAS
00124 24* KA = GAIN/(KVCO*KD1)
00125 25* ILAST = 1000/GAIN + 10
00126 26* IF (ILAST.LT. 200) ILAST = 200
00127 27* DO 990 ISTEP = 1,ILAST
00128 28* T = 63.0*ISTEP
00129 29* C COMMENT**UPDATE INPUT SIGNAL***
00130 30* C
00131 31* IF(ISTEP.EQ.10) VM = 1.0
00132 32* C
00133 33* COMMENT**INPUT AND FEEDBACK SUMMATION***
00134 34* C
00135 35* C

```

```

00146 36* V = VM - V4
00146 37* C COMMENT***VOLTAGE CONTROLLED OSCILLATOR SIMULATION***
00146 38* C
00146 39* C COMMENT***NONLINEAR VCO CURVE FIT***
00146 40* C IF(V.LT.6.0) GO TO 200
00147 41* C IF(V.GT.8.0) GO TO 201
00151 42* C F0 = (185.8 + (9.8)*V - (0.6)*V**2)*1.E+6
00153 43* C GO TO 202
00154 44* C F0 = (223. + (V-6.)*3.)*1.E+6
00155 45* C GO TO 202
00156 46* C F0 = (225.8 + (V-8.)*0.1)*1.E+6
00157 47* C 200 CONTINUE
00160 48* C
00160 49* C COMMENT***MIXER***
00160 50* C
00160 51* C FI = F0 - CN*FR
00161 52* C
00161 53* C COMMENT***DISCRIMINATOR***
00161 54* C
00161 55* C V1 = KD1*(FI - FD)
00162 56* C V2 = KD2*(FR-FD)
00163 57* C DELF = FI - FR
00164 58* C
00164 59* C COMMENT***DEVELOP ERROR SIGNAL***
00164 60* C
00164 61* C V5 = V1 - V2
00165 62* C
00165 63* C COMMENT***PULSE AMPLIFIER AND VCO BIAS***
00165 64* C
00165 65* C V6 = VBIAS + KA*V5
00166 66* C
00166 67* C COMMENT***INSERT LIMITER HERE***
00166 68* C
00166 69* C V6ABS = ABS(V6)
00167 70* C IF(V6ABS.LT.L) GO TO 300
00170 71* C IF(V6.LT.0.) GO TO 302
00172 72* C V3 = L
00174 73* C
00175 74* C GO TO 301
00176 75* C V3 = -L
00177 76* C GO TO 301
00200 77* C
00200 78* C V3 = V6
00201 79* C CONTINUE
00201 80* C COMMENT***SWITCHED RC NETWORK--SAMPLER***
00201 81* C
00202 82* C V4 = V4 + (V3 - V4)*CI
00202 83* C
00202 84* C COMMENT***PRINT***
00202 85* C
00203 86* C L1 = MOD(LINE,40)
00204 87* C L2 = MOD(LINE,5)
00205 88* C IF (L1) 52,50,52
00210 89* C 50 CONTINUE
00211 90* C WRITE(6,110) GAIN
00214 91* C FORMAT('1',20X,'LOOP GAIN ',F6.0)
00215 92* C WRITE(6,120)
00217 93* C FORMAT('0 STEP',7X,'VM',8X,'V3',11X,'F0',15X,'DELF',/
00217 94* C 11X,'MCSEC',4X,'VOLTS',5X,'VOLTS',9X,'HZ',16X,'HZ',/
00220 95* C 52 IF (L2 .EQ. 0) WRITE(6,125)
00223 96* C LINE & LINE + 1
00224 97* C WRITE(6,130) ISTEP,T,VM,V3,F0,DELF
00225 98* C FORMAT(' ',15,F10.0,2F10.4,E15.6,2X,F12.0)
00235 99* C
00235 100* C COMMENT***REPEAT FOR NEXT SAMPLING INTERVAL***
00235 101* C
00235 102* C 990 CONTINUE
00236 103* C STOP
00241 104* C END
00242 105* C

```

END OF COMPILATION: NO DIAGNOSTICS.

FREQUENCY CONTROL SIMULATION

LOOP GAIN 250.

STEP	T MCSEC	VM VOLTS	V3 VOLTS	F0 HZ	DELTA HZ
1	63.	.0000	-7.0004	.225000+09	-2.
2	126.	.0000	-7.0004	.225000+09	-2.
3	189.	.0000	-7.0000	.225000+09	0.
4	252.	.0000	-7.0000	.225000+09	0.
5	315.	.0000	-7.0000	.225000+09	0.
6	378.	.0000	-7.0000	.225000+09	0.
7	441.	.0000	-7.0000	.225000+09	0.
8	504.	.0000	-7.0000	.225000+09	0.
9	567.	.0000	-7.0000	.225000+09	0.
10	630.	1.0000	12.0000	.225800+09	799998.
11	693.	1.0000	12.0000	.225797+09	797026.
12	756.	1.0000	12.0000	.225794+09	793814.
13	819.	1.0000	12.0000	.225790+09	790362.
14	882.	1.0000	12.0000	.225787+09	786674.
15	945.	1.0000	12.0000	.225783+09	782740.
16	1008.	1.0000	12.0000	.225779+09	778572.
17	1071.	1.0000	12.0000	.225774+09	774162.
18	1134.	1.0000	12.0000	.225770+09	769514.
19	1197.	1.0000	12.0000	.225765+09	764632.
20	1260.	1.0000	12.0000	.225760+09	759512.
21	1323.	1.0000	12.0000	.225754+09	754154.
22	1386.	1.0000	12.0000	.225749+09	748564.
23	1449.	1.0000	12.0000	.225743+09	742736.
24	1512.	1.0000	12.0000	.225737+09	736678.
25	1575.	1.0000	12.0000	.225730+09	730380.
26	1638.	1.0000	12.0000	.225724+09	723854.
27	1701.	1.0000	12.0000	.225717+09	717090.
28	1764.	1.0000	12.0000	.225710+09	710098.
29	1827.	1.0000	12.0000	.225703+09	702872.
30	1890.	1.0000	12.0000	.225695+09	695414.
31	1953.	1.0000	12.0000	.225688+09	687724.
32	2016.	1.0000	12.0000	.225680+09	679804.
33	2079.	1.0000	12.0000	.225672+09	671656.
34	2142.	1.0000	12.0000	.225663+09	663280.
35	2205.	1.0000	12.0000	.225655+09	654674.
36	2268.	1.0000	12.0000	.225646+09	645838.
37	2331.	1.0000	12.0000	.225637+09	636778.
38	2394.	1.0000	12.0000	.225627+09	627490.
39	2457.	1.0000	12.0000	.225618+09	617976.
40	2520.	1.0000	12.0000	.225608+09	608234.

FREQUENCY CONTROL SIMULATION

LOOP GAIN 250.

STEP	T MCSEC	VM VOLTS	V3 VOLTS	F0 HZ	DELTA HZ
41	2583.	1.0000	12.0000	.225598+09	598266.
42	2646.	1.0000	12.0000	.225588+09	588072.
43	2709.	1.0000	12.0000	.225578+09	577658.
44	2772.	1.0000	12.0000	.225567+09	567016.
45	2835.	1.0000	12.0000	.225556+09	556156.
46	2898.	1.0000	12.0000	.225545+09	545066.
47	2961.	1.0000	12.0000	.225534+09	533756.
48	3024.	1.0000	12.0000	.225522+09	522224.
49	3087.	1.0000	12.0000	.225510+09	510470.
50	3150.	1.0000	12.0000	.225498+09	498496.
51	3213.	1.0000	12.0000	.225486+09	486300.
52	3276.	1.0000	12.0000	.225474+09	473892.
53	3339.	1.0000	12.0000	.225461+09	461256.
54	3402.	1.0000	12.0000	.225448+09	448402.
55	3465.	1.0000	12.0000	.225435+09	435332.
56	3528.	1.0000	12.0000	.225422+09	422042.
57	3591.	1.0000	12.0000	.225409+09	408534.
58	3654.	1.0000	12.0000	.225395+09	394812.
59	3717.	1.0000	12.0000	.225381+09	380874.
60	3780.	1.0000	12.0000	.225367+09	366718.
61	3843.	1.0000	12.0000	.225352+09	352348.
62	3906.	1.0000	12.0000	.225338+09	337764.
63	3969.	1.0000	12.0000	.225323+09	322962.
64	4032.	1.0000	12.0000	.225308+09	307948.
65	4095.	1.0000	12.0000	.225293+09	292724.
66	4158.	1.0000	12.0000	.225277+09	277282.
67	4221.	1.0000	12.0000	.225262+09	261630.
68	4284.	1.0000	12.0000	.225246+09	245764.
69	4347.	1.0000	12.0000	.225230+09	229690.
70	4410.	1.0000	12.0000	.225213+09	213400.
71	4473.	1.0000	12.0000	.225197+09	196904.
72	4536.	1.0000	12.0000	.225180+09	180198.
73	4599.	1.0000	12.0000	.225163+09	163280.
74	4662.	1.0000	12.0000	.225146+09	146156.
75	4725.	1.0000	12.0000	.225129+09	128822.
76	4788.	1.0000	12.0000	.225111+09	111280.
77	4851.	1.0000	9.7018	.225094+09	93530.
78	4914.	1.0000	6.9054	.225078+09	77870.
79	4977.	1.0000	4.5846	.225065+09	64874.
80	5040.	1.0000	2.6661	.225054+09	54130.

FREQUENCY CONTROL SIMULATION

LOOP GAIN 250.

STEP	T MCSEC	VM VOLTS	V3 VOLTS	F0 HZ	DELTA HZ
81	5103.	1.0000	1.0846	.225045+09	45274.
82	5166.	1.0000	- .2150	.225038+09	37996.
83	5229.	1.0000	-1.2807	.225032+09	32028.
84	5292.	1.0000	-2.1536	.225027+09	27140.
85	5355.	1.0000	-2.8671	.225023+09	23144.
86	5418.	1.0000	-3.4493	.225020+09	19884.
87	5481.	1.0000	-3.9246	.225017+09	17222.
88	5544.	1.0000	-4.3118	.225015+09	15054.
89	5607.	1.0000	-4.6279	.225013+09	13284.
90	5670.	1.0000	-4.8846	.225012+09	11846.
91	5733.	1.0000	-5.0939	.225011+09	10674.
92	5796.	1.0000	-5.2643	.225010+09	9720.
93	5859.	1.0000	-5.4025	.225009+09	8946.
94	5922.	1.0000	-5.5150	.225008+09	8316.
95	5985.	1.0000	-5.6064	.225008+09	7804.
96	6048.	1.0000	-5.6811	.225007+09	7386.
97	6111.	1.0000	-5.7414	.225007+09	7048.
98	6174.	1.0000	-5.7907	.225007+09	6772.
99	6237.	1.0000	-5.8307	.225007+09	6548.
100	6300.	1.0000	-5.8629	.225006+09	6368.
101	6363.	1.0000	-5.8896	.225006+09	6218.
102	6426.	1.0000	-5.9111	.225006+09	6098.
103	6489.	1.0000	-5.9282	.225006+09	6002.
104	6552.	1.0000	-5.9425	.225006+09	5922.
105	6615.	1.0000	-5.9543	.225006+09	5856.
106	6678.	1.0000	-5.9636	.225006+09	5804.
107	6741.	1.0000	-5.9711	.225006+09	5762.
108	6804.	1.0000	-5.9775	.225006+09	5726.
109	6867.	1.0000	-5.9821	.225006+09	5700.
110	6930.	1.0000	-5.9861	.225006+09	5678.
111	6993.	1.0000	-5.9896	.225006+09	5658.
112	7056.	1.0000	-5.9925	.225006+09	5642.
113	7119.	1.0000	-5.9943	.225006+09	5632.
114	7182.	1.0000	-5.9961	.225006+09	5622.
115	7245.	1.0000	-5.9979	.225006+09	5612.
116	7308.	1.0000	-5.9989	.225006+09	5606.
117	7371.	1.0000	-6.0000	.225006+09	5600.
118	7434.	1.0000	-6.0004	.225006+09	5598.
119	7497.	1.0000	-6.0014	.225006+09	5592.
120	7560.	1.0000	-6.0014	.225006+09	5592.

APPENDIX G

FORTRAN program for AFC system with alternate
sampler with limiter and nonlinear VCO model.


```

00152 IF (V.GT.8.0) GO TO 701
00154 F0 = (185.8 + (9.A)*V - (0.6)*V*V)*1.F+6
00155 GO TO 702
00156 F0 = (223. + (V-6.)*3.)*1.E+6
00157 GO TO 702
00160 F0 = (225.8 + (V-8.)*0.1)*1.F+6
00161 702 CONTINUE
00162 FI = F. - CH*FR
00163 V1 = KC1*(FI - FD)
00164 V2 = K 2*(FR - FD)
00165 D*LF = FI - FR
00166 V5 = V1 - V2
00167 V6 = VRIAS + KA*V5
00168 V6*BS = ABS(V6)
00170 IF (V6*BS.LT.L) GO TO 600
00171 IF ((6.LT.0.) GO TO 602
00173 V3 = L
00175 600 TO 601
00176 602 V3 = -L
00177 600 TO 601
00200 600 V3 = V6
00201 601 CONTINUE
00202 IF (M.EQ.1) GO TO 2-2
00203 V4 = V4 + C2*(V3 - V4)
00205 202 CONTINUE
00206 IF (ISTEP.GE.8) GO TO 300
00207 L2 = MOD(LINE,11)
00211 L1 = MOD(LINE,44)
00212 IF (L1) 52,50*52
00213 50 CONTINUE
00216 WRITE(6,110) GAIN
00217 110 FORMAT('1',20X,'LOOP GAIN ',F6.0)
00222 WRITE(6,120)
00223 120 FORMAT('0 STEP',7X,'T',7X,'VM',8X,'V3',11X,'F0',15X,'DELF',/
00225 11X,'MCSEC',4X,'VOLTS',5X,'HZ',9X,'HZ',16X,'HZ')
00226 52 IF (L2.(0.0) WRITE(6,125)
00227 125 FORMAT('H )
00231 LINE = LINE + 1
00232 TPRINT = ((ISTEP - 1)*TP + TSMALL)*1.E6
00233 WRITE(6,130) ISTEP,TPRINT,VM,V3,F0,DELF
00234 130 FORMAT(' ',15,F10.2,2F10.4,E15.6,2X,F12.0)
00244 GO TO 301
00245 300 IF (ISTEP.EQ.8) LINE = 0
00246

00250 L1 = MOD(LINE,40)
00251 L2 = MOD(LINE,5)
00252 IF (M.NE.1) GO TO 301
00254 IF (L1) 352,350,352
00257 350 CONTINUE
00260 WRITE(6,310) GAIN
00263 310 FORMAT('1',20X,'LOOP GAIN ',F6.0)
00264 WRITE(6,320)
00266 320 FORMAT('0 STEP',7X,'T',7X,'VM',8X,'V3',11X,'F0',15X,'DELF',/
00268 11X,'MCSEC',4X,'VOLTS',5X,'VOLTS',9X,'HZ',16X,'HZ')
00269 352 IF (L2.(0.0) WRITE(6,325)
00272 325 FORMAT('H )
00273 LINE = LINE + 1
00274 TPRINT = ((ISTEP - 1)*TP + TSMALL)*1.E6
00275 WRITE(6,330) ISTEP,TPRINT,VM,V3,F0,DELF
00305 330 FORMAT(' ',15,F10.2,2F10.4,E15.6,2X,F12.0)
00306 301 CONTINUE
00307 M = M + 1
00310 TSMALL = TSMALL + DELT
00311 IF (M.LF.10) GO TO 201
00313 M = 0
00314 TSMALL = 0.
00315 ISTEP = ISTEP + 1
00316 IF (ISTEP.LE.JR(II)) GO TO 201
00320 990 STOP
00322 EN
00323

```

END OF COMPILATION: NO DIAGNOSTICS.

LOOP G IN 250.

STEP	T MCSEC	VM VOLTS	V3 VOLTS	F0 HZ	DELTA HZ
0	-63.49	.0000	-7.0004	.225000+09	-2.
0	-63.34	.0000	-7.0004	.225000+09	-2.
0	-63.19	.0000	-7.0004	.225000+09	-2.
0	-63.04	.0000	-7.0004	.225000+09	-2.
0	-62.89	.0000	-7.0004	.225000+09	-2.
0	-62.74	.0000	-7.0004	.225000+09	-2.
0	-62.59	.0000	-7.0004	.225000+09	-2.
0	-62.44	.0000	-7.0004	.225000+09	-2.
0	-62.29	.0000	-7.0004	.225000+09	-2.
0	-62.14	.0000	-7.0004	.225000+09	-2.
0	-61.99	.0000	-7.0004	.225000+09	-2.
1	.00	1.0000	12.0000	.225800+09	79999.
1	.15	1.0000	12.0000	.225800+09	799712.
1	.30	1.0000	12.0000	.225799+09	799422.
1	.45	1.0000	12.0000	.225799+09	799132.
1	.60	1.0000	12.0000	.225799+09	798838.
1	.75	1.0000	12.0000	.225799+09	798544.
1	.90	1.0000	12.0000	.225798+09	798248.
1	1.05	1.0000	12.0000	.225798+09	797946.
1	1.20	1.0000	12.0000	.225798+09	797647.
1	1.35	1.0000	12.0000	.225797+09	797336.
1	1.50	1.0000	12.0000	.225797+09	797026.
2	63.49	1.0000	12.0000	.225797+09	797026.
2	63.64	1.0000	12.0000	.225797+09	796718.
2	63.79	1.0000	12.0000	.225796+09	796404.
2	63.94	1.0000	12.0000	.225796+09	796092.
2	64.09	1.0000	12.0000	.225796+09	795772.
2	64.24	1.0000	12.0000	.225795+09	795452.
2	64.39	1.0000	12.0000	.225795+09	795130.
2	64.54	1.0000	12.0000	.225795+09	794802.
2	64.69	1.0000	12.0000	.225794+09	794474.
2	64.84	1.0000	12.0000	.225794+09	794146.
2	64.99	1.0000	12.0000	.225794+09	793814.
3	126.98	1.0000	12.0000	.225794+09	793814.
3	127.13	1.0000	12.0000	.225793+09	793492.
3	127.28	1.0000	12.0000	.225793+09	793148.
3	127.43	1.0000	12.0000	.225793+09	792804.
3	127.58	1.0000	12.0000	.225792+09	792460.
3	127.73	1.0000	12.0000	.225792+09	792118.
3	127.88	1.0000	12.0000	.225792+09	791774.
3	128.03	1.0000	12.0000	.225791+09	791426.
3	128.18	1.0000	12.0000	.225791+09	791072.
3	128.33	1.0000	12.0000	.225791+09	790718.
3	128.48	1.0000	12.0000	.225790+09	790366.

LOOP GAIN 250.

STEP	T MCSEC	VM VOLTS	V3 VOLTS	F0 HZ	DELTA HZ
4	190.48	1.0000	12.0000	.225790+09	7a0366.
4	190.63	1.0000	12.0000	.225790+09	7a0004.
4	190.78	1.0000	12.0000	.225790+09	7a9646.
4	190.93	1.0000	12.0000	.225789+09	7a9282.
4	191.08	1.0000	12.0000	.225789+09	7a8916.
4	191.23	1.0000	12.0000	.225789+09	7a8550.
4	191.38	1.0000	12.0000	.225788+09	7a8176.
4	191.53	1.0000	12.0000	.225788+09	7a7802.
4	191.68	1.0000	12.0000	.225787+09	7a7428.
4	191.83	1.0000	12.0000	.225787+09	7a7052.
4	191.98	1.0000	12.0000	.225787+09	7a6670.
5	253.97	1.0000	12.0000	.225787+09	7a6670.
5	254.12	1.0000	12.0000	.225786+09	7a6292.
5	254.27	1.0000	12.0000	.225786+09	7a5902.
5	254.42	1.0000	12.0000	.225786+09	7a5518.
5	254.57	1.0000	12.0000	.225785+09	7a5128.
5	254.72	1.0000	12.0000	.225785+09	7a4736.
5	254.87	1.0000	12.0000	.225784+09	7a4342.
5	255.02	1.0000	12.0000	.225784+09	7a3946.
5	255.17	1.0000	12.0000	.225784+09	7a3546.
5	255.32	1.0000	12.0000	.225783+09	7a3144.
5	255.47	1.0000	12.0000	.225783+09	7a2740.
6	317.46	1.0000	12.0000	.225783+09	7a2740.
6	317.61	1.0000	12.0000	.225782+09	7a2336.
6	317.76	1.0000	12.0000	.225782+09	7a1924.
6	317.91	1.0000	12.0000	.225782+09	7a1512.
6	318.06	1.0000	12.0000	.225781+09	7a1100.
6	318.21	1.0000	12.0000	.225781+09	7a0688.
6	318.36	1.0000	12.0000	.225780+09	7a0264.
6	318.51	1.0000	12.0000	.225780+09	779846.
6	318.66	1.0000	12.0000	.225779+09	779422.
6	318.81	1.0000	12.0000	.225779+09	778998.
6	318.96	1.0000	12.0000	.225779+09	778572.
7	380.95	1.0000	12.0000	.225779+09	778572.
7	381.10	1.0000	12.0000	.225778+09	778140.
7	381.25	1.0000	12.0000	.225778+09	777706.
7	381.40	1.0000	12.0000	.225777+09	777270.
7	381.55	1.0000	12.0000	.225777+09	776836.
7	381.70	1.0000	12.0000	.225776+09	776396.
7	381.85	1.0000	12.0000	.225776+09	775954.
7	382.00	1.0000	12.0000	.225776+09	775508.
7	382.15	1.0000	12.0000	.225775+09	775066.
7	382.30	1.0000	12.0000	.225775+09	774612.
7	382.45	1.0000	12.0000	.225774+09	774158.

LOOP GAIN 250.

STEP	T MCSEC	VM VOLTS	V3 VOLTS	F0 HZ	DELTA HZ
8	445.94	1.0000	12.0000	.225770+09	769514.
9	509.44	1.0000	12.0000	.225765+09	764628.
10	572.93	1.0000	12.0000	.225760+09	759510.
11	636.42	1.0000	12.0000	.225754+09	754158.
12	699.91	1.0000	12.0000	.225749+09	748560.
13	763.40	1.0000	12.0000	.225743+09	742736.
14	826.90	1.0000	12.0000	.225737+09	736674.
15	890.39	1.0000	12.0000	.225730+09	730376.
16	953.88	1.0000	12.0000	.225724+09	723854.
17	1017.37	1.0000	12.0000	.225717+09	717090.
18	1080.87	1.0000	12.0000	.225710+09	710094.
19	1144.36	1.0000	12.0000	.2257-3+09	702868.
20	1207.85	1.0000	12.0000	.225695+09	695410.
21	1271.34	1.0000	12.0000	.225688+09	687724.
22	1334.83	1.0000	12.0000	.225680+09	679804.
23	1398.33	1.0000	12.0000	.225672+09	671656.
24	1461.82	1.0000	12.0000	.225663+09	663280.
25	1525.31	1.0000	12.0000	.225655+09	654674.
26	1588.80	1.0000	12.0000	.225646+09	645838.
27	1652.29	1.0000	12.0000	.225637+09	636774.
28	1715.79	1.0000	12.0000	.225627+09	627486.
29	1779.28	1.0000	12.0000	.225618+09	617972.
30	1842.77	1.0000	12.0000	.225608+09	608230.
31	1906.26	1.0000	12.0000	.225598+09	598262.
32	1969.75	1.0000	12.0000	.225588+09	588068.
33	2033.25	1.0000	12.0000	.225578+09	577650.
34	2096.74	1.0000	12.0000	.225567+09	567012.
35	2160.23	1.0000	12.0000	.225556+09	556148.
36	2223.72	1.0000	12.0000	.225545+09	545058.
37	2287.21	1.0000	12.0000	.225534+09	533752.
38	2350.71	1.0000	12.0000	.225522+09	522216.
39	2414.20	1.0000	12.0000	.225510+09	510462.
40	2477.69	1.0000	12.0000	.225498+09	498492.
41	2541.18	1.0000	12.0000	.225486+09	486296.
42	2604.67	1.0000	12.0000	.225474+09	473880.
43	2668.17	1.0000	12.0000	.225461+09	461250.
44	2731.66	1.0000	12.0000	.225448+09	448394.
45	2795.15	1.0000	12.0000	.225435+09	435320.
46	2858.64	1.0000	12.0000	.225422+09	422034.
47	2922.13	1.0000	12.0000	.225409+09	408526.

LOOP GAIN 250.

STEP	T MCSEC	VM VOLTS	V3 VOLTS	F0 HZ	DELTA HZ
48	2985.63	1.0000	12.0000	.225395+09	394804.
49	3049.12	1.0000	12.0000	.225381+09	380862.
50	3112.61	1.0000	12.0000	.225367+09	366710.
51	3176.10	1.0000	12.0000	.225352+09	352336.
52	3239.60	1.0000	12.0000	.225338+09	337752.
53	3303.09	1.0000	12.0000	.225323+09	322952.
54	3366.58	1.0000	12.0000	.225308+09	307936.
55	3430.07	1.0000	12.0000	.225293+09	292708.
56	3493.56	1.0000	12.0000	.225277+09	277270.
57	3557.06	1.0000	12.0000	.225262+09	261614.
58	3620.55	1.0000	12.0000	.225246+09	245750.
59	3684.04	1.0000	12.0000	.225230+09	229678.
60	3747.53	1.0000	12.0000	.225213+09	213386.
61	3811.02	1.0000	12.0000	.225197+09	196888.
62	3874.52	1.0000	12.0000	.225180+09	180182.
63	3938.01	1.0000	12.0000	.225163+09	163284.
64	4001.50	1.0000	12.0000	.225146+09	146140.
65	4064.99	1.0000	12.0000	.225129+09	128804.
66	4128.48	1.0000	12.0000	.225111+09	111262.
67	4191.98	1.0000	9.8221	.225094+09	94204.
68	4255.47	1.0000	7.2204	.225080+09	79634.
69	4318.96	1.0000	5.0282	.225067+09	67358.
70	4382.45	1.0000	3.1868	.225057+09	57046.
71	4445.94	1.0000	1.6439	.225048+09	48406.
72	4509.44	1.0000	.3539	.225041+09	41182.
73	4572.93	1.0000	-.7225	.225035+09	35154.
74	4636.42	1.0000	-1.6196	.225030+09	30130.
75	4699.91	1.0000	-2.3668	.225026+09	25946.
76	4763.40	1.0000	-2.9871	.225022+09	22472.
77	4826.90	1.0000	-3.5032	.225020+09	19582.
78	4890.39	1.0000	-3.9314	.225017+09	17104.
79	4953.88	1.0000	-4.2871	.225015+09	15192.
80	5017.37	1.0000	-4.5814	.225014+09	13544.
81	5080.86	1.0000	-4.8257	.225012+09	12176.
82	5144.36	1.0000	-5.0286	.225011+09	11040.
83	5207.85	1.0000	-5.1964	.225010+09	10100.
84	5271.34	1.0000	-5.3354	.225009+09	9322.
85	5334.83	1.0000	-5.4500	.225009+09	8680.
86	5398.33	1.0000	-5.5454	.225008+09	8146.
87	5461.82	1.0000	-5.6246	.225008+09	7702.

LOOP 6 IN 250.

STEP	T MCSEC	VM VOLTS	V3 VOLTS	F0 HZ	DELTA HZ
88	5525.31	1.0000	-5.6900	.225007+09	7336.
89	5588.80	1.0000	-5.7439	.225007+09	7034.
90	5652.29	1.0000	-5.7886	.225007+09	6784.
91	5715.79	1.0000	-5.8254	.225007+09	6578.
92	5779.28	1.0000	-5.8564	.225006+09	6404.
93	5842.77	1.0000	-5.8818	.225006+09	6262.
94	5906.26	1.0000	-5.9029	.225006+09	6144.
95	5969.75	1.0000	-5.9200	.225006+09	6048.
96	6033.25	1.0000	-5.9346	.225006+09	5966.
97	6096.74	1.0000	-5.9464	.225006+09	5900.
98	6160.23	1.0000	-5.9561	.225006+09	5846.
99	6223.72	1.0000	-5.9646	.225006+09	5798.
100	6287.21	1.0000	-5.9711	.225006+09	5762.

APPENDIX H

LISTINGS OF ALSAP ROUTINES

In addition to the ALSAP main routine, there are special subroutines for numerical integration (NINTEG), transformation matrix generation (GREG), and loading the input data (DATAIN). These routines are listed in this appendix. Also used but not listed here are two utility routines for finding the eigenvalues and eigenvectors of a matrix (MEGVEL and IGVEC).

```

COMMENT CCS BANDPASS FILTER 5/12/71 STEP RESPONSE
COMMENT ***** MAY 25, 1971 *****
C APPROXIMATE LINEAR SYSTEM ANALYSIS PROGRAM (ALSAP)
COMMON A(13,13),B(13,13),NORIG,M,N,A(13),NEVTBR,C(13,13),D(13,13),
1 LAMREL,LAMIMG,SCALE,PV(13),NLESS,I,TEMP,Z(13),IPRFG,IPR,FG
REAL LAMREL,LAMIMG
DOUBLE PRECISION PV
C *****
DIMENSION RSR(13),RSI(13),CYAT(13,13),MSKN(13),MSIN(13)
DOUBLE PRECISION VR(13),VI(13),RR,RI,IEMP
CALL DAIN
NORIG = N
DO 5011 I = 1,N
DO 5010 J = 1,N
5010 C(I,J) = 0.
5011 C(I,I) = 1.
DO 5012 I = 1,N
DO 5012 J = 1,M
5012 D(I,J) = 0.
C ***** FIND THE LARGEST AND SMALLEST NON-ZERO MAGNITUDE ELEMENTS OF MATRIX A
C FOR DETERMINING SCALING TO BE USED TO IMPROVE NUMERICAL ACCURACY
C IN THE SIMPLIFICATION PROCESS.
TEMP1 = 0.
TEMP2 = 1.E+30
DO 6000 I = 1,N
DO 6000 J = 1,N
TEMP = ABS(A(I,J))
IF(TEMP.LT.1.E-25) GO TO 6000
IF(TEMP.GT.TEMP1) TEMP1 = TEMP
IF(TEMP.LT.TEMP2) TEMP2 = IEMP
6000 CONTINUE
I = ALOG10(TEMP1)
J = ALOG10(TEMP2)
K = 1 + (I+J)/2.
SCALE = (10.0)**K
WRITE(6,6)
WRITE(6,6001) SCALE
6001 FORMAT(10X,48H"THE PROGRAM HAS CHOSEN THE SCALE FACTOR TO BE = ,E12
1.4)
COMMENT*****PRINT WARNING RELATIVE TO SCALE FACTOR AND EIGENVALUES*****
WRITE(6,6002)
WRITE(6,6003)
WRITE(6,6004)
WRITE(6,6005)
6002 FORMAT(10X,51H"NOTE--ALL PRINTED VALUES FOR EIGENVALUES AND FOR)
6003 FORMAT(10X,51H"ELEMENTS OF THE MATRIX A MUST BE MULTIPLIED BY)
6004 FORMAT(10X,51H"THE ABOVE SCALE FACTOR BEFORE EXTERNAL USE.*****)
6005 FORMAT(10X,54H"NO OTHER QUANTITIES IN THE PRINTOUT REQUIRE SCALI
NG)
COMMENT ***** END OF PRINT WARNING*****
WRITE(6,6)
WRITE(6,7000)
7000 FORMAT (1H1)
SCALIV = 1./SCALE
DO 40 I = 1,N
DO 40 J = 1,N
40 A(I,J) = A(I,J)*SCALIV
WRITE(6,6)
DO 999 IROOT = 1,NEVTBR
IF(IPRFG.EQ.0) GO TO 8001
WRITE(6,6)
WRITE(6,6006)
6006 FORMAT(10X,31HEIGENVALUES OF PRESENT MATRIX A)
8001 CONTINUE
WRITE(6,6)
CALL MEGVAL(N,A,RSR,RSI)
WRITE(6,6)
TEMP = RSR(1)
ITEMP = 1
DO 1100 I = 2,N
IF(TEMP.LT. RSR(I)) GO TO 1100
TEMP = RSR(I)
ITEMP = I
1100 CONTINUE
LAMREL = RSR(ITEMP)*SCALE
LAMIMG = RSI(ITEMP)*SCALE
RR = RSR(ITEMP)
RI = RSI(ITEMP)
CALL IGVEC(N,13,A,RR,RI,VR,VI)
IF(IPRFG.EQ.0) GO TO 8002
WRITE(6,42)
42 FORMAT(10X,38HEIGENVALUE WITH SMALLEST TIME CONSTANT)
WRITE(6,2) ITEMPT,RR,RI
WRITE(6,6)
WRITE(6,43)
43 FORMAT(10X,41HEIGENVECTOR FOR THE ABOVE FAST EIGENVALUE)
WRITE(6,6)
DO 5 J = 1,N
5 WRITE(6,2) VR(J),VI(J)
8002 CONTINUE

```

```

COMMENT--WRITE A*V FOR COMPARISON WITH LAMBDA*V
IEGVFC = 4
6500 CONTINUE
WRITE(6,6)
WRITE(IEGVFC,44)
44 FORMAT(10X,25HEIGENVECTOR VALIDITY TEST)
WRITE(6,6)
DO 32 KK = 1,N
PRINTR = RR*VR(KK) - PI*VI(KK)
PRINTI = RR*VI(KK) + KI*VR(KK)
VLAMR = 0.
DO 30 K = 1,N
30 VLAMR = VLAMR + A(KK,K)*VR(K)
VLAMI = 0.
DO 31 K = 1,N
31 VLAMI = VLAMI + A(KK,K)*VI(K)
IF((ABS(VLAMR-PRINTR).GT.ABS(VLAMR*1.E-3)).AND.(IEGVFC.NE.6)) GO
1 TO 6501
IF((ABS(VLAMI-PRINTI).GT.ABS(VLAMI*1.E-3)).AND.(IEGVFC.NE.6)) GO
1 TO 6501
GO TO 6502
6501 IEGVEC = 6
GO TO 6500
6502 CONTINUE
WRITE(IEGVFC,2) VLAMR,PRINTR,KK,VLAMI,PRINTI
32 CONTINUE
WRITE(6,6)
TEMP = DABS(VR(1))
ITEMP = 1
DO 1101 K = 1,N
IF(TEMP.GT.DABS(VR(K))) GO TO 1101
TEMP = DABS(VR(K))
ITEMP = K
1101 CONTINUE
TEMPD = VR(N)
VR(N) = VR(ITEMP)
VR(ITEMP) = TEMPD
IF(IPRTFG.EQ.0) GO TO 8003
WRITE(6,49) ITEMP,N
49 FORMAT(10X,20HROWS (AND COLUMNS) ,I2,7H AND ,I2,36H OF MATRIX
1A HAVE BEEN INTERCHANGED)
8003 CONTINUE
COMMENT----INTERCHANGE ROWS AND COLS. OF MATRIX A
DO 1102 K = 1,N
TEMP = A(K,N)
A(K,N) = A(K,ITEMP)
1102 A(K,ITEMP) = TEMP
DO 1103 K = 1,N
TEMP = A(N,K)
A(N,K) = A(ITEMP,K)
1103 A(ITEMP,K) = TEMP
DO 1200 J = 1,M
TEMP = B(N,J)
B(N,J) = B(ITEMP,J)
1200 B(ITEMP,J) = TEMP
WRITE(6,6)
NLESS1 = N - 1
WRITE(6,6)
IF(IPRTFG.EQ.0) GO TO 8004
WRITE(6,45)
45 FORMAT(10X,46HFIRST N-1 COMPONENTS OF NORMALIZED EIGFVECTOR)
8004 CONTINUE
DO 1001 I = 1,NLESS1
1001 PV(I) = VR(I)/VR(N)
IF(IPRTFG.EQ.0) GO TO 8005
WRITE(6,2) (PV(J),J = 1,NLESS1)
WRITE(6,6)
8005 CONTINUE
IF(ABS(LAMIMG).LT.ABS(LAMREL*1.E-25)) GO TO 5000
WRITE(6,5015)
5015 FORMAT(10X,26HCOMPLEX ROOT TO BE REMOVED)
GO TO 998
5000 CALL GREG
DO 1000 I = 1,NLESS1
A(I,N) = 0.
DO 1000 J = 1,NLESS1
1000 A(I,J) = A(I,J) - PV(I)*A(N,J)
A(N,N) = LAMREL/SCALE
IF(IPRTFG.EQ.0) GO TO 8006
WRITE(6,46)
46 FORMAT(10X,20HTRANSFORMED MATRIX A)
WRITE(6,6)
DO 1002 I = 1,N
1002 WRITE(6,2) (A(I,J),J = 1,N)
WRITE(6,6)
WRITE(6,47)
47 FORMAT(10X,35HEIGENVALUES OF TRANSFORMED MATRIX A)
CALL MEUVAL(N,A,RSR,RSI)
8006 CONTINUE

```

```

COMMENT--GENERATE (N-1) BY (N-1) MATRIX AND FIND ITS EIGENVALUES
DO 1205 I = 1,NLESS1
DO 1205 J = 1,NLESS1
1205 CMAT(I,J) = A(I,J)
WRITE(6,6)
DO 1203 I = 1,NLESS1
DO 1203 J = 1,M
1203 B(I,J) = B(I,J) - PV(I)*B(N,J)
IF(IPRTFG.EQ.0) GO TO 8007
WRITE(6,6)
WRITE(6,1204)
1204 FORMAT(10X,29HMATRIX B AFTER TRANSFORMATION)
WRITE(6,6)
DO 1207 I = 1,N
1207 WRITE(6,2) (B(I,J),J = 1,M)
WRITE(6,1500)
1500 FORMAT(1H1)
8007 CONTINUE
N = N - 1
DO 1502 I = 1,N
DO 1502 J = 1,N
1502 A(I,J) = CMAT(I,J)
999 CONTINUE
WRITE(6,6)
WRITE(6,7000)
WRITE(6,1206)
1206 FORMAT(10X,29HEIGENVALUES OF FINAL MATRIX A)
CALL MEGVAL(NLESS1,CMAT,RSRN,RSIN)
COMMENT*****THE MATRICES NEEDED FOR DIFFERENTIAL EQUATION SOLUTION
C*****ARE PREPARED HERE*****
C THE MATRIX A MUST BE UN-SCALED****
DO 3000 I = 1,NLESS1
DO 3000 J = 1,NLESS1
3000 A(I,J) = A(I,J)*SCALE
C*****THE MATRIX B IS CORRECT-AS IS*****
C*****THE MATRICES C AND D ARE USED TO RECOVER THE ORIGINAL STATE FROM
C**** THE SOLUTION OF THE REDUCED DIFFERENTIAL EQUATION---
C* * * * (X = C*Z+D*U)* * * * *
COMMENT* * * INITIALIZATION * * * * *
DO 3004 I = 1,N
3004 Z(I) = 0.
C* * * * PRINT MATRICES* * * * *
WRITE(6,6)
WRITE(6,3005)
3005 FORMAT(10X,49HMATRICES FOR NUMERICAL INTEGRATION AND CONVERSION)
WRITE(6,3006)
3006 FORMAT(10X,19HZDOT=AZ+BU, X=CZ+DU)
WRITE(6,6)
WRITE(6,6)
WRITE(6,3007)
3007 FORMAT(10X,8HMATRIX A)
DO 3008 I = 1,N
3008 WRITE(6,2) (A(I,J),J = 1,N)
WRITE(6,6)
WRITE(6,3009)
3009 FORMAT(10X,8HMATRIX B)
DO 3010 I = 1,N
3010 WRITE(6,2) (B(I,J),J=1,M)
WRITE(6,6)
WRITE(6,3011)
3011 FORMAT(10X,8HMATRIX C)
DO 3012 I = 1,NORIG
3012 WRITE(6,2) (C(I,J),J = 1,N)
WRITE(6,6)
WRITE(6,3013)
3013 FORMAT(10X,8HMATRIX D)
DO 3014 I = 1,NORIG
3014 WRITE(6,2) (D(I,J),J= 1,M)
C* * * * *END OF MATRIX PRINTING* * * * *
2 FORMAT ( )
6 FORMAT (1H )
CALL NINTEG(N,NORIG,M,A,B,C,D,Z)
998 CONTINUE
STOP
END

SUBROUTINE NINTEG(N,NORIG,M,A,B,C,D,Z)
DIMENSION A(13,13),B(13,13),C(13,13),D(13,13),Z(13),X(13),ZDOT(13)
1,U(13)
C DIMENSION IBUF(10000)
C COMPLEX AA(2500)
C CALL PLOTS(IBUF(1),10000,2)
C IPLOT = 0
C PRD = 20.E-6
C DT = .5E-9
C PI = 3.1415927
C F = 1.024E+6

```

```

      TF = 1.0E-6
      IPPRINT = 19
      T = -DT
      WRITE(6,11)
11  FORMAT(1H1)
      WRITE(6,12)
12  FORMAT(10X,21HNUMERICAL INTEGRATION)
      WRITE(6,10)
      WRITE(6,21)
21  FORMAT(6X,4HTIME,8X,5HINPUT,8X,4HX(1),9X,4HX(2),9X,4HX(3),9X,4HX(4
      1))
      WRITE(6,22)
22  FORMAT(6X,4HX(5),7X,4HX(6),9X,4HX(7),9X,4HX(8))
      WRITE(6,8)
7  CONTINUE
      T = T + DT
      IPPRINT = IPPRINT + 1
      U(1) = 1.
      DO 4 I = 1,N
      ZDOT(I) = 0.
      DO 5 J = 1,N
5  ZDOT(I) = ZDOT(I) + A(I,J)*Z(J)
      DO 4 J = 1,M
4  ZDOT(I) = ZDOT(I) + B(I,J)*U(J)
      DO 6 I = 1,N
6  Z(I) = Z(I) + DT*ZDOT(I)
      IF(IPRINT.LE.19) GO TO 7
      IPPRINT = 0
      DO 2 I = 1,NORIG
      X(I) = 0.
      DO 1 J = 1,N
1  X(I) = X(I) + C(I,J)*Z(J)
      DO 2 J = 1,M
2  X(I) = X(I) + D(I,J)*U(J)
      WRITE(6,8)
      WRITE(6,8) T,U(1),(X(I),I=1,NORIG)
C  IPLOT = IPLOT + 1
C  AA(IPLOT) = CMPLX(X(1),0.)
      8  FORMAT ( )
10  FORMAT(1H )
      IF(T.LE.TF) GO TO 7
C  CALL TIMPLT(AA,IPLOT,PRD)
999  CONTINUE
      RETURN
      END

```

```

SUBROUTINE GREG
COMMON A(13,13),B(13,13),NORIG,M,N,X(13),NEVTR,C(13,13),D(13,13),
1  LAMREL,LAMIMG,SCALE,PV(13),NLESS1,ITEMP,Z(13),IROOT,IPRTFG
REAL LAMREL,LAMIMG
DOUBLE PRECISION PV
C * * * * *
REAL MATTMP(13,13)
DIMENSION CTEMP(13,13),DTEMP(13,13)
XLAM = 1./LAMREL
C * * * * * CALCULATION OF CTEMP * * * * *
DO 2101 I = 1,NLESS1
DO 2100 J = 1,NLESS1
2100 CTEMP(I,J) = -XLAM*PV(I)*A(N,J)*SCALE
2101 CTEMP(I,I) = CTEMP(I,I) + 1.
DO 2102 J = 1,NLESS1
2102 CTEMP(N,J) = -XLAM*A(N,J)*SCALE
DO 2103 J = 1,NLESS1
TEMP = CTEMP(N,J)
CTEMP(N,J) = CTEMP(ITEMP,J)
2103 CTEMP(ITEMP,J) = TEMP
6  FORMAT(1H )
2  FORMAT( )
C * * * * * CALCULATION OF DTEMP
DO 2110 I = 1,NLESS1
DO 2110 J = 1,M
2110 DTEMP(I,J) = -XLAM*PV(I)*B(N,J)
DO 2111 J = 1,M
2111 DTEMP(N,J) = -XLAM*B(N,J)
DO 2113 J = 1,M
TEMP = DTEMP(N,J)
DTEMP(N,J) = DTEMP(ITEMP,J)
2113 DTEMP(ITEMP,J) = TEMP
COMMENT  D = D + C*DTEMP * * * * *
C  C = C*CTEMP * * * * *
C  SEQUENCE OF THESE TWO STEPS IS CRITICAL
C  * * * * * UPDATE OF MATRIX D * * * * *
DO 3000 I = 1,NORIG
DO 3000 J = 1,M
DO 3000 K = 1,N
3000 D(I,J) = D(I,J) + C(I,K)*DTEMP(K,J)

```

```

C * * * * * UPDATE OF MATRIX C * * * * *
DO 3001 I = 1,NORIG
DO 3001 J = 1,N
3001 MATTMP(I,J) = C(I,J)
DO 3002 I = 1,NORIG
DO 3002 J = 1,NLESS1
C(I,J) = 0.
DO 3002 K = 1,N
3002 C(I,J) = C(I,J) + MATTMP(I,K)*CTEMP(K,J)
IF(IPRTFG.EQ.0) GO TO 8008
WRITE(6,2)
WRITE(6,100) IROOT
100 FORMAT(10X,9HMATRIX C(I,I2,1H))
DO 6502 I = 1,NORIG
6502 WRITE(6,2) (C(I,J),J = 1,NLESS1)
WRITE(6,2)
WRITE(6,101) IROOT
101 FORMAT(10X,9HMATRIX D(I,I2,1H))
DO 6503 I = 1,NORIG
6503 WRITE(6,2) (D(I,J),J = 1,M)
WRITE(6,2)
8008 CONTINUE
RETURN
END
SUBROUTINE DATAIN
COMMON A(13,13),B(13,13),NORIG,M,N,X(13),NEVTBR,C(13,13),D(13,13),
1 LAMREL,LAMIMG,SCALE,PV(13),NLESS1,ITEMP,Z(13),IROOT,IPRTFG
REAL LAMREL,LAMIMG
DOUBLE PRECISION PV
C * * * * *
REAL LFACT1,LFACT2,LT1,LM,LT2,L3,L4,L5,L2
IPRTFG = 0
NEVTBR = 2
N = 13
M = 1
C * * * * * INPUT PARAMETERS * * * * *
R1 = 51.
LT1 = -5.358E-6
LM = 6.06E-6
LT2 = 5.194E-5
RT2 = 9.11
R2 = 5.1E3
C1 = 4.8E-10
L2 = 1.08E-5
RL2 = 1.7
C2 = 1.368E-9
C3 = 5.1E-10
L3 = 5.1E-5
RL3 = 8.01
L4 = 1.6E-5
RL4 = 2.51
C4 = 2.2E-9
C5 = 3.44E-10
L5 = 5.1E-5
RL5 = 8.01
C6 = 5.7E-10
R3 = 4.7E3
C7 = 1.8E-9
RL = 6.2E2
LFACT2 = 1./((LT1*LT2+LM*(LT1+LT2))
LFACT1 = LFACT2*(LT2+LM)/LM
WRITE(6,1500)
1500 FORMAT(1H1)
C * * * * * LOAD MATRIX A * * * * *
DO 1091 I = 1,N
DO 1091 J = 1,N
1091 A(I,J) = 0.
A(1,10) = 1./C1
A(1,11) = 1./C1
A(2,10) = 1./C2
A(3,11) = 1./C3
A(4,11) = 1./C4
A(4,13) = -1./C4
A(5,11) = 1./C5
A(5,12) = -1./C5
A(5,13) = -1./C5
A(6,6) = -1./(R3*C6)
A(6,13) = 1./C6
A(7,7) = -1./(RL*C7)
A(7,13) = 1./C7
A(8,8) = -LM*R1*LFACT1
A(8,9) = -(RT2+R2)*(LT1+LM)*LFACT1+(R2+RT2)/LM
A(8,10) = R2*(LT1+LM)*LFACT1-R2/LM
A(8,11) = R2*(LT1+LM)*LFACT1-R2/LM
A(9,8) = -LM*R1*LFACT2
A(9,9) = -(RT2+R2)*(LT1+LM)*LFACT2
A(9,10) = R2*(LT1+LM)*LFACT2

```

```

A(9,11) = R2*(LT1+LM)*LFACT2
A(10,1) = -1./L2
A(10,2) = -1./L2
A(10,9) = R2/L2
A(10,10) = -(R2+RL2)/L2
A(10,11) = -R2/L2
A(11,1) = -1./L3
A(11,3) = -1./L3
A(11,4) = -1./L3
A(11,5) = -1./L3
A(11,9) = R2/L3
A(11,10) = -R2/L3
A(11,11) = -(R2+RL3)/L3
A(12,5) = 1./L4
A(12,12) = -RL4/L4
A(13,4) = 1./L5
A(13,5) = 1./L5
A(13,6) = -1./L5
A(13,7) = -1./L5
A(13,13) = -RL5/L5
C * * *   LOAD MATRIX B   * * * * *
DO 4000 I = 1,N
DO 4000 J = 1,M
4000 B(I,J) = 0.
B(8,1) = LM*LFACT1
B(9,1) = LM*LFACT2
C   * * * * *   INITIAL CONDITIONS   * * * * *
DO 4001 I = 1,N
4001 X(I) = 0.
C * * *   PRINT INPUT DATA   * * * * *
WRITE(6,100)
100 FORMAT(10X,48HTHE INPUT SYSTEM IS OF THE FORM   XDOT = AX + BU)
WRITE(6,6)
WRITE (6,101) N,M
101 FORMAT(10X,28HTHE INPUT LINEAR SYSTEM HAS ,12,35H STATE VARIABLE C
10COMPONENTS AND HAS ,12,19H CONTROL COMPONENTS)
WRITE(6,6)
6 FORMAT(1H )
2 FORMAT( )
WRITE(6,6)
WRITE(6,102)
102 FORMAT(10X,34HTHE INPUT MATRIX A IS AS FOLLOWS)
WRITE(6,6)
DO 200 I = 1,N
200 WRITE(6,2) (A(I,J),J=1,N)
WRITE(6,6)
WRITE(6,103)
103 FORMAT(10X,34HTHE INPUT MATRIX B IS AS FOLLOWS)
WRITE(6,6)
DO 201 I = 1,N
201 WRITE(6,2) (B(I,J),J = 1,M)
WRITE(6,6)
WRITE(6,104)
104 FORMAT(10X,42HTHE INITIAL STATE VECTOR X IS AS FOLLOWS)
WRITE(6,6)
WRITE(6,2) (X(I),I = 1,N)
WRITE(6,6)
WRITE(6,105) NEVTBR
105 FORMAT(10X,49HTHE SYSTEM IS TO BE SIMPLIFIED BY THE REMOVAL OF ,12
1,12H EIGENVALUES)
RETURN
END

```

PRECEDING PAGE BLANK NOT FILMED

APPENDIX I

ROOT REMOVAL FOR A COMPLEX CONJUGATE PAIR

APPENDIX I

ROOT REMOVAL FOR A COMPLEX CONJUGATE PAIR

Although a complex conjugate pair of fast characteristic roots can be "removed" one at a time with ALSAP as described in the body of the report, the use of complex arithmetic in the simulator can be avoided by approximating the two modes simultaneously. This appendix presents the equations describing the reduced state equation, the initial conditions for the new state variables, and the transformation relating the original and the new state variables.

The original system will be of the form

$$\dot{\underline{x}} = A \underline{x} + B \underline{u} ,$$

where $\underline{x} = (x_1, x_2, \dots, x_n)^T$ is the state vector and $\underline{u} = (u_1, u_2, \dots, u_n)^T$ is the control vector. Let the fast pair of complex conjugate roots be λ and $\bar{\lambda}$, and let their eigenvectors be \underline{v} and $\bar{\underline{v}}$, respectively (the over-bar designates the complex conjugate). As before, let the eigenvectors be normalized and partitioned such that

$$\underline{v} = \begin{bmatrix} \underline{p} \\ \hline 1 \end{bmatrix} \quad \text{and} \quad \bar{\underline{v}} = \begin{bmatrix} \bar{\underline{p}} \\ \hline 1 \end{bmatrix} .$$

The reduced state equation will be

$$\dot{\underline{x}}^n = A^n \underline{x}^n + B^n \underline{u}$$

where the new state vector is given by $\underline{x}^n = (x_1^n, x_2^n, \dots, x_{n-2}^n)^T$, and the original state vector can be recovered using the relationship

$$\underline{x} = C \underline{x}^n + D \underline{u} .$$

The initial conditions for the new state variables and the elements of the matrices A^n , B^n , C , and D are given by the following expressions. The superscript "re" refers to the real part of the complex number while "im" refers to the imaginary part; subscripts refer to matrix element indices.

Initial Conditions

$$x_i^n = x_i - \left(\frac{p_i^{im}}{p_{n-1}^{im}} \right) x_{n-1} + \left[\left(\frac{p_i^{im} p_{n-1}^{re}}{p_{n-1}^{im}} \right) \left(\frac{p_i^{im}}{p_{n-1}^{im}} \right) - p_i^{re} \right] x_n$$

for $i = 1, 2, \dots, n-2$,

New State Distribution Matrix, A^n

$$a_{ij}^n = a_{ij} + \left[\left(\frac{p_{n-1}^{re}}{p_{n-1}^{im}} \right) p_i^{im} - p_i^{re} \right] a_{nj} - \left[\left(\frac{p_i^{im}}{p_{n-1}^{im}} \right) \right] a_{n-1,j} \quad , \quad i, j = 1, 2, \dots, n-2.$$

New Control Distribution Matrix, B^n

$$b_{ij}^n = b_{ij} - \left(\frac{p_i^{im}}{p_{n-1}^{im}} \right) b_{n-1,j} + \left[\left(\frac{p_i^{im}}{p_{n-1}^{im}} \right) p_{n-1}^{re} - p_i^{re} \right] b_{nj} \quad ,$$

$i = 1, 2, \dots, n-2; j = 1, 2, \dots, m.$

State-to-State Relating Matrix, C

The elements of the C-matrix are best described in three separate groups.

For $i = 1, 2, \dots, n-2$ and $j = 1, 2, \dots, m$ one has

$$c_{ij} = \frac{1}{|\lambda|^2} \left\{ a_{n-1,j} \left[\frac{\lambda^{im} p_i^{re} - \lambda^{re} p_i^{im}}{p_{n-1}^{im}} \right] \right. \\ \left. + a_{nj} \left[\frac{p_{n-1}^{re}}{p_{n-1}^{im}} \left(\lambda^{re} p_i^{im} - \lambda^{im} p_i^{re} \right) - \left(\lambda^{im} p_i^{im} \right. \right. \right. \\ \left. \left. \left. + \lambda^{re} p_i^{re} \right) \right] + |\lambda|^2 \delta_{ij} \right\}, \text{ where}$$

$$\delta_{ij} = \begin{cases} 0, & \text{if } i \neq j \\ 1, & \text{if } i = j. \end{cases}$$

For $i = n-1$ and $j = 1, 2, \dots, m$ one has

$$c_{n-1,j} = \frac{1}{|\lambda|^2} \left\{ a_{n-1,j} \left[\frac{\lambda^{im} p_{n-1}^{re} - \lambda^{re} p_{n-1}^{im}}{p_{n-1}^{im}} \right] - a_{nj} \lambda^{im} \left[p_{n-1}^{im} \right. \right. \\ \left. \left. + \left(p_{n-1}^{re} \right)^2 / \left(p_{n-1}^{im} \right) \right] \right\}.$$

For $i = n$ and $j = 1, 2, \dots, m$ one has

$$c_{nj} = \frac{1}{|\lambda|^2} \left\{ -\lambda^{re} a_{nj} + \lambda^{im} \left(a_{n-1,j} - a_{nj} p_{n-1}^{re} \right) / p_{n-1}^{im} \right\}.$$

Control-to-State Relating Matrix, D

The elements of the D-matrix are also described in three groups.

For $i = 1, 2, \dots, n-2$, and $j = 1, 2, \dots, m$ one has

$$\begin{aligned}
d_{ij} = & \frac{-1}{|\lambda|^2} \left\{ b_{nj} \left[\lambda^{\text{re}} \left(p_i^{\text{re}} - p_{n-1}^{\text{re}} p_i^{\text{im}} / p_{n-1}^{\text{im}} \right) \right. \right. \\
& + \left. \lambda^{\text{im}} \left(p_i^{\text{im}} + p_{n-1}^{\text{re}} p_i^{\text{re}} / p_{n-1}^{\text{im}} \right) \right] \\
& \left. + b_{n-1,j} \left[\left(\lambda^{\text{re}} p_i^{\text{im}} - \lambda^{\text{im}} p_i^{\text{re}} \right) / p_{n-1}^{\text{im}} \right] \right\} .
\end{aligned}$$

For $i = n-1$ and $j = 1, 2, \dots, m$ one has

$$\begin{aligned}
d_{n-1,j} = & \frac{-1}{|\lambda|^2} \left\{ b_{nj} \left[2\lambda^{\text{im}} p_{n-1}^{\text{im}} + \lambda^{\text{im}} \left(\left[p_{n-1}^{\text{re}} \right]^2 - \left[p_{n-1}^{\text{im}} \right]^2 \right) / \left(p_{n-1}^{\text{im}} \right) \right] \right. \\
& \left. + b_{n-1,j} \left[\lambda^{\text{re}} - \lambda^{\text{im}} p_{n-1}^{\text{re}} / p_{n-1}^{\text{im}} \right] \right\} .
\end{aligned}$$

For $i = n$ and $j = 1, 2, \dots, m$ one has

$$\begin{aligned}
d_{nj} = & \frac{-1}{|\lambda|^2} \left\{ b_{nj} \left[\lambda^{\text{re}} + \lambda^{\text{im}} \left(p_{n-1}^{\text{re}} / p_{n-1}^{\text{im}} \right) \right] \right. \\
& \left. + b_{n-1,j} \left[-\lambda^{\text{im}} / p_{n-1}^{\text{im}} \right] \right\} .
\end{aligned}$$